

# Design and Implementation of the Precision Personnel Locator Digital Transmitter System

A Thesis

submitted to the Faculty

*of the*

WORCESTER POLYTECHNIC INSTITUTE  
Worcester, Massachusetts, USA

*in partial fulfillment of the requirements of the*

Degree of Master of Science

*in*

Electrical and Computer Engineering

*by*

---

Hauke C. Dämpfling

December 2006

Approved:

---

Prof. R. James Duckworth, Major Advisor

---

Prof. David Cyganski, Committee Member

---

Prof. John A. Orr, Committee Member



## **Abstract**

The *Precision Personnel Locator* project is an ongoing research project funded by the Department of Justice, the goal of which is to provide sub-meter accuracy tracking and location of first responders inside of buildings with no pre-existing infrastructure, especially in emergency situations. The PPL system consists of wearable, battery-powered *Locator* devices that transmit a multi-carrier “ranging signal” waveform and *Reference Units* that receive this ranging signal and relay the information to a *Base Station* for location estimation processing and display.

This thesis describes the design and implementation of a subset of the *Locator* devices’ functionality, including: the digital generation of the ranging signal waveform; the coordination of the transmissions of many *Locator* devices using time-sharing methods to prevent overlap of the signals; and finally, the gathering of environmental data such as temperature and movement of the wearer and the relaying of this data back to the *Base Station*.

To perform these tasks, two subsystems were designed and implemented as printed circuit boards. The first of these is the *Data Channel*, which is a low power, general-purpose communications platform that is capable of controlling the transmissions of the *Locator* devices with support for up to 100 *Locators* transmitting every second, and it can control the power of the *Locator* devices by switching portions of the system off when they are not in use. It also includes sensors to measure the ambient temperature, movement of the device, and a “distress button” that a first responder can press to trigger a distress signal to be transmitted to the outside of the building. The second subsystem is the *Digital Waveform Generator*, which consists of a Field-Programmable Gate Array (FPGA) and Digital-to-Analog Converter (DAC) that are capable of generating waveforms of up to 200 MHz bandwidth. The new *Locator* hardware can operate on battery power for many days.

The two subsystems were successfully tested and will serve as an important step towards the goal of developing a deployable location and tracking system.

## **Acknowledgements**

I would like to thank my advisor, Prof. James Duckworth, for his support and guidance throughout my time as a graduate student and my work on this project, and especially for his contributions and help reviewing this thesis. I would also like to thank Prof. John Orr and Prof. David Cyganski for serving as my thesis committee members.

I am grateful to the many people who have directly contributed to my work on this thesis: Robert Boisse, Jeffrey Cho, Jack Coyne, Gerry Harrington, Thomas Lui, Candemir Orsan, and Hemish Parikh all assisted me greatly during the design and evaluation process.

I would like to thank the rest of the Precision Personnel Locator team for their support of the overall project and their input to my work: Prof. Sergey Makarov, Prof. William Michalson, Vincent Amendolare, Jason Farmer, David Holl, Jason Huang, Shashank Kulkarni and Benjamin Woodacre have all greatly contributed to the success of the PPL project.

Finally, I would like to thank the National Institute of Justice at the Department of Justice, who funded this research project.

Hauke Daempfling

December 2006

## **Table of Contents**

Abstract .....	i
Acknowledgements .....	ii
List of Figures .....	v
List of Tables .....	vi
Chapter 1. Introduction .....	1
Chapter 2. Background.....	6
2.1. Overall System Requirements.....	6
2.1.1. Meeting with Worcester Firefighters .....	8
2.1.2. PPL Workshops.....	9
2.2. PPL Project History.....	10
2.3. Existing Digital Hardware Design .....	12
2.4. Locator Design Requirements.....	15
Chapter 3. Data Channel and Communication Protocol .....	18
3.1. Multi-Transmitter Support .....	18
3.2. Time-Division Multiplexing .....	20
3.3. Free-Running Transmitter Calculations.....	23
3.4. Random Transmissions .....	27
3.4.1. Conclusions .....	31
3.5. Bi-Directional Communication.....	32
3.6. Hardware Specifications .....	34
3.7. Hardware Implementation.....	38
3.8. Communications Protocol.....	41
3.8.1. Data Format.....	43
3.8.2. Communications Concept.....	46
3.9. Protocol Implementation.....	48
3.9.1. Synchronization and Timing.....	51
Chapter 4. Digital Waveform Generation .....	57
4.1. Digital-to-Analog Converter Design.....	58
4.1.1. Sampling Clock.....	60
4.2. Data Supplying System Design.....	62
4.2.1. High Speed Memory and CPLD .....	63
4.2.2. Field Programmable Gate Array .....	63
4.2.3. FPGA Configuration .....	65
4.2.4. Package Selection.....	66
4.3. Hardware Implementation.....	67
4.3.1. Power Supply Design.....	68
4.3.2. PCB Design.....	71
4.3.3. FPGA Digital Design .....	74
Chapter 5. Experimental Results.....	77
5.1. Data Channel.....	77
5.1.1. Hardware Performance.....	77
5.1.2. Outdoor / Indoor Range Tests .....	78
5.1.3. Outdoor Range Test .....	84
5.1.4. Data Rate vs. Receiver Sensitivity Test.....	85

5.1.5. Antenna Configuration Test.....	86
5.1.6. Timer Accuracy Test.....	88
5.1.7. Timer Drift Test .....	89
5.1.8. Synchronization Accuracy Test .....	90
5.1.9. Time Division Multiplexing Protocol .....	91
5.2. Digital Waveform Generator.....	94
5.2.1. RF Characterization.....	94
5.2.2. Power Analysis.....	100
Chapter 6. Conclusion and Future Work.....	104
6.1. Future Work .....	107
Chapter 7. References .....	108
Appendix A. Detailed Data Channel Experimental Results .....	111

## **List of Figures**

Figure 1: PPL System Concept .....	2
Figure 2: Locator Unit Concept Drawings .....	3
Figure 3: Locator Overview .....	4
Figure 4: PPL System Overview .....	7
Figure 5: Audio Proof-of-Concept System .....	10
Figure 6: RF Proof-of-Concept Receiver .....	11
Figure 7: Current Transmitter Hardware .....	13
Figure 8: Multi-Carrier Signal .....	14
Figure 9: Previous Digital Waveform Generation Hardware .....	14
Figure 10: Overview of Locator Hardware Design .....	16
Figure 11: Data Channel as Part of Overall Locator Design .....	18
Figure 12: Time-Division Multiplexing .....	19
Figure 13: Frequency-Domain Multiplexing, Bands (left) vs. Interleaving (right) .....	19
Figure 14: TDM Overview .....	23
Figure 15: Clock Drift .....	24
Figure 16: Sample Failure Times .....	26
Figure 17: Random Transmission Scheme .....	28
Figure 18: General Locator Block Diagram .....	35
Figure 19: Data Channel Hardware Block Diagram .....	38
Figure 20: Completed Data Channel Hardware .....	39
Figure 21: Data Channel Movement Detection Circuit .....	41
Figure 22: System Overview .....	42
Figure 23: Packet Format .....	46
Figure 24: Protocol Overview .....	47
Figure 25: Basic Protocol Overview .....	50
Figure 26: Timeslot Overview .....	52
Figure 27: Synchronization .....	54
Figure 28: Data Transmission .....	55
Figure 29: Digital Waveform Generator as Part of Overall Locator Design .....	57
Figure 30: Digital Waveform Generator Concept .....	58
Figure 31: Proposed DAC Clock Generation Circuit .....	61
Figure 32: Modifications to Clock Circuit .....	62
Figure 33: Xilinx Spartan-3 Configuration Times (Source: Xilinx XAPP452) .....	64
Figure 34: Digital Waveform Generator Block Diagram .....	68
Figure 35: Digital Side Power Distribution .....	69
Figure 36: Analog Side Power Distribution .....	69
Figure 37: DAC and FPGA Packages .....	72
Figure 38: Routed LVDS Data Lines .....	72
Figure 39: Completed Digital Waveform Generator Board, Top (Digital) Side .....	73
Figure 40: Completed Digital Waveform Generator Board, Bottom (Analog) Side .....	74
Figure 41: DDR Timing Diagram (Source: AD9726 Data Sheet) .....	74
Figure 42: FPGA Internal Hardware Design .....	75
Figure 43: Slave “Street” (left) and “Back” (right) Location .....	79
Figure 44: Range Test Data Rate Results .....	80

Figure 45: Range Test Distance Results .....	81
Figure 46: Range Test Antenna Results .....	82
Figure 47: Range Test Results Overview Map .....	83
Figure 48: Outdoor Range Test Locations .....	84
Figure 49: Outdoor Range Test Results .....	85
Figure 50: Data Rate vs. Receiver Sens. Results .....	86
Figure 51: Antenna Configuration Test Set-Up .....	87
Figure 52: Antenna Configuration Test Results .....	88
Figure 53: Actual Protocol Overview .....	92
Figure 54: Actual Synchronization .....	93
Figure 55: Actual Data Transmission .....	94
Figure 56: Multi-Carrier Test Waveform .....	95
Figure 57: Spurious Signal Comparison .....	97
Figure 58: Sampling Clock vs. Spurious Levels .....	98
Figure 59: Output Spectrum at 220 MSPS with On-board clock .....	99
Figure 60: Output Spectrum at 400 MSPS .....	99
Figure 61: Locator Power-Up Sequencing .....	101
Figure 62: Power Consumption and Timing .....	102
Figure 63: Newly Developed Locator Hardware .....	106

## **List of Tables**

Table 1: Allotted Frequency Bands .....	11
Table 2: Symbols Used .....	24
Table 3: Sample Failure Times (h:mm:ss) .....	27
Table 4: Required Frequency Stability for Specific Failure Times .....	27
Table 5: Simulation Verification Results .....	30
Table 6: Sample Probability Calculations .....	31
Table 7: Transceiver Modules .....	34
Table 8: Data from Locator to Base Station .....	45
Table 9: Data from Base Station to Locator .....	45
Table 10: Xemics Module Mode Switch Times .....	52
Table 11: DAC Comparison .....	60
Table 12: Current Consumption Estimates .....	70
Table 13: Regulator Selection .....	70
Table 14: Outdoor / Indoor Test Runs .....	80
Table 15: Timer Drift Test Results .....	89
Table 16: SNR Comparison Results .....	95
Table 17: Harmonic Distortion Test .....	96
Table 18: Signal Power Levels .....	96
Table 19: Battery Life Calculation .....	102
Table 20: Outdoor / Indoor Range Test Raw Results .....	112
Table 21: Outdoor Range Test Raw Results .....	113
Table 22: Synchronization Accuracy Test Results .....	114

## **Chapter 1. Introduction**

On December 3, 1999, six firefighters were killed in a disastrous fire at the Worcester Cold Storage and Warehouse in Worcester, Massachusetts [3, 26, 27, 30]. Most, if not all, of these deaths could possibly have been prevented if the firefighters had had some better way to navigate inside the building despite the thick smoke and complicated layout of the corridors. This event led to the authoring of a whitepaper by Prof. John Orr [17] outlining the basic requirements for a system to locate and track first responders inside of buildings, and the subsequent launch of the *Precision Personnel Locator* research project, or *PPL*, which has been funded with a total of about \$3 million by the US Department of Justice.

In general, precise location estimation of persons inside of buildings without preexisting infrastructure for such purposes is a highly useful yet technically challenging problem. As will be described in more detail later, this is due largely to the fact that radio signals reflect from metal objects, creating multiple copies of the same signal and obscuring the direct path to the radio transmitter. Currently, there are no commercially available systems that can accomplish precise location and tracking. If such systems can be developed, the applications include uses for law enforcement, correctional facilities, and emergency first responders, such as firefighters [28]. The Precision Personnel Locator research project aims to develop technology for these applications by building an RF-based location and tracking system.

The PPL system consists of wearable *Locator* devices that transmit a multi-carrier “ranging signal” waveform that spans as much as a few hundred MHz and *Reference Units* that receive this ranging signal and relay the information to a *Base Station* for processing and location estimation. Figure 1 depicts this situation for the case of firefighters. The concept is that every person to be tracked wears a Locator unit (in the figure these are referred to as “transmitter badges”), most likely as part of their standard turnout gear. The Reference Units either are mounted directly on the first responders’ vehicles or are deployed from them, allowing for a rapid setup of the entire system. The incident commander has a tactical display as part of the Base Station, most likely on their command vehicle, to view the positions of the persons being tracked. This tactical display would have the capability to display the location of all or only a few selected Locator units in real-time and the paths they have followed over time. Such information could in turn be disseminated off-site or to hand-held units such as PDAs. The location and path



information could then be used either to guide a lost user out on the path they entered the building, or to guide a rescue team into the building and directly to the person in need of assistance.

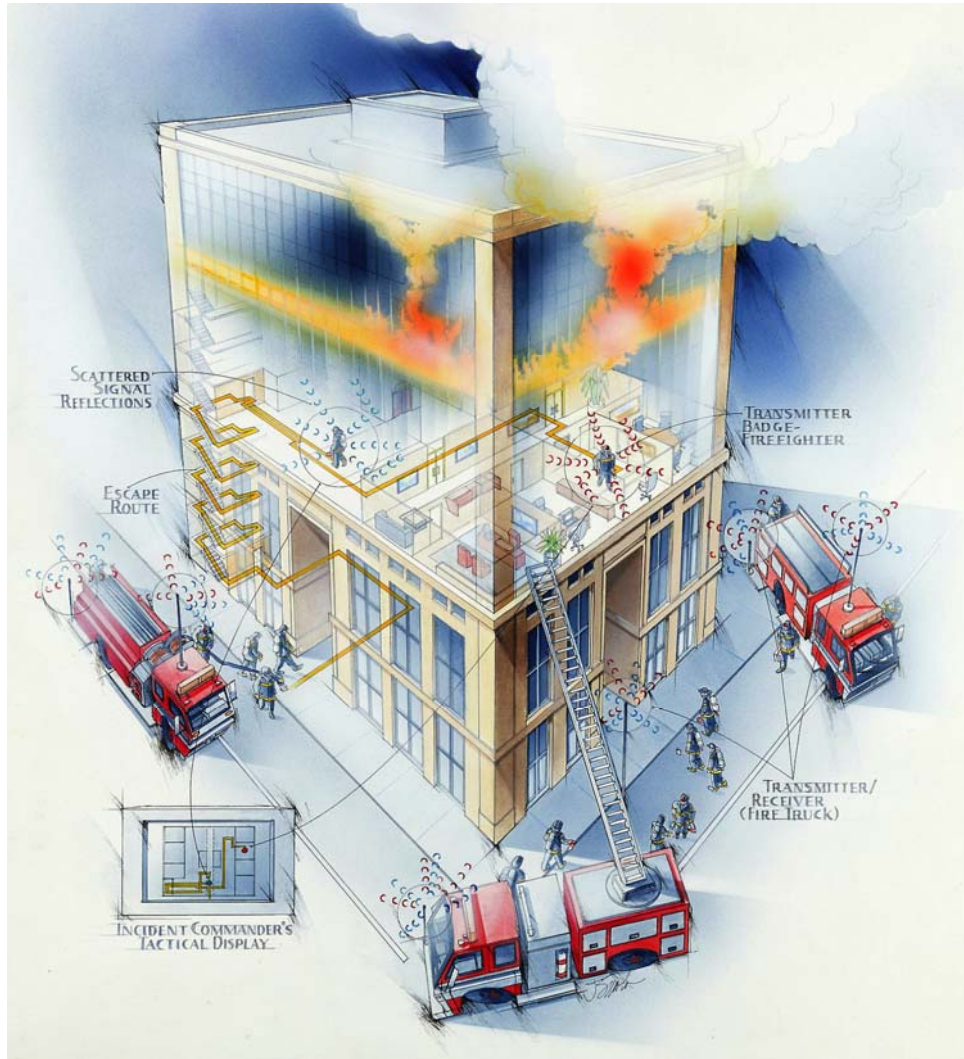
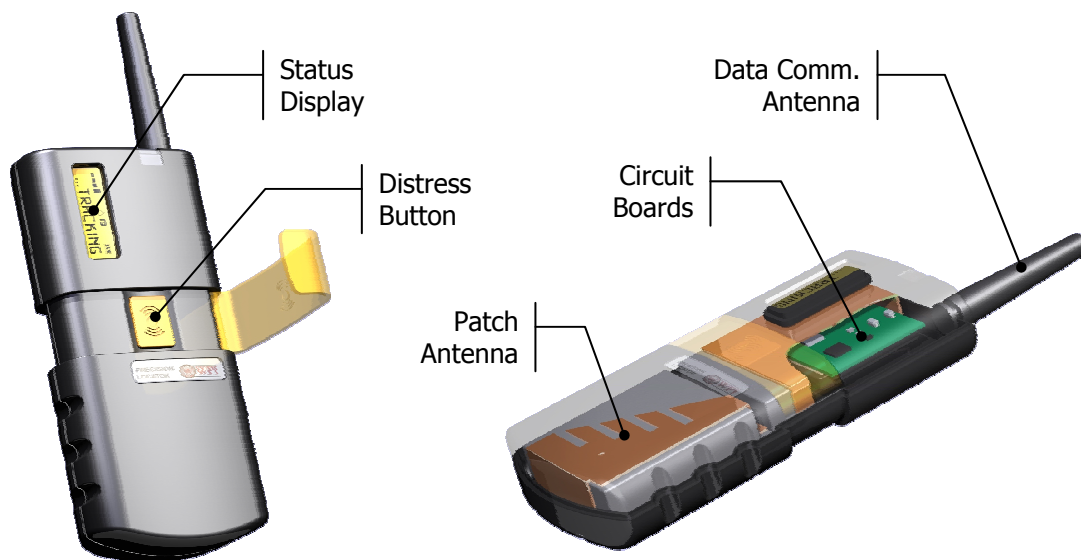


Figure 1: PPL System Concept

The figure above makes another important point, which is that the signal transmitted by the Locator devices is reflected by metal objects and scatters. This effect is called *multipath*, because each reflected signal that reaches the receiver is seen as a different “path” to the transmitter. The receiver then has the difficult task of selecting the true path, which is usually the shortest path, but not necessarily the strongest signal. Multipath effects can also cause certain frequencies in the signal to be faded out and others to be amplified. This problem is solved by the unique signal structure, algorithms and system architecture of the PPL system [6].

The function of the Locator units is to transmit the “ranging signal”, consisting of many carriers, at pre-determined time intervals, so that multiple units may time-share their transmissions. Figure 2 shows a concept drawing of what a Locator device might look like. The units would be hand-held, being the size of a cell phone or walkie-talkie. They feature a distress button that can be used by a first responder to trigger a distress call to be sent to the outside of the building in case of emergency, and a status display for information such as battery charge status. As can be seen in the figure, there are two separate antennas – a PIFA-type antenna for the ranging signal, and a monopole antenna for data communication. Note that the reasons for implementing these two radio channels separately will be discussed in this thesis.



**Figure 2: Locator Unit Concept Drawings**

The ranging signal is generated on the Locators by a “software radio” type system. Digital samples of the signal waveform are generated by a Field Programmable Gate Array (FPGA) and provided to a Digital-to-Analog Converter (DAC) at a high speed – at least twice the bandwidth of the signal, i.e. a few hundred MHz. The DAC passes the generated signal to a radio frequency (RF) front-end, which up-converts the signal in the analog domain to the desired center frequency. In addition, the entire Locator must be able to be switched off when it is not in use to conserve power and in order to allow for the time-sharing of ranging signal transmissions. Figure 3 shows this system, in which the Locator has been divided into three subsystems: the digital generation of the ranging signal waveform via the FPGA and DAC, the radio frequency front-end that upconverts and transmits this signal, and lastly a control module that handles tasks such as

powering the other two parts of the Locator on and off as necessary and communicating commands and status data. This control module is known as the *Data Channel*.

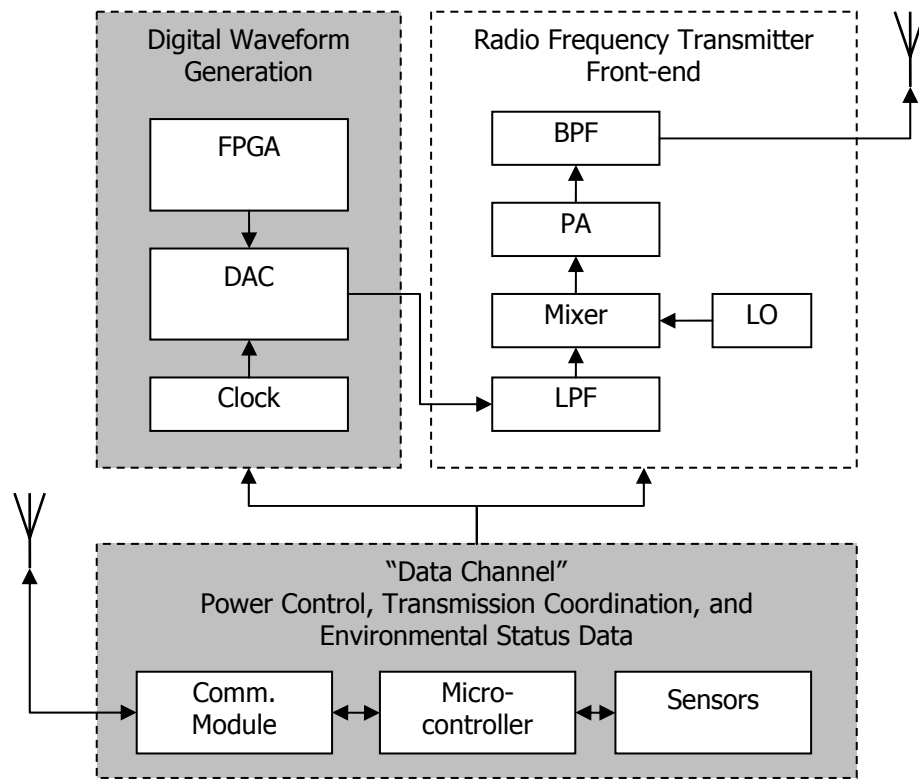


**Figure 3: Locator Overview**

The focus of the work described in this thesis lies in the design, implementation and testing of the digital portion of the Locator units, consisting of the power control, transmission coordination, and digital waveform generation subsystems shown (shaded) above. Some additional tasks of the Locator units are to monitor the status of the environment, the physiological status of its wearer and to provide limited communication capabilities, such as a “distress call” to the outside of the building. There are several challenges in these tasks. The Locator units must be capable of running on battery power for several days. The waveform generation system must be capable of supplying data to the DAC at a high speed and still have a low power consumption, for example by enabling the circuit for only short periods of time. In addition, the transmissions of multiple Locators must be coordinated, and the status information and possible distress call must be communicated to the Base Station.

In order for the Locator to be modular for testing and to be able to better shield the different systems from one another in case of problems, it was decided to implement the subsystems shown above as three separate printed circuit boards (PCBs). The first PCB is the

*Data Channel*, which is intended to take over the power control, transmission control, status monitoring, and general data communication tasks of the Locator, and the second PCB is the *Digital Waveform Generator*, which is intended to replace the existing prototype waveform generators and produce the ranging signal waveform for the RF front-end. Note that the RF front-end is currently being developed as a third subsystem by other members of the PPL team.

The Data Channel subsystem was developed as a more general-purpose platform for two-way wireless communications on an RF band separate from the ranging signals. It was implemented as a small, battery powered printed circuit board (PCB). The PCB includes a low-power microcontroller, a communications module capable of communications in the license-free 900 MHz “Industrial, Scientific and Medical” (ISM) radio band, and several peripherals such as an accelerometer for movement detection and a temperature sensor. The hardware is capable of operating on battery power for several days and has several interface ports to connect to other parts of the Locator, such as for overall power control of the Locator device. Because the PCBs operate on a wireless channel separate from the ranging signal, they could even be used as a backup for basic communication in case the ranging signal fails, for example to communicate the distress signal.

The Digital Waveform Generator subsystem is a redesign of an existing version of waveform generator hardware and is intended to be used in conjunction with a new RF transmitter front-end currently under development. It was implemented as a small PCB that attaches directly to the new RF front-end. The boards’ major components are a Xilinx Spartan-3 FPGA and an Analog Devices DAC, accompanied by supporting circuitry such as clock generation for the DAC. This new hardware was developed to better approximate a final product in terms of size, power consumption, and sampling rate, as the previous generation of hardware was larger, and the FPGA and DAC were not optimal compared to the required sampling rate, and therefore also consumed more power.

This thesis presents the design, implementation and testing of the Data Channel and Digital Waveform Generator subsystems. In the next chapter, the background of the PPL project will be presented, including its history and the overall design requirements. Then, in the following chapters, the design of each subsystem will be discussed, followed by the implementation and testing of each.

## **Chapter 2. Background**

In this chapter, the requirements for the different portions of the PPL system with a focus on the Locator device will be presented, followed by a brief history of the PPL project. The previous generation of Locator hardware is presented, followed by the design requirements for the new Locator hardware, with a focus on the digital subsystems of the Locator.

### **2.1. Overall System Requirements**

At the beginnings of the PPL project in 1999 [17], several requirements for the system were laid out, many of which evolved over time to meet the requirements of users and the technical realities of implementing the system [18]. This section describes the system requirements as they stood at the time of writing, with some mention to the origins of these requirements. It should be noted that, in several cases, there were two sets of requirements for two different goals: the theoretical “final production system” level requirements, and the prototype system requirements that apply to the systems described in this thesis, which represent a step towards the final requirements.

An overview of the PPL system is presented in Figure 4. The Locator units transmit the ranging signal, which is received by the Reference Units, which in turn relay the data back to the Base Station. For this reason, the Locators are often referred to simply as transmitters, and the Reference Units as receivers. The Locator units are worn by the first responders entering the building or structure, and the units collect environmental and psychological status information and transmit it outside the building, in addition to transmitting the ranging signal. The Reference Units could be mounted on a first responder vehicle (such as a fire truck), or they could be deployed from the vehicles as mobile reference units. The Base Station could be mounted on, for example, the vehicle of the incident commander. It is obvious that the Locator units must be completely free to operate on their own, with “no wires attached” and powered by a battery.

It should be noted that many of the discussions of the PPL project are in the context of firefighters, but the system is actually very general-purpose. Market studies and focus groups were conducted [28] that showed that there is interest in this kind of technology from groups such as law enforcement and correctional facilities as well. In some cases, the requirements differ, but the basic work being done on the PPL systems and algorithms can be adapted to meet these different needs.

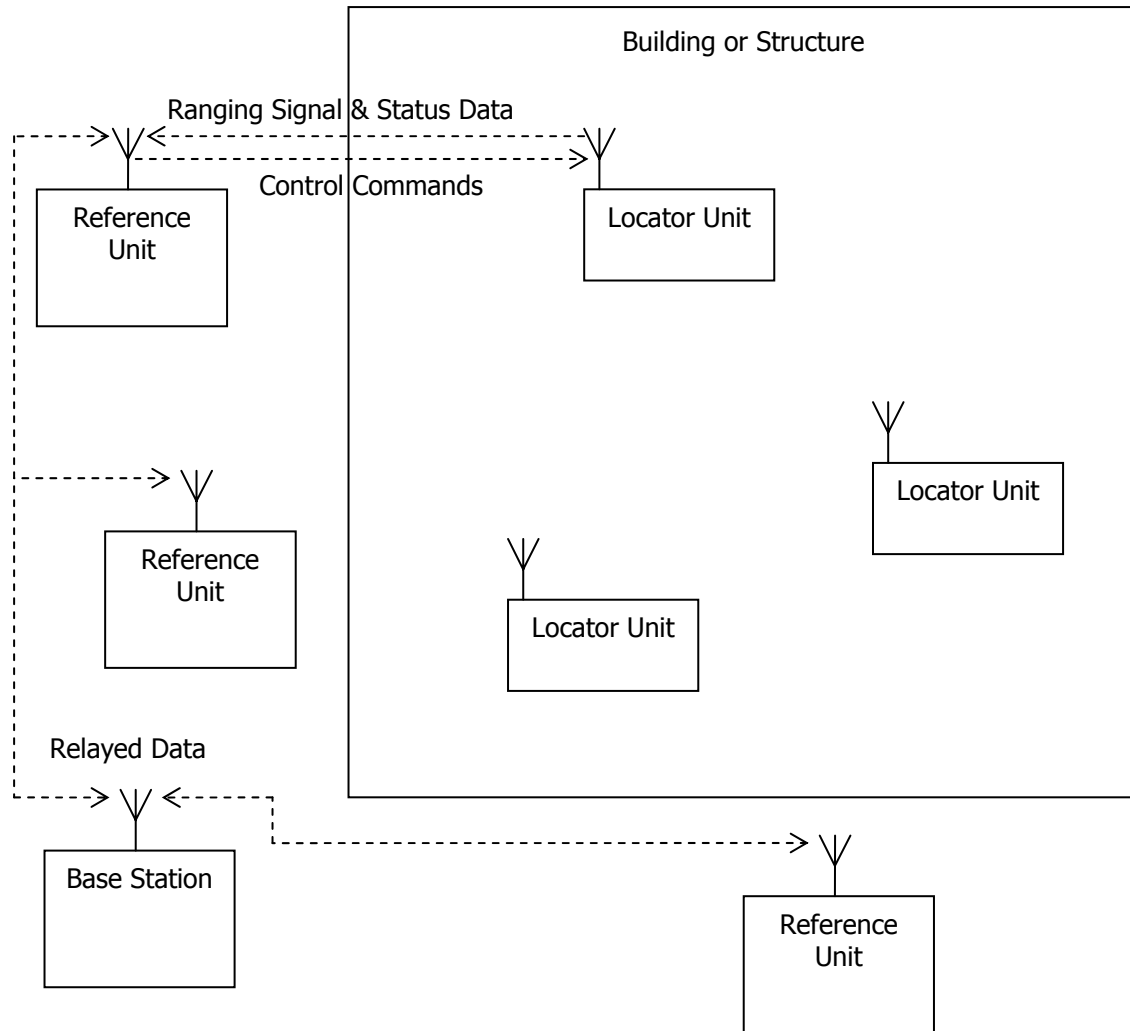


**Figure 4: PPL System Overview**

The most obvious requirements for the system are accuracy and reliability. The system must be able to provide real-time location information in three dimensions for each separate user of the system. The accuracy of the position should be good enough to let the users know which side of a wall a person is on, to be able to direct a search and rescue team to the correct room, so the positioning requirement calls for  $\pm 1$  foot accuracy. The system must support up to 100 users simultaneously, allowing for use in large-scale emergencies where this number of first responders is likely.

The operating range of the system was originally specified to be at least 2000 ft (about 610 m), so that it would be able to cover an entire city block. However, in order to stay within FCC regulations and because such a range is not yet required for testing, the prototype system specifications stated that a range of 100 m is enough. This range covers the Atwater-Kent

building at WPI, which is often used for testing, and is representative of other large, commercial buildings. In addition, it can be assumed that the existing transmitters would need to only be modified for a higher transmission power to achieve a greater range.

The system should track the path users have taken over time by periodically recording their location. In order to acquire this tracking information, and in order to provide real-time location information to the users, the system must update the position of each Locator device at least once a second. The path information that is gathered could be displayed on the Base Station, and it could also be relayed to hand-held units, possibly even ones carried by the first responders themselves. This would allow for a “self-rescue” type operation, where users who may have become lost or disoriented could find their own way out.

Finally, the Locator devices should collect environmental and psychological information, so that this information can be relayed to the Base Station and the status of the person inside the building is better known. This should include a “distress signal” that a first responder can trigger when in need of assistance in emergencies.

### **2.1.1. Meeting with Worcester Firefighters**

In October 2005, researchers from the WPI PPL project met with officials from the Worcester Fire Department to discuss both system requirements and to get an idea of existing firefighter equipment [29]. Several important insights into how the PPL system might integrate into fire departments’ equipment and routines were gained. In general, one must realize that typical fire departments may not have a great deal of funding and that most firefighters operate without “high-tech gadgets” – the standard *turnout gear* includes only boots, pants, a jacket, a helmet, a flashlight and possibly a radio. Other equipment, such as axes, is taken from the fire truck only when needed. So-called “self contained breathing apparatuses” (SCBAs) are also part of the equipment of a fire department, but there may not be enough for every firefighter. SCBAs are also sometimes forgotten, or even abandoned by firefighters when they are out of air. The SCBAs typically also include a “Personal Alert Safety System” (PASS), which is a device that emits a loud beeping noise when it detects non-movement of the firefighter, allowing for other firefighters to find a downed colleague.

The main theme that became apparent at this meeting was that the Locator devices must be very simple to use, hard to lose or forget, and be robust. When arriving at the scene of an incident, firefighters should not need to remember to pick up a Locator device (in case it is

attached to some kind of charging station or something similar), or to turn it on. This means that it would be preferable to be able to issue a Locator device to every firefighter so that it can be worn at all times, or even that it is sewn into or otherwise securely attached to the firefighter's turnout gear, such as the jacket. This shows the need for two more requirements: The devices must be low-cost, so that one could be issued for every firefighter in a department, and they must be very low-power, preferably even with the ability to remotely turn off a device when it is not at the scene of an incident. However, another important point is that if a device is so low-power that it does not need to be recharged often, this might actually be a disadvantage, as it does not build a habit for firefighters to regularly recharge their devices.

In respect to the possible "self-rescue" feature of the system, the point was made that inside a burning building there is often very low or absolutely no visibility, due to thick smoke and/or the power being cut off to the building. Therefore, it would be difficult for a firefighter to see the screen of a device providing self-rescue information, or the device could be dropped and easily lost. In addition, the environment can often be very noisy, making audio clues also somewhat troublesome.

In summary, the meeting with the firefighters confirmed that the top priorities for the Locator devices are small size, robustness, as well as low cost. In addition, the fact that every fire is an "organized chaos" makes it clear that rapid deployment and ease-of-use are especially important to the system as well.

### **2.1.2. PPL Workshops**

The first workshop concerning the PPL project was held in June of 2004 [22] and was attended by representatives from government, fire departments, law enforcement offices, and correctional facilities. At this workshop, the system requirements and priorities for the PPL system were established; many of these requirements are reflected in the above sections.

In August 2006, a workshop entitled "Precision Indoor Personnel Location and Tracking for Emergency Responders" was held at WPI [21]. At this workshop, representatives from industry and research gathered to present their different approaches to the issue of indoor location and tracking, and discussed common requirements for such systems. Through working group sessions, several conclusions for requirements were reached [31]. Many of these conclusions simply confirm the need for reliability, accuracy, etc. and underline the different requirements for different end users. However, one point differs from the previous discussion here, which is that



self-rescue could actually be a very important feature. This is because a firefighter is not always in a zero-visibility environment, and may easily be in a situation where he or she must escape from a building or structure, without the time for a rescue team to enter the building. So, although for the design of the Locator devices, self-rescue was not deemed a required functionality, this feature should not be eliminated from the list of general, future system requirements.

To summarize all these requirements for the focus of this thesis, which is on the Locator devices, it is clear that the Locators must be small and low-power, able to reliably transmit the ranging signal, and to communicate status information back to the Base Station.

## **2.2. PPL Project History**

The PPL project has benefited much from the work being done at WPI in the areas of radio navigation, radar sensing, and super-resolution techniques. In a paper by Professors Cyganski, Orr, and Michalson of WPI, a novel approach to range estimation is described [6]. This approach uses a multi-carrier signal structure and a matrix decomposition algorithm to analyze the relative phase shifts of each carrier to determine the time difference of arrival (TDOA) which can in turn be used to calculate the distance to the transmitter from two receivers. In addition, this algorithm allows for the separation of the direct-path and multipath signals, and its multi-carrier structure allows it to be robust against frequency selective fading.

This algorithm was implemented in a proof-of-concept system that used audio waves instead of RF frequencies [13]; this allowed for rapid prototyping with standard PC hardware. The original signal consisted of 101 carriers generated at 44100 samples per second, and the wavelengths of the kHz-range audio signals in air correspond to the wavelengths of an RF signal in the GHz range. This system, shown in Figure 5, showed that this approach is feasible, and thus paved the way for the next stage of the project, which was an RF-based prototype system.

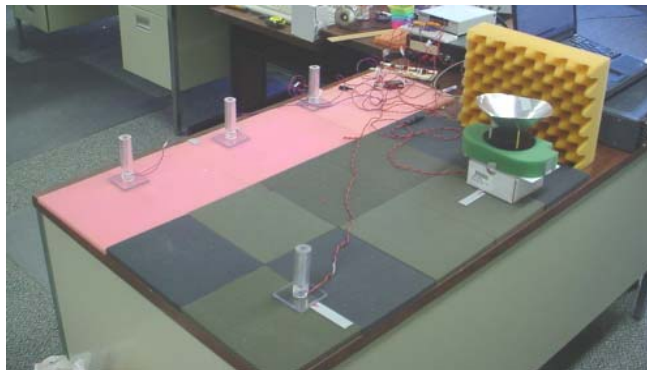


**Figure 5: Audio Proof-of-Concept System**

The first RF prototype system consisted of off-the-shelf components connected to form the transmitter and receiver portions of the system. A photo of the receiver portion of this prototype system is shown in Figure 6. This prototype served as the basis for the “second generation” custom prototype system presented in the following section.

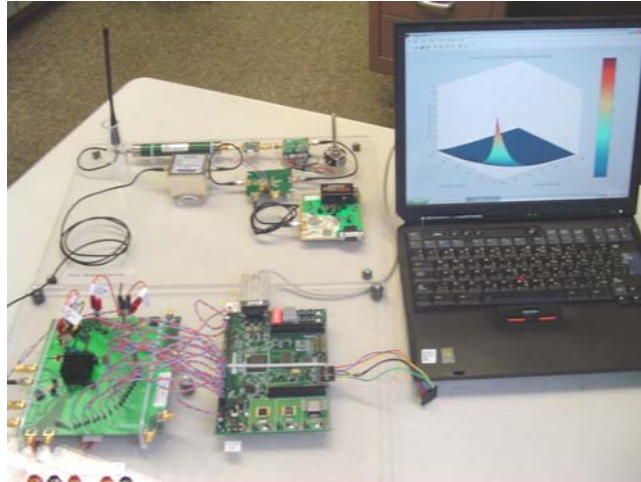


**Figure 6: RF Proof-of-Concept Receiver**

Originally, the RF prototypes operated at a center frequency of about 440 MHz, depending on the experimental set-up. However, the FCC recently granted the PPL project more frequencies to use, as listed in Table 1. Band 1 is the previously allotted frequency span around the 440 MHz center frequency. As can be seen, the new “bands” that have been granted, Bands 2 and 3, can actually be seen as a continuous band with a gap in the middle.

<b>Band</b>	<b>Lower Freq. (MHz)</b>	<b>Upper Freq. (MHz)</b>
1	410	470
2	512	608
3	614	698

**Table 1: Allotted Frequency Bands**

Since the implementation of the second generation of prototype hardware, many tests to evaluate system performance using the TODA algorithms have been performed, and improvements and additions to the hardware and algorithm software have been made. Some of the improvements and tests are described here:

- The TDOA range estimation algorithm originally required that one must specify the number of multipath reflections to solve for. Since one cannot know the number of reflections in a real-world multipath environment, and solving for the wrong number of

signals may perturb the correct solution, an addition to the algorithm known as “auto-Nsig” allowed for it to automatically determine the best number of signal paths to solve for.

- The initial versions of the algorithms used only one of the sidebands of the received signal. Algorithm improvements that allowed processing of both sidebands of the signal meant a doubling of the bandwidth available for range estimation.
- A Windows-based GUI for data collection was developed. This had previously been done with tedious manual editing and execution of MATLAB scripts. This GUI made the process of collecting data during testing much more efficient, allowing more tests to be performed.

An important point that is raised above is increasing the bandwidth. It has been shown [7, 20] that, generally speaking, increased bandwidth results in better range estimates. Therefore, tests were performed in which the original transmitter bandwidth of 25 MHz was increased to 50 MHz and above, which allowed for better range estimation.

During the testing of the TDOA algorithm, some important benchmarks were reached, for example, a first test was performed that showed that the TDOA algorithm could be used to accurately locate a transmitter in two dimensions in an outdoor environment. An important element of this test was that the transmitter did not share any clock signals with the receivers, i.e. it was completely free-running “with no wires attached”, as a transmitter in the real world would be.

### **2.3. Existing Digital Hardware Design**

The work described in this thesis involved improving the design of the Locator devices, which was based on the previous generation of simple transmitter hardware described in [8]. Because this thesis focuses on the digital hardware of the Locator devices, we will describe this portion of the previous version of hardware, a diagram of which is reproduced from [8] in Figure 7. The “Digital Controller” and “High Speed D/A” portions were completely redesigned as part of the work on this thesis, and a redesign of the RF front-end is currently underway by other members of the PPL team.

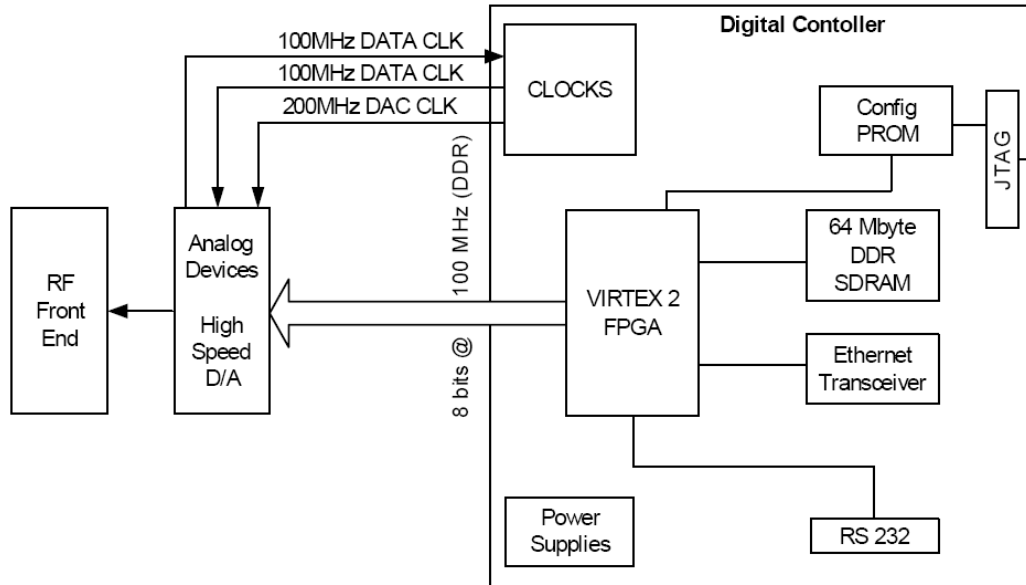


**Figure 7: Current Transmitter Hardware**

The digital portion of the previous transmitter prototype was responsible for generating a 100 MHz bandwidth signal that contains the multi-carrier waveform. This waveform normally is adapted for different bandwidths in different experiments, but in general, it consists of 50 or 51 equally spaced carriers. In [8], 50 carriers are spaced 244 kHz apart, beginning at 2.44 MHz, resulting in about 12.2 MHz total bandwidth (see Figure 8).

The transmitter hardware consists of two separate boards as shown in Figure 9, a general-purpose digital controller board (bottom) that was also used on the receiver, and a digital-to-analog conversion board (top). The digital controller board features a Xilinx Virtex-2 FPGA with the required configuration PROM and power supplies. In addition, it has a 64 MB SDRAM, an Ethernet transceiver, and an RS232 interface. A number of FPGA pins are present on pin headers to provide for up to 16 bits of data or 14 bits of data and two clock signals using the low-voltage differential signaling (LVDS) standard to interface to the DAC board.

The digital-to-analog conversion board contains an Analog Devices AD9736 DAC, which is capable of sampling rates of up to 1.2 GSPS with 14 bits of resolution. The DAC receives its sampling clock from either an external clock via an SMA connector or a clock from the digital controller board. The DAC features an LVDS interface, and expects an input of 14 bits of data together with an additional data clock signal from the FPGA. In addition, the DAC can optionally provide a clock signal to the FPGA.

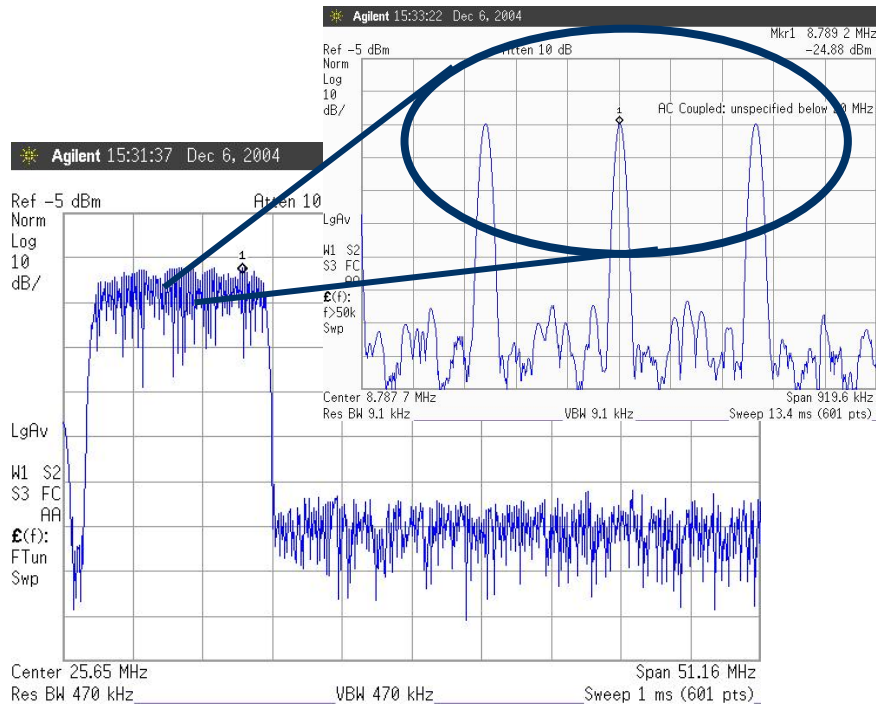


**Figure 8: Multi-Carrier Signal**

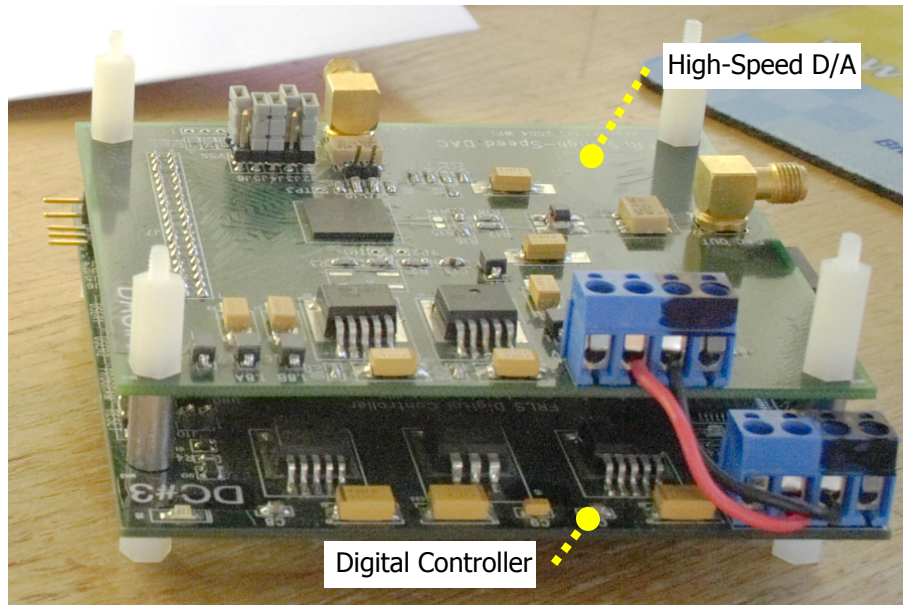


**Figure 9: Previous Digital Waveform Generation Hardware**

The ranging signal generated by these boards consisted of 8192 samples, making up a *symbol*, that were sampled at 200 MSPS, giving a symbol duration of 40.96  $\mu$ s. The samples were stored in the FPGA’s block memory and were provided to the DAC using double data rate (DDR) transfer, in which data is sampled on both the rising and falling clock edge, allowing for a clock frequency of half the data rate. The signal generated by this digital waveform generation system

was passed along to the RF front-end, which upconverted the signal to a center frequency depending on the experimental set-up.

The disadvantage of this previous version of hardware was that it was unnecessarily powerful for a deployable system, because it was intended as a general-purpose platform. For example, the digital controller board contains features such as a large SDRAM and an Ethernet controller, which are not necessary for the final Locator device. Also, the FPGA contains much more logic than is actually needed to generate the waveform (only 1% of its logic resources were actually used, and only 17% of its Block RAM), and the entire design had not been tested for use with higher bandwidths than 100 MHz. In addition, the boards are large and do not show what a final Locator device might look like in terms of size.

Another large disadvantage was that the previous version of the hardware was not optimized in terms of current consumption. The hardware was not designed to enable easy or fast power control, meaning that the boards were powered either completely on or completely off. In addition, as will be shown in a later chapter, supporting multiple Locators requires time-sharing of the transmission of the ranging signal. This means that the Locator should be switched off when it is not needed, both to prevent overlap of two transmitters' signals, and to conserve power. However, the previous design required too much time to power on and off, effectively preventing duty cycling of the hardware and preventing support for multiple transmitters.

One should note that the previous generation of hardware was purely a transmitter for the ranging signal and did not include any provisions for several of the features that have been described as requirements in the previous sections, such as environmental status information, or any other kind of data communication ability that would allow for implementation of a time-sharing scheme. This was one of the reasons for developing a new version of the hardware, with the requirements as set forth in the following section.

## **2.4. Locator Design Requirements**

In late 2005, the existing prototype transmitter and receiver hardware worked well and many tests had been performed with it. However, this hardware had several shortcomings, as described in the previous sections. Therefore, it was decided to develop the new Locator hardware described in this thesis. This section presents the specifications for this new generation of hardware.

It was decided to implement the new Locator hardware subsystems as three separate printed circuit boards. These subsystems, as described in the Introduction and pictured in Figure 10 below, are the Digital Waveform Generation of the ranging signal waveform, the RF transmission of the waveform, and lastly the control of the transmissions and communication of commands and data, which was named the “Data Channel”. The work done for this thesis concerned the digital portions of the Locator, which are the *Digital Waveform Generation* and the *Data Channel* (shaded in figure).

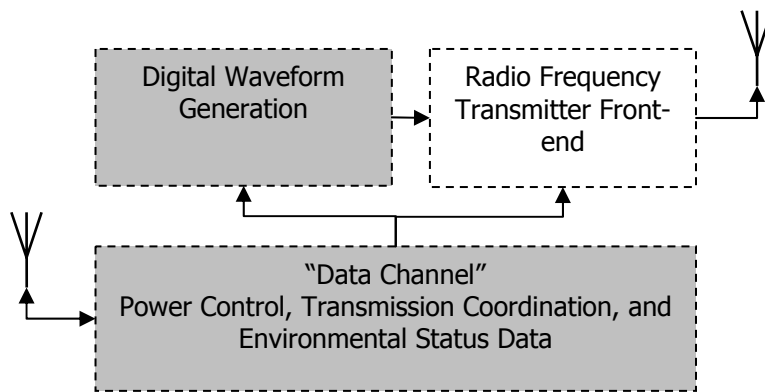


**Figure 10: Overview of Locator Hardware Design**

The separation of the prototype Locator hardware into these subsystems had the advantage of one being able to develop and test each subsystem individually, it allowed the hardware to be modular, and it additionally prevented any errors in one design, such as excessive electrical noise or other faults, from leaking into another board. The PCBs of each subsystem were designed to be small, with the ability to be connected together to best approximate a final Locator design.

For the ranging signal generation by the Digital Waveform Generator, a signal bandwidth of 150 MHz was required in order to generate a signal spanning the new frequency bands granted by the FCC (described as Bands 2 and 3 in Section 2.2), which span from 512 MHz to 698 MHz, with a gap from 608 to 614 MHz. The same number of samples as in previous versions, 8192, was selected, except the signal was now be sampled at the new rate of 300 MSPS. The output levels of the waveform generator were required to be -40 to -50 dBm per subcarrier (but the design should be able to produce more than this) with low spurious levels. The DAC was required to provide for at least 14 bits of resolution and its sampling clock should be generated on-board.

The system had to support up to 100 simultaneous users, giving location updates at least once a second. In addition, the Locators were required to be low-power, consuming as little power as possible when running, to provide detailed power control for individual portions of the circuits, and to have rapid turn-on times for power saving through duty cycle reduction. The system was required be able to operate continually on battery power for at least several (on the order of 6-12) hours. Some additional requirements were that the Locator must be able to measure ambient temperature and detect non-movement of the device, and be able to transmit a user-triggered “distress signal” to the Base Station (via the Reference Units). The minimum communication range was at specified to be least 100 m.

In the following two chapters, we will show how these design requirements were implemented in the Data Channel, followed by the Digital Waveform Generation.



## **Chapter 3. Data Channel and Communication Protocol**

In this chapter, the design process will be presented that addresses the issues of supporting multiple users and gathering and communicating status data, which ultimately led to the development of the Data Channel hardware. The relationship of the Data Channel subsystem to the other hardware in the Locator is shown in Figure 11. First, the theory behind supporting multiple Locator devices will be addressed, followed by possible implementations. This will be narrowed down to the system that was finally implemented, and details on the hardware as well as protocol software will be presented.

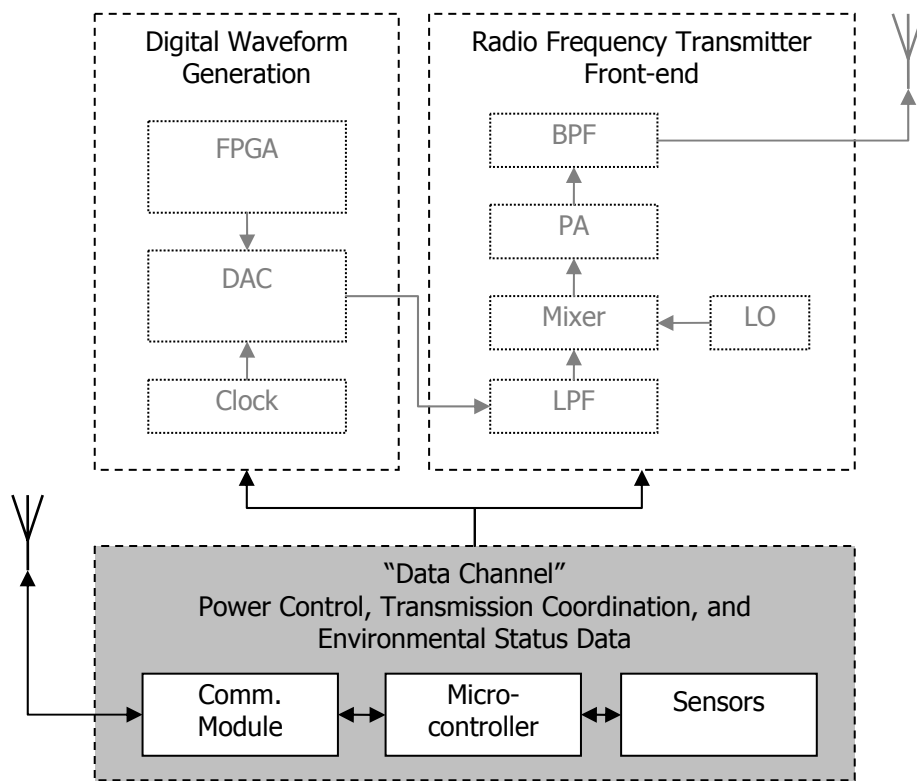
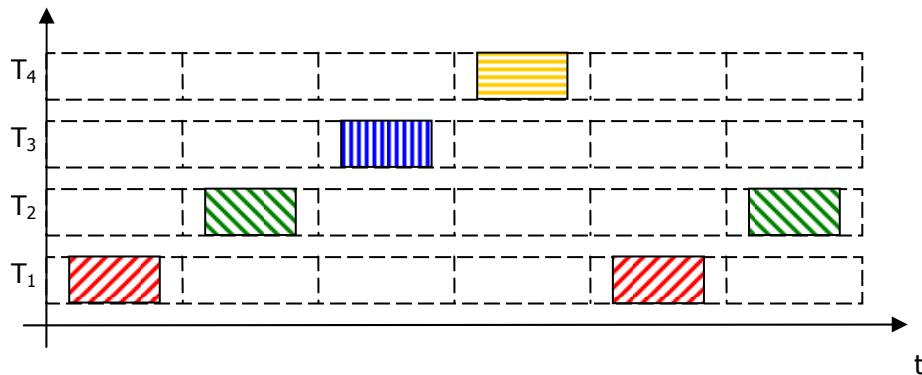


Figure 11: Data Channel as Part of Overall Locator Design

### **3.1. Multi-Transmitter Support**

In order to support multiple users, the PPL system must be able to receive signals from multiple Locators, which in turn means that multiple Locators must be able to operate in parallel. This section discusses the two basic approaches to supporting such parallel operation: frequency-domain multiplexing (FDM) and time-domain multiplexing (TDM). For completeness, we also briefly discuss code-division multiplexing (CDM).

In TDM, the Locators, or simply transmitters (as their main function is to transmit the ranging signal), do not actually transmit in parallel, but a “virtual parallelism” is achieved by having the transmitters transmit for short durations in rapid succession. An overview of this situation with four transmitters,  $T_1$  through  $T_4$ , is shown in Figure 12. The major advantage of this approach is that it is very straightforward to implement, and can be used to conserve power as well, as the transmitter’s duty cycle is much reduced. However, this requires the circuitry to be able to power on and off quickly, otherwise this power-saving advantage disappears. In addition, a trade-off must be made between the minimum time to transmit for each transmitter, number of transmitters in the system, and messaging frequency. This means that this approach may require the active coordination of the transmitters, depending on the restrictions on clock drift, which will be discussed in detail in later sections.



**Figure 12: Time-Division Multiplexing**

In FDM, the different transmitters transmit at different frequencies, allowing for concurrent operation. This is theoretically possible because the PPL signal consists of individual carriers, each of which takes theoretically zero bandwidth. Figure 13 shows two approaches: on the left, the different transmitters’ carriers are consecutive and use completely different frequency bands; on the right, the different transmitters’ carriers are interleaved.

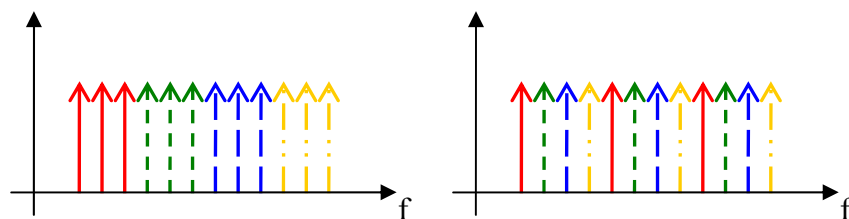


**Figure 13: Frequency-Domain Multiplexing, Bands (left) vs. Interleaving (right)**

The advantage to this approach is that one does not have to worry about turning a transmitter on and off and coordinating between different transmitters, so no control hardware is needed for these tasks. However, there are also several disadvantages. This approach is harder to implement on both the transmitter and receiver: The transmitter has to span a larger number of possible transmission frequencies, while the receiver has the added task of disassembling the received signal into its different transmitter components. Also, and most importantly, implementing such a system for a large number of transmitters (up to 100) with the current waveform (at least 50 carriers) means that five thousand carriers would have to fit in a frequency range limited by the bandwidth of the receiver, which may only be a few hundred MHz. Such tight packing of the waveform carriers may lead to other problems, such as a reduction of the multipath-resistant characteristics of the ranging signal due to the chance of different transmitters interfering with each other (for example through clock drift or harmonics). Hence, it may be that in order to support the targeted number of transmitters (100), the system would have to employ some kind of control hardware to manipulate the transmitted signals to prevent interference, similar to what is needed for TDM, which eliminates this advantage of FDM and raises the question of whether it would not just be simpler to only implement TDM.

A final approach that is used for multiplexing data together is CDM (also known as CDMA, or code-division multiple access), the very basic idea of which is that two transmitters transmit at the same time and on the same frequencies, and only by a special encoding scheme can a receiver recover the data transmitted from each source. One of the disadvantages of this scheme is that the transmit power of each unit must be closely controlled, otherwise one transmitter might “drown out” another. However, the major disadvantage is that for our purposes, it is unacceptable to overlap two different carriers, as this disrupts the phase information that is required for the range estimation. Therefore, it is clear the CDM is useful only for binary data transmission and not for our system.

In conclusion, while FDM may offer advantages for systems with a smaller number of transmitters, it is clear that TDM is the best approach due to its simplicity. The following section investigates this multiplexing method.

### **3.2. Time-Division Multiplexing**

In time-division multiplexing, it is clear that the transmitter’s emissions must be controlled so that no two transmitter’s transmissions overlap. For example, the system

specifications state that 100 transmitters should be able to provide location updates once a second, so each transmitter has only 10 ms to transmit. In this section, we will verify that TDM is indeed feasible in this situation, and then discuss different schemes that allow this kind of control.

We will verify that our goal of multiplexing 100 transmitter units to provide updates once a second is realistic, considering that each transmitter only has 10 ms to transmit. There are several factors to keep in mind: whether this time allows for enough of the ranging waveform to be transmitted, how much data can be transmitted during this time (assuming some kind of data communication is taking place), and whether this provides a tight enough resolution for tracking.

The current signal consists of “symbols” of 8192 samples, sampled at 200 MSPS, which gives a symbol period of 40.96  $\mu$ s. This allows for 244 symbols to be transmitted in a 10 ms period. Although the capture of a single symbol is sufficient for range estimation, multiple symbols can be “time fused” to provide better SNR: each doubling of the number of symbols gives a SNR boost of about 3 dB. However, one must keep in mind that clock drift might cause transmitters to drift, which means a guard time should be implemented in the beginning and end of the 10 ms period – this will be discussed in detail in the following section. Therefore, while a balance between the number of symbols transmitted and the required guard time has to be found, we can assume that 10 ms is sufficient time to transmit a ranging signal.

Assuming that some kind of data communication other than the transmitters’ ranging signal waveforms is implemented, we can quickly calculate that at a relatively slow baud rate of 19.2 kbits/second, 24 bytes could be transferred in a 10 ms period. For a simple control/command protocol, this may be sufficient, but may not be if larger amounts of data needed to be transferred. This issue will be discussed in more detail in a later section, but one can see that this time period does allow for a transfer of a small amount of data.

Finally, we would like to know what resolution an update rate of once per second gives. A human walks at a normal rate of about 1.2 m/s [15] (for reference, the fastest human running speed is about 10 m/s [10], while a human falling at terminal velocity is about 60 m/s [9]), and we can assume that a firefighter who is loaded down by heavy gear may not walk as quickly. In addition, firefighters often crawl along the floor, below any smoke that may be in the air, further reducing their rate of movement. So, we can see that a position update of once per second should give a resolution of better than one meter. In addition, we can imagine that a future system might be able to dynamically adjust the number of updates per second depending on the actual number

of users that require accurate tracking. This would mean that certain users' positions (such as those who are outside the building or who are not moving often) could be updated less frequently, resulting in a higher resolution for other users. Similar variations on this scheme to further increase accuracy could also be implemented, but in general, a tracking resolution of typically better than one meter is on the order of the overall system accuracy and is therefore sufficient.

We must now discuss methods with which to implement a TDM scheme. There are many medium access control schemes in existence for communications on shared mediums, such as ALOHA, Slotted Time (with beacons or shared clocks), Carrier Sense Multiple Access (CSMA) with Collision Avoidance or Detection, Bit-Map or Binary Countdown protocols, and so on [25]. Current widely used communications standards such as Wireless LAN (802.11 [12]), Bluetooth (802.15.1 [5]) or ZigBee (802.15.4 [33]) all use variations of the previously listed medium access control methods. However, these protocols all have one thing in common that make them unsuited for direct application to the current system: they assume that every station is a transceiver, or at the very least a transmitter with the capability to detect communications or collisions on the medium.

The previous generation of transmitter/receiver hardware allowed only for one-way communication. The multi-carrier waveforms were generated on the transmitter by feeding data from a static memory inside an FPGA into a DAC, and on the receiver end, the waveforms were digitized by an ADC and FPGA and transferred to a MATLAB script to extract the range information. This means that modulating or in any way actively manipulating the generated waveform on the transmitter side would involve complex calculations and therefore complex hardware on the transmitter FPGA. Another issue is the power question: the transmitter chain of FPGA plus DAC plus RF front-end consumed on the order of many hundred milliamps, and constantly running this system would require a large battery or the run time would be reduced to unacceptably. Similarly, the receivers in this system required a large amount of hardware (RF front-end, ADC, etc.) that make it unfeasible to add receiver hardware to each transmitter. Therefore, it is clear that the previous version of transmitter hardware was only fitting to generate a ranging signal waveform and not for bi-directional or data communication.

Therefore, in the following two sections, we will investigate the question of how a system in which the transmitters have no receive capability might function.

### 3.3. Free-Running Transmitter Calculations

We seek to investigate an “open-loop” system where the transmitters do not have any form of receive capability. Therefore, the transmitters will have free-running clocks with only the possibility of synchronization through some kind of physical connection with a base station. In this kind of a system, the issue of clock drift becomes crucial, because it defines how much time it takes for this system to fail. In this section, we will delve into some more detail on the TDM system, and then derive a “time until failure” equation for this scheme, and show some calculation examples.

In a TDM system, time is divided into “time slots”, with each slot having a guard time at its beginning and end to allow for some amount of clock drift. This system will fail when clock drift causes transmissions to drift over the bounds of the guard time and to overlap. In the worst case, if  $n$  transmitters are at the upper and lower bounds of their frequency range given by their ppm rating  $ppm$ , and they make an update every  $t_u$  seconds consisting of  $s$  symbols (each symbol being of duration  $t_d$ ), we shall derive the worst-case time until failure  $t_f$ . Figure 14 shows an overview of this situation using four transmitters as an example, and Table 2 shows the symbols used for these calculations.

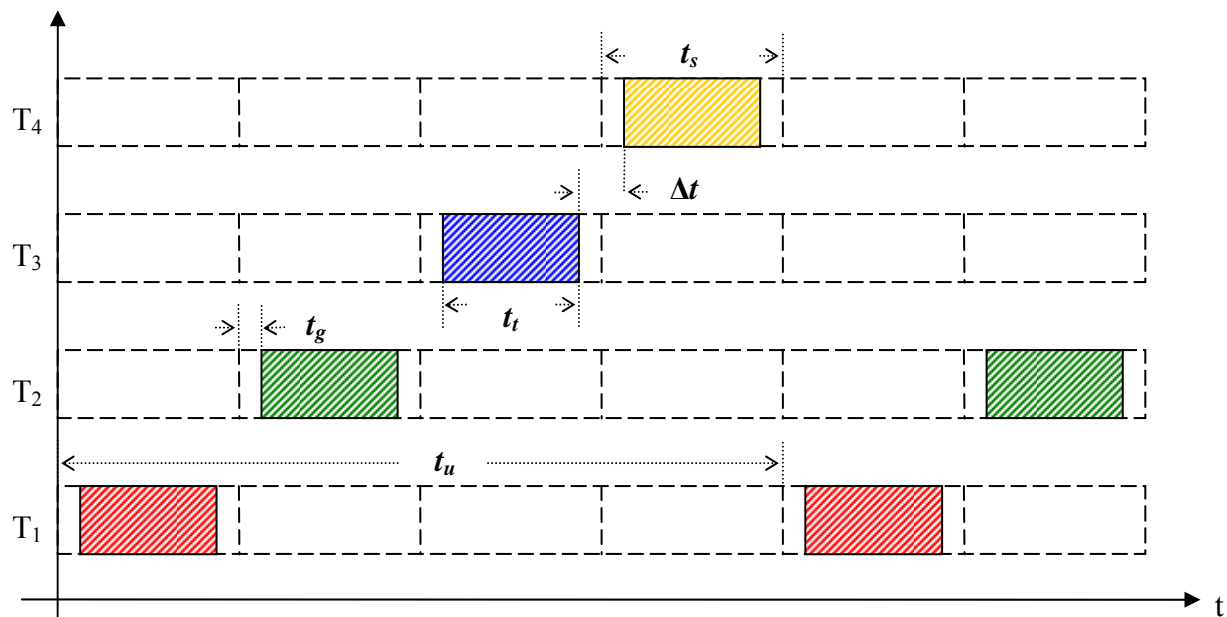


Figure 14: TDM Overview

Symbol	Description	Notes & Relationships
$n$	Number of Transmitters	
$s$	Symbols per Transmission	$s \geq 1$
$t_d$	Symbol Duration	Currently: 8192 samples at 200 MSPS gives 40.96 $\mu$ s symbol duration
$t_u$	Update Period	(see Figure 14) updates per second = $1/t_u$
$ppm$	Crystal ppm Rating	Example: A 50 ppm crystal is $ppm = 50 \times 10^{-6}$
$t_s$	Time Slot	(see Figure 14) $t_s = \frac{t_u}{n}$
$t_g$	Guard Time	(see Figure 14)
$t_t$	Transmit Time	(see Figure 14) $t_t = t_d \cdot s = t_s - 2 \cdot t_g$
$\Delta t$	Time Between Transmissions	(see Figure 14) $\Delta t = 2 \cdot t_g$

Table 2: Symbols Used

We should note that throughout this analysis we ignore the propagation delay of signals through the air. The propagation delay of a radio signal through air is the distance traveled divided by  $c$ , the speed of light (299792458 m/s). The propagation delay over 1 m is therefore 3.3356 ns and 333.56 ns over 100 m. Because the guard times we will consider below are higher than this by several orders of magnitude, this delay is negligible for our applications.

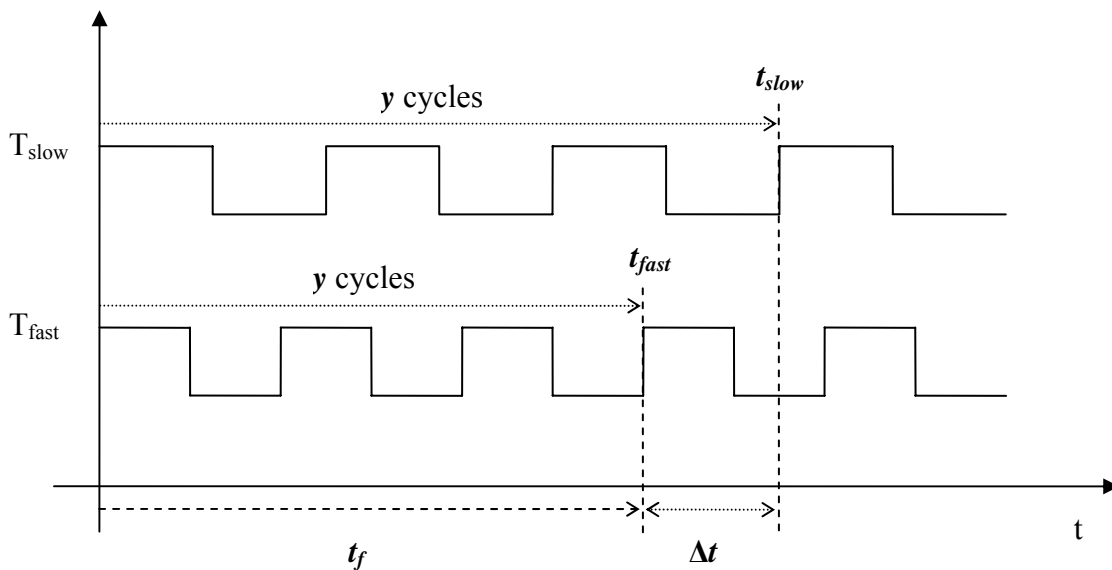


Figure 15: Clock Drift

We will investigate two transmitters whose clocks are at the lower and higher end of their allowable frequency range as given by their ppm rating, as shown in Figure 15. In other words, given a nominal frequency of  $f_0$  and a frequency range  $\pm \Delta f = \pm f_0 \cdot ppm$ , the “slow”

transmitter's ( $T_{slow}$ ) clock frequency is  $f_{slow} = f_0 - \Delta f$  and the "fast" transmitter's ( $T_{fast}$ ) clock frequency is  $f_{fast} = f_0 + \Delta f$ .

After  $y$  clock cycles,  $T_{slow}$  and  $T_{fast}$  will "think" they are at the same point in time, however their actual times (the times at which they actually complete  $y$  clock cycles) are, respectively,  $t_{slow} = \frac{y}{f_0 - \Delta f}$  and  $t_{fast} = \frac{y}{f_0 + \Delta f}$ . We are interested in the point in time when the difference in these two times,  $\Delta t = t_{slow} - t_{fast}$ , grows too large, because at this time the guard time will be overstepped and transmissions will begin to overlap. Since the "fast" transmitter will cause an error (overlapping transmission) first, this point in time is  $t_{fast}$ , and we shall call this the time until failure,  $t_f$ .

Using the above information, we derive  $t_f$  as follows. First, we will combine the above equations for the difference in the two clocks:

$$\Delta t = \frac{y}{f_0 - f_0 \cdot ppm} - \frac{y}{f_0 + f_0 \cdot ppm}$$

Solving  $t_f = t_{fast} = \frac{y}{f_0 + f_0 \cdot ppm}$  for  $y$  and substituting:

$$\Delta t = \frac{t_f \cdot (f_0 + f_0 \cdot ppm)}{f_0 - f_0 \cdot ppm} - \frac{t_f \cdot (f_0 + f_0 \cdot ppm)}{f_0 + f_0 \cdot ppm}$$

Simplifying and solving for  $t_f$ :

$$t_f = \Delta t \cdot \frac{1 - ppm}{2 \cdot ppm} \quad \text{Equation 1}$$

Now we would like to express this time until failure in terms of the system parameters  $ppm$ ,  $n$ ,  $s$ ,  $t_d$ , and  $t_u$  (see Table 2). We can derive an expression for  $\Delta t$  using the relationships given in Table 2 as follows:

Solving  $t_d \cdot s = t_s - 2 \cdot t_g$  for  $2 \cdot t_g$  and substituting into  $\Delta t = 2 \cdot t_g$ :

$$\Delta t = t_s - t_d \cdot s$$

Substituting the given equation for  $t_s$ :

$$\Delta t = \frac{1}{n} \cdot t_u - t_d \cdot s$$

Finally, inserting this into the above equation for  $t_f$ :



$$t_f = \left( \frac{1}{n} \cdot t_u - t_d \cdot s \right) \cdot \frac{1 - ppm}{2 \cdot ppm} \quad \text{Equation 2}$$

We can now use this formula to calculate some sample failure times for different system configurations. For example, we can see how different crystals and a different number of updates per second and/or number of users (transmitters) affect failure times; this is shown in Table 3. The crystal ppm rating  $ppm$  is varied over the rows while the number of updates per second multiplied by the number of transmitters (i.e.  $n / t_u$ ) is varied over the columns of the table. Note that currently, we use 50 ppm crystals as the default for these calculations, however we assume that down to 10 ppm crystals can be used at an acceptable price. Similarly, Figure 16 shows a plot of the failure times for smaller numbers of  $n / t_u$ . The number of symbols is fixed at  $s = 1$ . Note that varying this parameter does not affect these calculations by a significant amount, however at a higher number of transmitters and/or updates per second, it may not be possible to transmit a larger number of symbols ( $\sim 256$ ) per time slot and a smaller number of symbols must be used ( $\sim 16$ ).

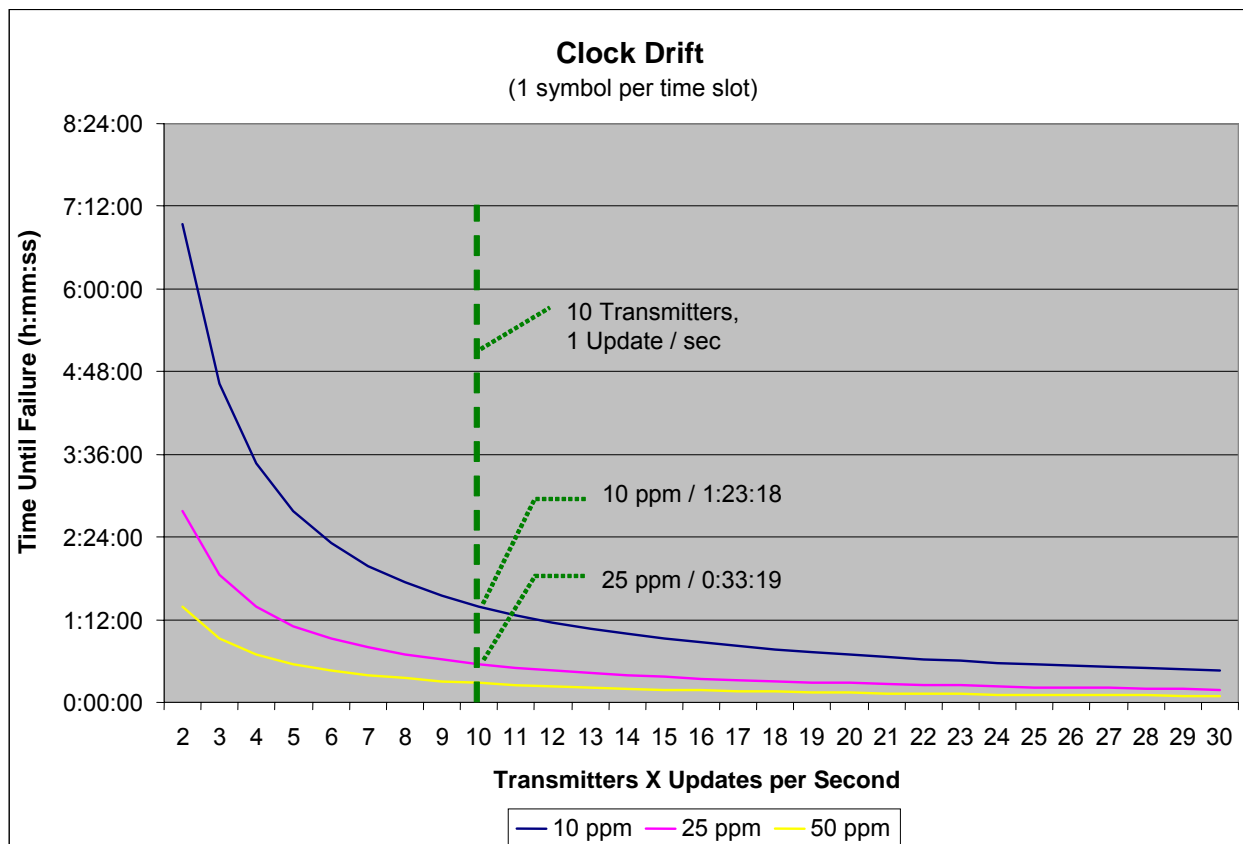


Figure 16: Sample Failure Times

Tx's x Upd / s	2	5	10	25	50	100	250	500	1000
<b>10 ppm</b>	6:56:38	2:46:38	1:23:18	0:33:18	0:16:38	0:08:18	0:03:18	0:01:38	0:00:48
<b>25 ppm</b>	2:46:39	1:06:39	0:33:19	0:13:19	0:06:39	0:03:19	0:01:19	0:00:39	0:00:19
<b>50 ppm</b>	1:23:19	0:33:19	0:16:40	0:06:40	0:03:20	0:01:40	0:00:40	0:00:20	0:00:10
<b>100 ppm</b>	0:41:40	0:16:40	0:08:20	0:03:20	0:01:40	0:00:50	0:00:20	0:00:10	0:00:05

Table 3: Sample Failure Times (h:mm:ss)

To learn what ppm ratings would be required to enable the system to run for a certain amount of time, the above equation can be solved for  $ppm$ . Table 4 shows some sample systems and the required crystal ppm rating. It shows five different system configurations that may be likely to be used in different situations such as an actual production system (System 3), a system with lower update frequency (i.e. no tracking; System 4), and systems that may be used during demonstration and testing (Systems 1, 2, and 5).

Parameters	Sys. 1	Sys. 2	Sys. 3	Sys. 4	Sys. 5
Number of Transmitters ( $n$ )	10	10	100	100	3
Update Period ( $t_u$ )	1 sec	10 sec	1 sec	60 sec	1 sec
Symbols per Transmission ( $s$ )	256	256	16	256	256
<b>Calculations</b>	-	-	-	-	-
Time Until Failure ( $t_f$ ) for 50 ppm	15 min	2.8 hr	1.6 min	1.6 hr	54 min
<b>Required ppm Ratings</b>	-	-	-	-	-
1 hour	12	137	1.3	81	45
6 hours	2	23	0.2	13	8
24 hours	0.5	6	0.05	3	2

Table 4: Required Frequency Stability for Specific Failure Times

We can see from these results that in any case, a long system run time is only achievable through a very high-quality crystal. In addition, a system with no feedback other than the ranging signal transmissions is vulnerable to failure in case any one unit loses its synchronization through some kind of software or hardware fault. Therefore, we wish to investigate a system that would not suffer from such a problem.

### 3.4. Random Transmissions

A radically different approach to a time-multiplexed system is one where the transmitters do not attempt to stay synchronized at all. In other words, the transmitters choose a random time within their update period at which to transmit. To be able to perform calculations, a simplified model is used where the update period  $t_u$  is divided into  $N$  slots, each slot having the duration of a transmission (i.e. no guard time). Note that this section re-uses several symbols from Table 2 in Section 3.3. We will derive the probability  $p_a$  that none of the  $n$  transmissions will overlap in one

update period. In order to calculate the probability that a certain number of transmitters will be successful in one update period, simulations were performed and the results are given below.

For simplicity, these calculations will assume that the update period is divided into discrete “slots” of length  $t_t$ , making the calculations possible in discrete time. This situation is pictured in Figure 17. Note that this definition of “slot” is slightly different as compared to the previous sections, as these time slots do not include a guard time at the beginning and end of each slot.

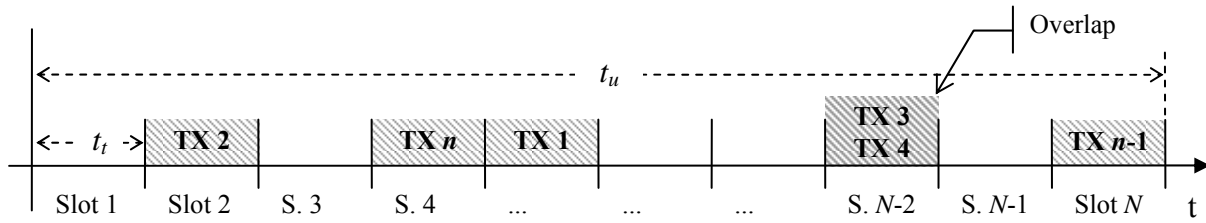


Figure 17: Random Transmission Scheme

Each transmitter would need to encode a unique ID into its transmitted signal so that the receiver can tell the different transmissions apart. This could be accomplished by encoding the transmitter ID into the transmitted waveform via a kind of OFDM modulation, or a separate data channel could be used to communicate the transmitter’s ID (more discussion on both these methods will be given in following sections).

If we make the assumption that a receiver can detect when multi-symbol transmissions have overlapped partially, and that the receiver can use only the non-overlapping part of each transmission for its calculations, then the above “slots” assumption can still be used when a transmission drifts partially into an adjacent slot that contains another transmission. Hence, we can simplify the state of transmissions as being either completely overlapping (or so closely overlapping that they cannot be recovered), or non-overlapping (or partially overlapping, so that they can be recovered), and the “slots” assumption holds. For this reason, compression or expansion of the update period  $t_u$  of each individual transmitter due to clock drift is ignored in these calculations.

We will now derive the probability  $p_a$  that none of the  $n$  transmissions will overlap in one update period. As stated above, the update period  $t_u$  is divided into  $N$  slots of length  $t_t$ , so the

number of slots is given by  $N = \left\lfloor \frac{t_u}{t_t} \right\rfloor = \left\lfloor \frac{t_u}{s \cdot t_d} \right\rfloor$ . During the update period, each of the  $n$

transmissions fills exactly one slot, and these transmissions are uniformly distributed over the  $N$  slots. Two questions can be asked: First, what is the probability that, for each transmitter's transmission, no other transmissions will fall in that same slot, and second, what is the probability that there will be no two transmissions in the same slot during an update period? This is very similar to the "Birthday Pairing" problem in [19] (Example 2-20, pp. 39), and the derivation is as follows:

For one transmission, there are  $N - 1$  slots for other transmissions, so for each of those  $n - 1$  other transmissions the probability of falling in those other slots is  $(N - 1) / N$ . Therefore, the probability that none of those other transmissions will fall in the same slot as this transmission is  $p_s = \left(1 - \frac{1}{N}\right)^{n-1}$ . Note that this does not address the question of whether or not the other transmissions will overlap; this will be addressed below. However, we can use this probability to show that in subsequent update periods, the chance of one transmitter being repeatedly overlapped becomes very low. The chance that a specific transmitter's transmission is overlapped by at least one other transmission is the inverse of the above event, i.e.  $1 - p_s$ . The chance that this happens in  $k$  subsequent update periods is  $(1 - p_s)^k$ . In the situation of 100 transmitters updating with 16 symbols once a second, we see that the probability of one transmitter being overlapped is 6.3%. In the following three update periods, we see that this probability drops to 0.4%, 0.03% and 0.002% respectively; showing that for one transmission to be corrupted repeatedly becomes very unlikely.

The second question that can be asked is, what is the probability that no two of  $n$  independent transmissions will fall into the same of  $N$  slots? There are a total of  $N^n$  ways of arranging  $n$  transmissions into  $N$  slots. However, if we take overlap into account, then the first transmission has a choice of  $N$  slots, while the second transmission has a choice of  $N - 1$  slots, the third  $N - 2$ , and so on, up to  $N - n + 1$  slots for the last transmission. This gives a probability that no two transmissions will overlap of:

$$p_a = \frac{N \cdot (N - 1) \cdot \dots \cdot (N - n + 1)}{N^n} = \prod_{k=1}^{n-1} \left(1 - \frac{k}{N}\right) \quad \text{Equation 3}$$

While  $p_a$  analytically gives the probability that none of the transmissions will overlap (and this analytical result is confirmed by simulations, as will be shown below), we may wish to learn what the probability that most (say, 90%) of the transmissions in one update period will not

overlap with others. In order to calculate these numbers, the following simulations were performed.

Since it is very impractical to calculate all the ways  $n$  transmissions can be arranged into  $N$  slots (there are  $N^n$  possible arrangements), we must approximate such calculations by randomly assigning  $n$  transmissions into  $N$  slots a large number of times (in these simulations 1,000 to 100,000 times) and drawing our statistics from these samples.

The computer model used is an  $N$ -element array to represent the “slots”, with  $n$  “transmissions” randomly assigned to elements of the array. Each of the slots begins at a count of zero and is incremented when a transmission falls into that slot, allowing for overlapping transmissions. This set-up can be visualized as in Figure 17. This assignment is performed (“run”) a large number of times, and each time the number of slots that contain exactly one transmission is counted as the “number of successful transmissions”. Over the large number of runs, statistics on how many transmissions are successful can be calculated.

To verify these simulations, a small number of slots and transmitters were chosen to be able to accurately calculate the above statistics for all  $N^n$  arrangements. If one chooses  $N = 6$  and  $n = 5$ , one can visualize this as five dice being thrown, with each die representing a transmitter and the number it shows as being the slot that the transmitter has chosen. There are  $N^n = 7776$  ways to arrange the transmissions into the slots.

Table 5 shows the results of the accurate calculations and the simulations. Clearly the simulation results (acquired over 100,000 runs) match well with the calculations. Note that if one wishes to know, for example, the probability that “three or more transmitters succeed”, one must sum the probability of three, four and five successful transmissions (i.e.  $0.463 + 0 + 0.0926 = 0.556$ ). Also, note that the probability that all transmitters succeed matches exactly with the analytical result for this system,  $p_a = 0.0926$ . (This match was checked and held true for all systems investigated.)

<b>Successful Transmissions</b>	<b>Calculated Probability</b>	<b>Simulated Probability</b>
0	0.0394	0.0388
1	0.251	0.251
2	0.154	0.156
3	0.463	0.461
4	0	0
5	0.0926	0.0942

**Table 5: Simulation Verification Results**

Table 6 shows some sample calculations and simulations of the above probabilities for more realistic systems (the same systems as in Table 4 in Section 3.3). All simulations had 100,000 runs.

<b>Parameters</b>	<b>Sys. 1</b>	<b>Sys. 2</b>	<b>Sys. 3</b>	<b>Sys. 4</b>	<b>Sys. 5</b>
Number of Transmitters ( $n$ )	10	10	100	100	3
Update Period ( $t_u$ )	1 sec	10 sec	1 sec	60 sec	1 sec
Symbols per Transmission ( $s$ )	256	256	16	256	256
<b>Calculations</b>	-	-	-	-	-
Number of Slots ( $N$ )	95	953	1525	5722	95
All transmitters succeed ( $p_a$ )	0.612	0.954	0.0362	0.419	0.969
90% of transmitters succeed (simulation)	0.614	0.954	0.908	0.9998	0.969

**Table 6: Sample Probability Calculations**

### **3.4.1. Conclusions**

Using the argumentation from Sections 3.3 and 3.4, several conclusions were drawn that reflected on the design of the Data Channel. The calculations above showed that a system where the transmitters have no receive capability may be practical depending on the requirements for the number of transmitters and number of updates per second.

For a TDM-type system where transmitters attempt to stay synchronized, the calculations show that – unless we are able to use very high-accuracy oscillators – the system would be unfeasible. Also, there are some practical issues that need to be considered, such as how any synchronization would take place: the transmitters would need to be physically connected to a central unit, which is impractical at the scene of an incident, so the system would need to run for a long time without failing and synchronization could take place – for example – when recharging the transmitters. Even if one assumes that synchronization could take place at the scene of an incident, one needs to consider that firefighters may be trapped in a building for a long period of time, and the ability to rescue them should not be impaired over time. Therefore, it makes sense to consider the case of random transmissions.

If we assume that clock drift does not affect the performance of the random transmission scheme significantly and the update period is fixed, then the transmitters would not need to be synchronized at all. In this case, the question is “how well” the system performs, i.e. how many transmissions make it through successfully, which depends only on the number of transmitters and the number of transmissions per second. One can consider the following scenarios as examples.

In a live demonstration version of the system, it would be desirable to have a fairly high update rate (once per second), but a large number of transmitters would not be required. In this case, the calculations show that it seems feasible to have free-running transmitters.

For a production-level system, a higher number of transmitters is required (100). The calculations show that a system with a high number of updates (once per second) would not perform very well. The possibility exists of offering a lower-cost version with, for example, a lower number of updates (such as every 60 seconds), but this does not meet the production level system requirements of providing real-time tracking of Locator units. In any case, the random transmission scheme would always involve some transmissions colliding.

From these arguments, it became clear that to be able to coordinate a large number of transmitters and updates per second, only a system where the transmitters can be coordinated wirelessly in some kind of TDM scheme gives a high reliability. There are several advantages to designing transmitters with added receiver or transceiver capability, including the fact that such a capability could always be dropped later to offer a lower-cost and lower-performance version of the system as discussed above.

Other advantages of such a system are, for example, that a higher level of control is possible over the transmitters. Transmitters could be turned off remotely to conserve power when not at the scene of an incident, and the number of updates per second and number of transmitters could be reconfigured on-the-fly. Transmitters would not need to encode a unique ID into their transmitted signal and receivers would not need to be able to detect overlapping transmissions. In addition, other data could be transmitted over the extra communication channel, such as device status or environment or physiological information.

It was clear from these arguments that the realization of the Data Channel was justified. In the following sections, we will discuss the implementation of the Data Channel.

### **3.5. Bi-Directional Communication**

As we can see from the previous sections, in order to achieve the full functionality of the Locator units, a system capable of communicating on a channel separate from the ranging waveforms had to be designed. First, the option of a “receive only” functionality on the Locator units was investigated, which would reduce the cost of the units. Then, both standardized and custom different bi-directional communications systems were investigated. This section discusses these design decisions.

In order to keep the Locator units simple and therefore cheaper, we can imagine a system where each Locator unit is equipped only with a transmitter for the ranging signals and a receiver for the command and control communications. While such a system would provide enough functionality for basic TDM operation and power control, there would be no direct way for the Locator to relay data back to the Base Station, such as status information or at the very least a device ID. However, this information could theoretically be “piggybacked” onto the transmitted ranging waveform. Since the ranging signal follows a traditional OFDM structure, data could be modulated onto this signal (a common technique in communications systems). However, it is clear that adding a system that modulates the transmitted ranging waveform would add a relatively large amount of complexity, as compared to simply giving the Locators a separate, bi-directional communications channel via a separate transceiver module, as we will see below.

There are several existing, widely used communications standards that were briefly considered. Wi-Fi (IEEE 802.11, [12]) has an average (indoor) range of about 30 m, and latencies in the tens of ms [4, 14]. Bluetooth (IEEE 802.15.1, [5]) is a protocol for “personal area networks”, and with a maximum output power of 100 mW, can theoretically cover distances of 100 m. However, one of the downsides of both these communications standards is that they require relatively large protocol stacks and are in most cases not suitable for prototype implementation. Finally, ZigBee (IEEE 802.15.4, [33]) is a relatively new protocol for close-range communications (10-75 m), which may not be enough for our purposes. In addition, at the time this system was being designed, there was not yet a wide selection of ZigBee transceivers and stack implementations available, indicating that the technology might not be mature yet.

For our applications, it seemed that using these existing communications standards would be “overkill”, so simpler transceiver IC’s and modules were investigated. A broad search of different vendors’ offerings showed that there are several similar products available that operate in the license-free 433 MHz and/or 900 MHz bands. Table 7 shows a summary of the most promising modules.

The ChipCon CC1100 seemed the most advanced of the chips as it supports internal buffers, automatic generation of checksums, automatic receive polling, received signal strength indicator (RSSI), and a standardized SPI interface to communicate with the chip. However, the maximum transmit power it supports is 10 dBm, and there was concern that this would not be able to cover enough distance. Initial tests with evaluation boards showed that the coverage from



a vehicle parked outside a large building (such as Atwater Kent Laboratories at WPI) may not be able to cover the full building (a range of about 100m).

Product	Freq. Range (MHz)	Data Rate	Output Power	Receiver Sens.	Interface	Notes
ChipCon CC1020	402-408, 804-940	153.6 kbps	-20 to 10 dBm	-118 dBm	Sync. Digital	
ChipCon CC1100	300-348, 400-464, 800-928	500 kbit/s	-30 to 10 dBm	-110 dBm	SPI & Others	with buffers, CRC, etc.
Atmel AT86RF211S	400-480, 800-950	100 kbps	15 dBm	-107 dBm	Sync. Digital	better documentation than ChipCon
Xemics DP1205	868-870, 902-928	152.3 kbit/s	15 dBm	-113 dBm	Sync. Digital	Complete module with external components
Micrel MICRF505	850-950	200 kbps	10 dBm	-97 dBm	Sync. Digital	

**Table 7: Transceiver Modules**

There are two transceivers with a higher output power than the ChipCon transceivers, and one of these, the Xemics DP1205, stood out because it is a complete solution in a small, shielded module that includes the Xemics XE1205 transceiver IC and all necessary passive components. It does not support all the advanced features of the CC1100, but still includes a smaller buffer (16-byte, vs. 64-byte buffer in the CC1100) for burst transmissions and support for automatic transmission detection and synchronization with the incoming bit stream. While this module is not as advanced as the ChipCon variant, it supports all the basic necessary features and supports a higher output power, so it was decided that this module should be used in the design.

### **3.6. Hardware Specifications**

The Data Channel Hardware development began in late 2005. At the time, a functioning TDM control hardware was required to be completed for a demonstration of a multi-transmitter system in mid-2006, so outside contractors were hired to speed the development and design the details of the Data Channel hardware and provide basic firmware. This section describes the specifications for the PPL Data Channel hardware that were used to develop the new hardware. Figure 18 shows a conceptual block diagram of the transmitter as it existed at the time (before the development of the new Digital Waveform Generator hardware also described in this thesis) and the proposed Data Channel hardware.

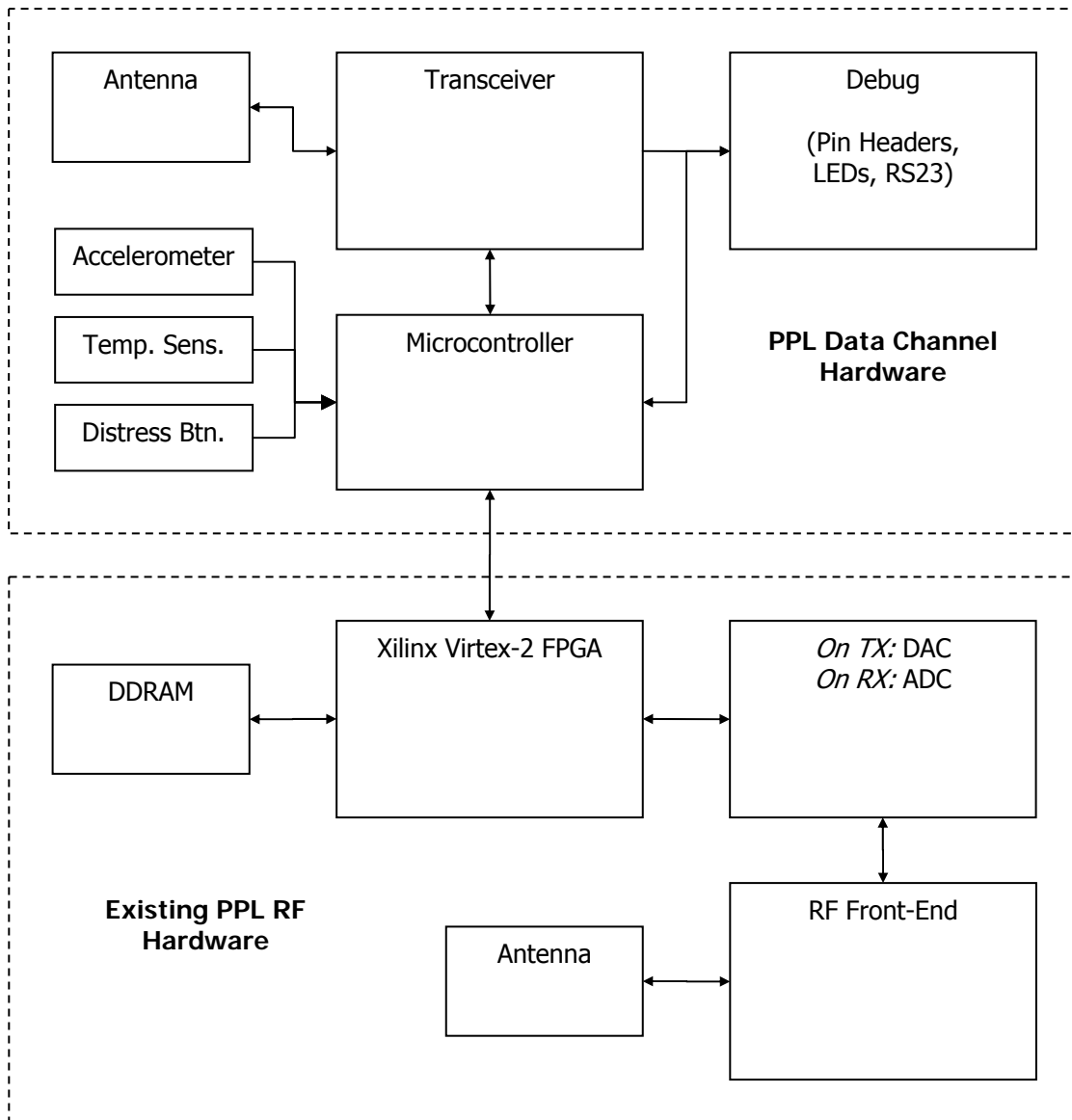


Figure 18: General Locator Block Diagram

Several decisions on details of the design were made before the final specifications were established. The most important of these was the selection of the TI MSP430 microcontroller family as the microcontroller in the system. This decision was made because the MSP430F161x family is a very low-power microcontroller that had been used in previous, similar designs. The following is a list of the specifications for the Data Channel hardware.

- **Conceptual Tasks**

- Coordinate and control TDM of Locator transmissions
- Manage power of entire Locator device
- Monitor and communicate “environmental data” (movement, temperature, distress button)

- **PCB Layout**

- System should fit on a PCB with dimensions of 2.5 x 3 inches.
- Mounting holes must be compatible with existing boards.

- **Power**

- System should include a low-power voltage regulator that provides 3.3 V to power the entire Data Channel hardware.
- System should have the capability of being powered from a DC power supply or conventional batteries (AA/AAA).
- The components in this system must either be low-power (<1mA), have the ability to be put into a low-power “sleep mode”, or to be powered off in some other fashion.

- **Wireless**

- System must support wireless communication with a Xemics DP1205 module.
- Minimum Range: 100m indoors
- Minimum Data Rate: approx. 10 kbps
- Must be FCC compliant and support Frequency Hopping Spread Spectrum (FHSS)
- Interface of transceiver must provide for low-latency communications – i.e. interrupts generated on reception of packets and streaming data output

- **Microcontroller**

- System must include Texas Instruments MSP430F1611 microcontroller
- Must include JTAG interface for programming

- **Accelerometer**

- System must include an accelerometer to detect non-movement of device
- Accelerometer should be at least two-axis for better general movement measurement

- **Distress Button**
  - System must include a pushbutton connected to the microcontroller (to trigger transmission of a distress signal)
  - Suggested to connect to a microcontroller port capable of generating interrupts (MSP430 ports P1 and P2)
- **Temperature Sensor**
  - System must be able to measure ambient temperature
- **Interface**
  - System must be able to interface to existing hardware (operates at 3.3 V)
  - Several pin headers (about 16) connected to microcontroller ports required; suggested: MSP430 ports P1 and P4. These pin headers should be laid out as groups of eight pin headers with a ground connection at each end (ten pins to a row).
  - System must have a way to configure a board ID (such as through a rotary DIP switch), can be shared with microcontroller ports
- **Debugging**
  - System must provide RS232 interface
  - System must provide test points, pin headers and status LEDs
  - Suggested to include an additional pushbutton for user input
- **Firmware**
  - Code must be written in C, compatible with IAR compiler
  - Low-level drivers for interfacing to the Xemics DP1205 and the Accelerometer will be provided.

Figure 19 shows a block diagram that represents many of these specifications, and shows how the components of the Data Channel system were connected. Note that in addition to the items listed here, a simple graphical user interface (GUI) on a PC for test and debug of the units was implemented.

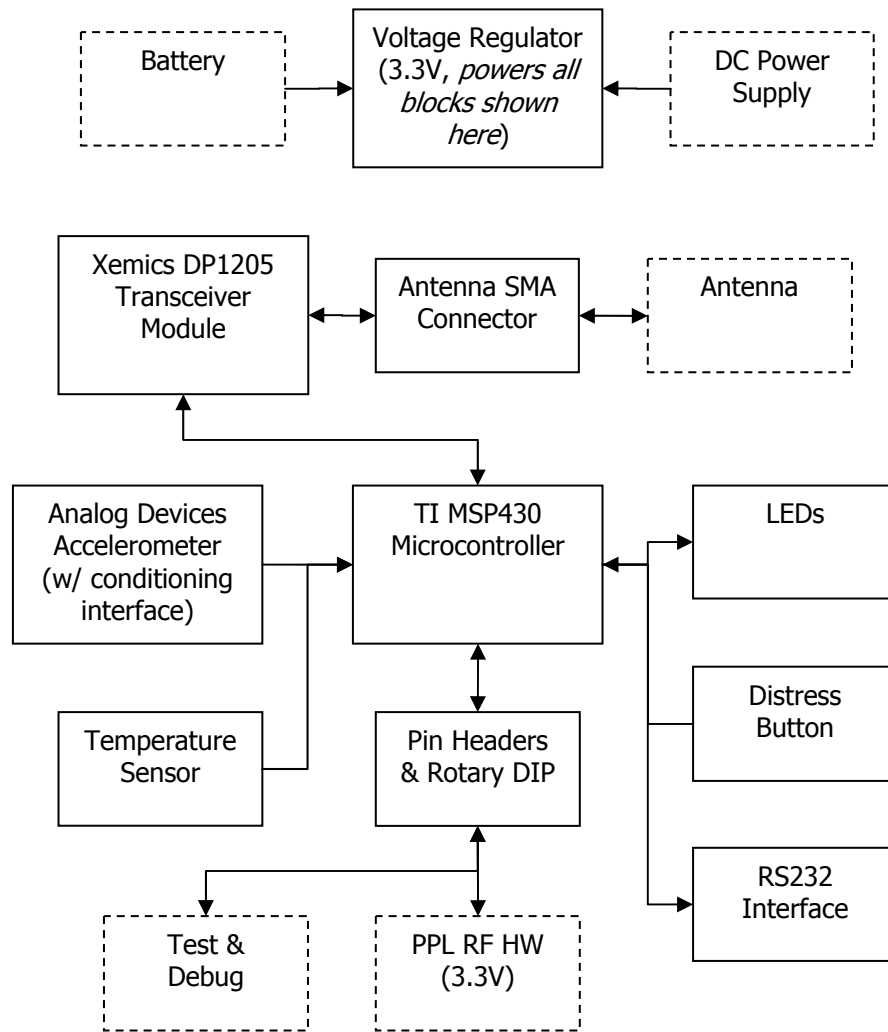
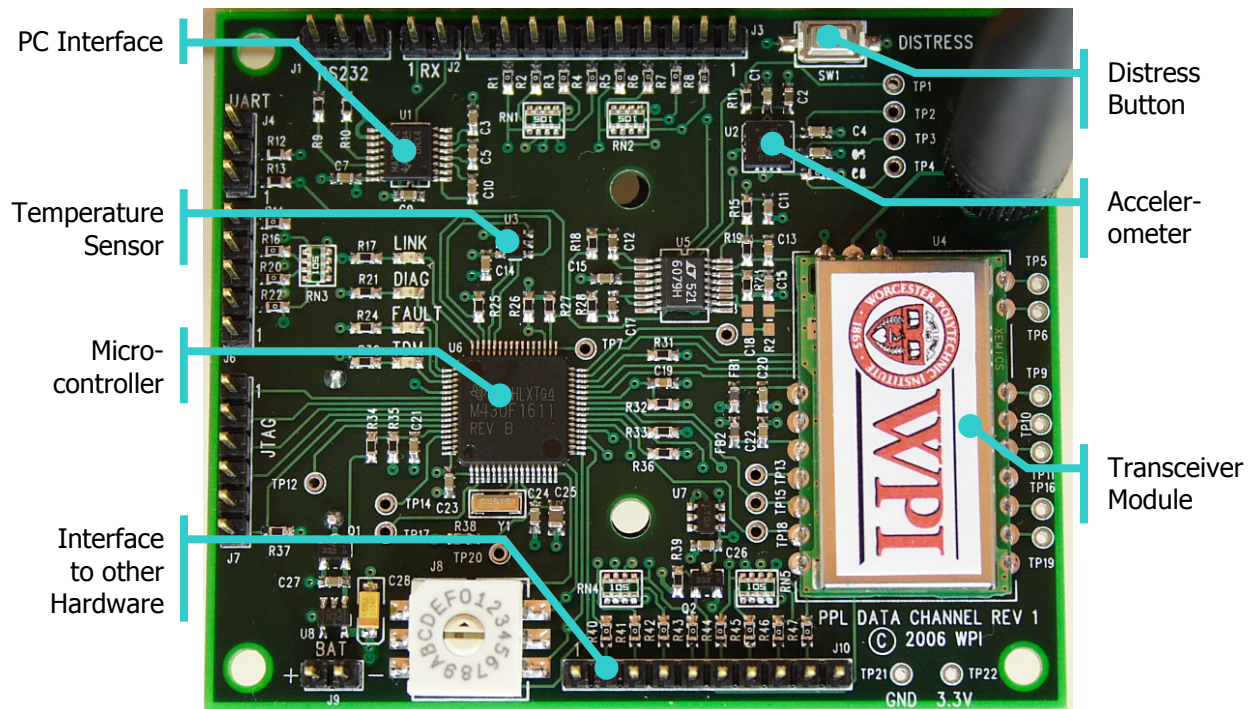


Figure 19: Data Channel Hardware Block Diagram

### 3.7. Hardware Implementation

The Data Channel boards were designed, ordered and populated during February and March 2006. Although parts of the circuit design, the schematic entry and PCB layout were done by outside consultants, all other tasks were done at WPI. The WPI tasks included the overall design as described in the previous section, selection of the major parts in the system, basic circuit design, parts ordering, board assembly and testing. A total of ten boards were completed and tested to be functional (please see the Experimental Results chapter for details). Figure 20 shows a completed Data Channel board. In this section, some of the elements of the Data Channel hardware will be described.



**Figure 20: Completed Data Channel Hardware**

In general, the design of the Data Channel hardware corresponds to the block diagram shown in the previous section (Figure 19). The functionality of the Xemics module [32] is described in Section 3.9 on the implementation of the protocol, and in this section, we will describe some of the other noteworthy features of the boards.

The MSP430F1611 microcontroller [16] has a total of six I/O ports, many of which are shared with other functions, such as USARTs or a built-in analog-to-digital converter. Along with three pin headers that connect directly to three different MSP430 ports, the microcontroller also interfaces to the Xemics module through one of its USARTs in SPI mode, to an RS232 level shifter through the second USART, and to the temperature sensor through an SPI interface that is implemented with general-purpose I/O. In addition, the battery voltage is applied to one of the pins of the built-in ADC through a voltage divider (so as not to overload the input pin) so that the code on the MSP430 is capable of determining the current battery voltage.

The only crystal on the board is a 32.768 kHz crystal, which drives the MSP430. The MSP430 features a “digitally controlled oscillator” (DCO), which is a digital PLL that multiplies the basic clock up to a much higher frequency, so it can be used as a fast instruction clock. In our implementations, we chose a 4 MHz instruction clock to allow for near-maximum speeds. However, we chose to operate the timers, which are also an important feature of the MSP430, to

run of the 32.768 kHz crystal, to avoid any problems with PLL jitter and to be able keep the CPU timers operating while the CPU is put into a low-power mode. The timers operate by running a counter to which a number of “capture and compare” modules are connected. In essence, these modules trigger an interrupt when certain timer values are reached (a “tick”), and they can therefore be used to time multiple different events off a single, continually running timer.

The MSP430 supports several different low-power modes that allow for disabling of different parts of the CPU such as the DCO, the CPU core itself, and other oscillators in the system. These modes can be entered from software, and can be exited by different events such as a timer tick (if the timers are enabled during the low power mode) or an event on the RS232 receive line. Note that the boards are typically powered by three AA batteries that can be installed in a batter holder in the back of the PCB.

The movement detection circuitry (also referred to simply as the “analog” circuitry because it is the only analog circuitry on the board) features an Analog Devices ADXL330 accelerometer [23]. A special movement detection circuit was designed; it is shown in Figure 21. This circuit takes the output of each of the axes of the accelerometer, which is a voltage that is proportional to the acceleration of the IC and first low-pass, then sums and high-pass filters it. The effect of this circuit is that the voltage at the “ACC” output generally rests at about 1.5V, except when there is movement, in which case the output voltage changes, but still quickly settles back to the nominal output if there is no more acceleration. As a result, one must merely watch the output of this circuit, which feeds directly into one of the microcontroller ADC pins, for changes, and if any changes are observed, this indicates movement. This circuitry has the ability to be powered down via a control signal from the microcontroller, to conserve power when it is not in use.

As the boards were being completed, development on the firmware that was provided by the outside contractors was continued. Several of the drivers that had been provided had to be rewritten for efficiency and bug fixes, such as the drivers to interface for the Xemics radio module, and the driver for RS232 communication with the PC. The firmware was written and compiled in IAR Systems Embedded Workbench for the TI MSP430.

Because the Data Channel is actually a very general platform, providing wireless communications, a low-power microcontroller, expansion ports, and a PC interface, it was also used for several other purposes in supporting the PPL system and experiments. For example,

code was written that interfaces it to a variable gain amplifier on the PPL receiver boards; to an Analog Devices PLL chip, and to analog switches that control RF input from multiple antennas. Most notably however, the Data Channel was also interfaced to the newly built Digital Waveform Generators in order to test the functionality of the power control of those boards, and eventually the entire Locator device.

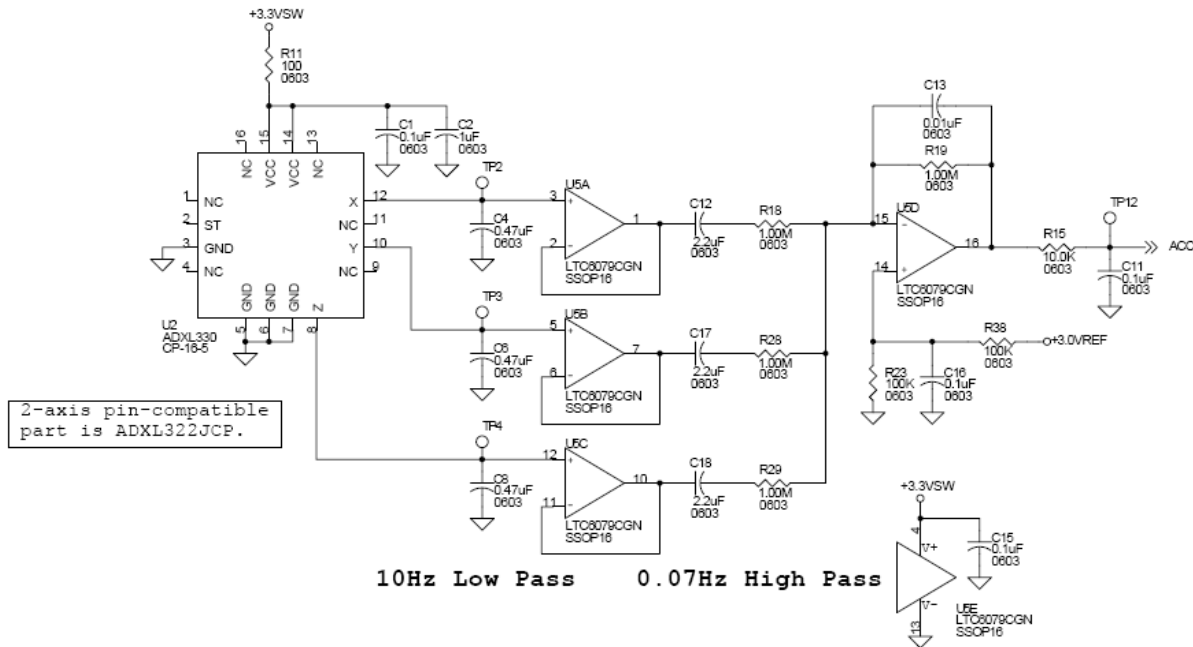


Figure 21: Data Channel Movement Detection Circuit

Having built this hardware as described in the previous sections, we will now describe protocol that provides the Time-Division Multiplexing scheme described earlier.

### 3.8. Communications Protocol

In order for the Data Channel units to communicate amongst one another and accomplish the tasks set forth in the previous sections, a wireless communications protocol must be developed. It is important to note that the focus of the project work changed after the Data Channel hardware development had been completed in mid-2006, and supporting multiple transmitters received a lower priority than other developments. Because, among other things, using the Data Channel as a general platform for supporting the PPL project became more important than a full protocol implementation, note that only a proof-of-concept of the protocol framework described in this section was implemented, as is described in the subsequent section.



Although the Data Channel hardware will eventually be merged with the hardware of the entire Locator device, the boards were designed separately from the other prototype parts of the system. Figure 22 shows an overview of the concept of how the Data Channel units fit into the system. Both Locator units (LU) and Reference Units (RU) are each given a Data Channel board (DC). The first “layer” of communication is the Reference Units communicating with the Locators. The second layer of communication is the Base Station communicating with the Reference Units. In the future, this second layer can be implemented through a high-speed link, such as 802.11. However, in the proof-of-concept implementation, the major goal was to show that the “time slot” TDM system is functional, so only one layer of communications was implemented and only one Data Channel board is present at the Base Station, instead of one at each Reference Unit. This concept can then be extended, as the Reference Units only function as a “relay” or “repeater” for the data that is communicated between the Locators and the Base Station, as will be described below.

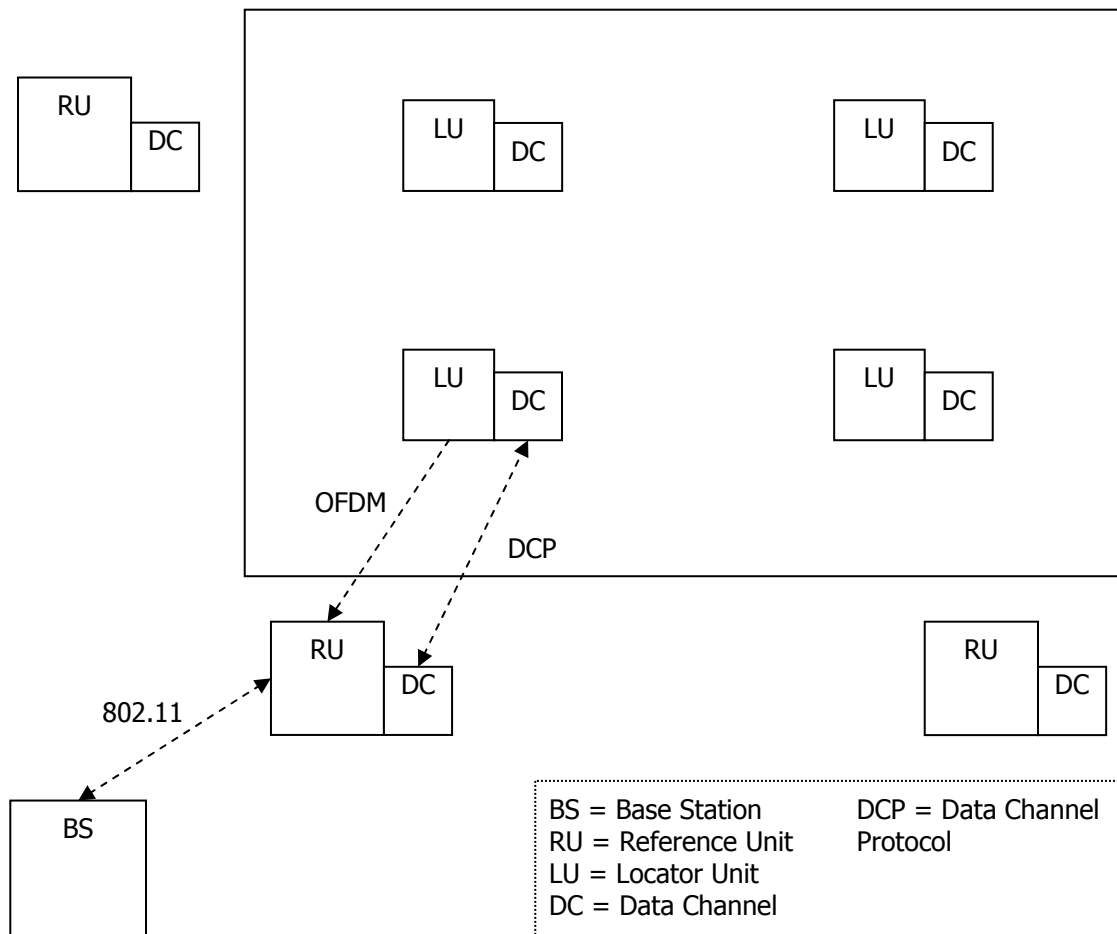


Figure 22: System Overview

Because the correct functioning of the ranging signal transmission is essential, the Data Channel's main responsibility is providing TDM control for the Locator devices. This is achieved by receiving time-synchronizing information from the units outside the building. The other data, namely commands for the Locator units and status information, is included with the time synchronization.

As we have seen in the previous sections, 100 Locator units in the system communicating once a second gives each unit a 10 ms time slot within which to communicate, both for their Data Channel and for their ranging signal transmission, although these do not necessarily need to happen in the same slot. In the proof-of-concept system, only sixteen time slots were implemented, because only ten Data Channel boards were built initially and the rotary DIP switch used to encode the board ID has only sixteen positions. However, the slot length was kept at 10 ms, and the number of slots can easily be increased by adjusting the configuration of the firmware.

Because it is important for the Locators to conserve power, an important feature for the Data Channel units is to be able to be wirelessly commanded to power down. As we have seen from the hardware description, the Data Channel boards have the ability to go into a very low-power sleep mode out of which they can be awakened by timer interrupts. We can assume that the Data Channel is capable of powering on and off the rest of the Locator sections and controlling ranging signal transmissions through its expansion ports with the same accuracy as it can control its own timings and power. We will assume that this "sleep mode" feature can be implemented by programming the Data Channel to regularly wake up and listen for any wireless commands to power itself up and return to normal operations.

### **3.8.1. Data Format**

In order to describe the protocol, we must first know what data we are communicating. The data that needs to be sent from the Locators to the Base Station (via the Reference Units) are: distress signal, movement data, temperature, diagnostics, and acknowledge for previously sent commands. Data from the Base Station to the Locators would be mainly power commands. In addition, we will assume that a Data Channel board can synchronize its timer to the reception of a packet, which we will refer to as a synchronization packet or synchronization signal. Note that this packet can include regular data as well. The implementation details are described in the

subsequent section. We will now describe a framework data packet format for the communication of this information.

First, we must determine the possible size of the packet. Because the time available in which to communicate is limited by the slot length, the data rate is a limiting factor. As the Experimental Results chapter will show, the optimal baud rate for the boards is 19200 baud. At this rate, the maximum number of bytes that can be transmitted in 10 ms is 24 bytes. If we assume 1 ms guard time at either end of the slot, this reduces to 19 bytes that can be transmitted in each slot. We will keep this in mind in the following discussion to and determine if this is sufficient to transmit all necessary data.

The Xemics module provides for the detection of a preamble of alternating ones and zeroes and a unique identifier of up to four bytes, which also serves as a synchronization pattern to align the incoming bit stream into bytes. The suggested preamble length is 3 bytes, and for our purposes, we would like to avoid false pattern detection in random noise, so we will use the maximum identifier length of four bytes. While these bytes have to be manually inserted at the transmitter, the Xemics module automatically detects and strips these bytes at the receiver.

During testing of the modules, it was determined that even when radio conditions are good, single-bit errors may still occur in packets. Therefore, it was decided to implement a forward error correction scheme using a (12,8) Hamming code, which can correct single-bit errors. The use of this code increases the number of bits necessary to encode a message by 50% (i.e. one byte of parity information for every two bytes of data), but allows for one bit error in every twelve bits of data. In addition, to further reduce the chances of errors occurring in the case of the Hamming code failing, a “checksum” byte consisting of a byte-by-byte XOR of the contents of the packet is appended prior to Hamming encoding. Any packets received that show errors can be discarded. Both the Hamming Code and the checksum are applied to the payload of the packet, which does not include the preamble and unique identifier. Although Hamming encoding normally involves interleaving the check bits into the data, for ease of implementation we will merely append the check bits to the end of the packet, giving one byte of check bits for every two bytes of data.

As will be shown in detail below, the Reference Units do not communicate directly amongst one another, and the Locators do not communicate amongst one another, but every Reference Unit receives every packet from every Locator and vice versa. Therefore, an

addressing scheme to uniquely identify each unit only requires a “source” address, which can be a single byte consisting of the board’s unique ID. Furthermore, the unique identifier implemented in the Xemics module can differ for transmissions from Locators to Reference Units and vice versa, so that accidental communication amongst Reference Units and amongst Locators can be avoided. Therefore, the destination of a packet is always clear.

Finally, we must encode the data into the remaining bytes of the packet. Table 8 shows the data that must be transmitted from Locator to Base Station, and Table 9 shows the data that must be transmitted from Base Station to Locator. As we can see, the communications require only three bytes of payload for either communication in addition to the one-byte address, the one-byte checksum and the Hamming parity data. Because the Hamming code is more efficient for an even number of bytes to encode, an additional “reserved” byte can be added to the payload, which could later be used for other psychological status or other data. Figure 23 shows the resulting packet, which is 16 bytes long and can be transmitted in 6.67 ms. One should note that if required, two more payload bytes could be added, resulting in one more Hamming byte and a total packet length of 19 bytes, which can be transmitted in 7.92 ms. Therefore, our assumptions on baud rate being fast enough and the length of the guard time are shown to be acceptable.

Field	Size	Description
User Distress Signal	1 bit	Distress signal triggered by user
Temperature Alert	1 bit	Automatic distress for high temperature
Non-Movement Alert	1 bit	Auto. distress on non-movement detection
Low Battery Alert	1 bit	Warning for low battery voltage
Diagnostics	3 bits	Reserved for diagnostic codes to indicate other hardware problems
Acknowledge	1 bit	Acknowledges the receipt of a command
Ack. Packet Identifier	1 byte	Packet identifier of the packet which contained the command being ack’ed
Temperature	1 byte	Temperature value in Celsius (-40 to 150 deg C)

**Table 8: Data from Locator to Base Station**

Field	Size	Description
Packet Identifier	1 byte	Unique packet identifier
Target Locator ID	1 byte	The ID to which a command is being sent (if any)
Power Up Command	1 bit	Tells a sleeping Locator to power up
Power Down Command	1 bit	Tells a Locator to go to sleep
Alert/Distress Ack.	1 bit	Acknowledges reception of alerts

**Table 9: Data from Base Station to Locator**

Preamble (3)	Unique Identifier (4)	Addr (1)	Payload (4)	Chk sum (1)	Hamming Parity Data (3)
--------------	-----------------------	-------------	-------------	-------------------	----------------------------

Figure 23: Packet Format

### 3.8.2. Communications Concept

Now that the data format has been determined, a system for relaying this data to and from the Base Station will be described. There are several assumptions that are made during this discussion. We assume that all Reference Units are able to communicate with the Base Station on a separate, high-speed data link. In addition, we assume that every Locator Unit is within the communication range of at least one Reference Unit, but not necessarily more than one or even all Reference Units. The latter assumption provides a challenge for the protocol. It is obvious that the distress signal triggered by a person wearing the Locator is of high priority. Therefore, we must devise a system in which the distress signal and other information can be relayed to the Base Station even in situations where the Locator is not within communications range of every Reference Unit. However, one also had to consider the possibility of a Locator unit completely falling out of range of the Reference Units as well.

In the event that a Locator unit falls out of the range of all Reference Units, the ability exists for it to continue transmitting for a certain amount of time. As we have previously developed equations for clock drift and time until failure, we can now apply these to calculate the time until failure. Using Equation 1 from Section 3.3, and setting  $ppm$  to the actual crystal rating of 20 ppm and calculating for a guard time of  $\Delta t = 1$  ms, we see that the time until failure is 25 seconds. This means that a Locator can still be confident of hitting its time slots (both ranging signal and Data Channel communication) for that period after it has received its last synchronization signal. Once that 25 s time limit has passed however, the Locator must assume that it will overlap with other communications and must stop transmitting and switch to an active receive mode until it receives a new synchronization packet. During the time that a Locator is out of communications range, the Base Station would also be aware that it has not received any data from that particular Locator and display an alert that it may be outside of the Reference Units' communication range.

How a final protocol implementation would work is shown in Figure 24. In this figure, four Locators,  $LU_0$  to  $LU_3$ , and three Reference Units,  $RU_0$  to  $RU_2$ , are shown. A "T" indicates a transmission, an "R" indicates a reception, and synchronization is represented with arrows. The

different elements of the operation of the protocol are circled and indicated with letters, and are described below.

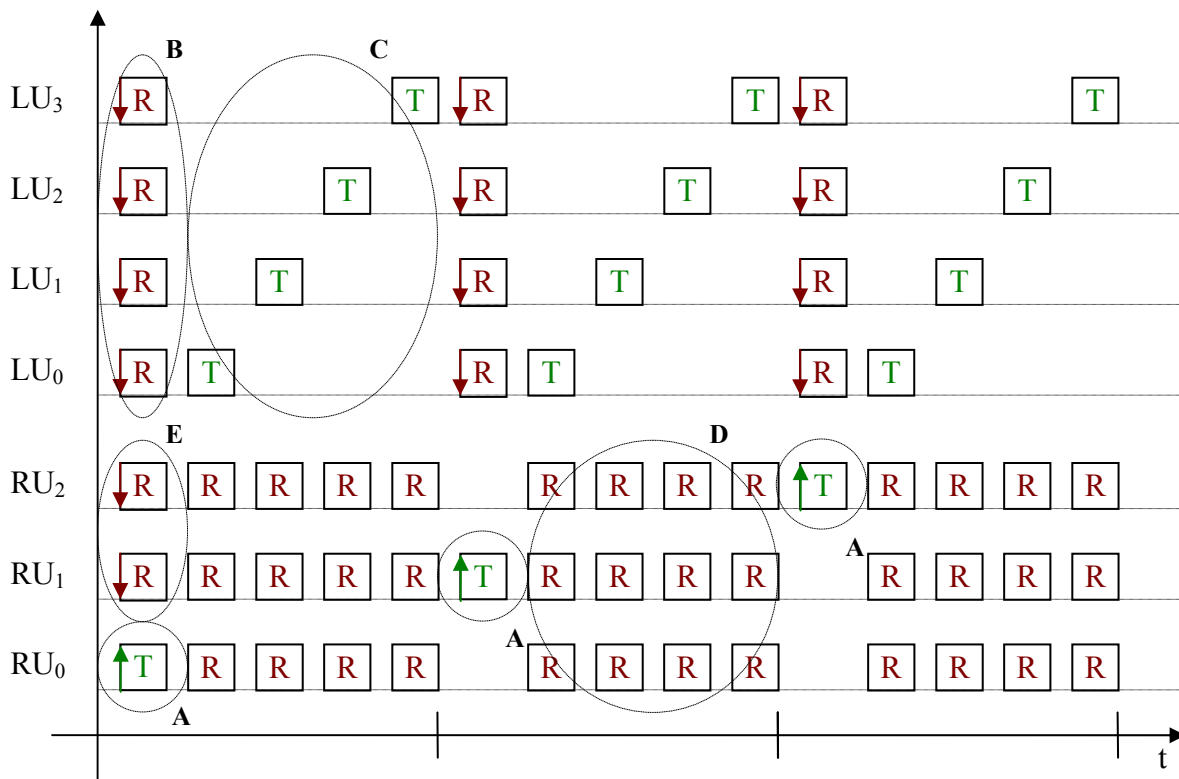


Figure 24: Protocol Overview

- **A:** All Reference Units in the system take turns at transmitting synchronization and data packets. This is important because we assume that not every Locator can communicate with every Reference Unit, but with at least one. Therefore, every Reference Unit must take a turn at transmitting synchronization and data to ensure that all Locators receive it, even if they do not receive it in every communications cycle.
- **B:** Every Locator attempts to receive synchronization and data whenever it is transmitted by one of the Reference Units.
- **C:** The Locators transmit in their assigned slots. Locators derive these slot assignments from a unique ID (as is currently implemented in the proof-of-concept implementation). In a future implementation, they could be dynamically configured by commands from the Base Station, or assigned via other means.
- **D:** While the Locators are transmitting, all Reference Units attempt to receive every packet, so that in the event that a Locator cannot reach all Reference Units, at least one

will receive the data and be able to relay it back to the Base Station. This is essential in relaying a distress signal to the Base Station. In case more than one Reference Unit receives the data, the Base Station can simply disregard the other copies.

- **E:** One of the Reference Units is designated the “master” Reference Unit that provides the overall timing for the entire system. The other Reference Units synchronize their clocks from the master, so that they can then pass this synchronization timing on to the Locators.

One protocol feature that was mentioned above for possible future implementation is dynamic slot assignment, in which the Base Station would assign Locators a slot within which to transmit. The details of such a scheme fall under future work, but it mentioned here because it should be noted that the bytes remaining unused in the packet (up to three) could be used to implement this feature.

As previously mentioned, a future implementation of the system will include a high-speed data link (802.11 or similar) between the Reference Units and the Base Station. However, because it is not clear when this link will be in place, we can also plan for the Data Channel being used for this purpose. In this situation, it is clear that at the maximum number of users, the “air time” of the Data Channel is completely occupied. Therefore, to support this second layer of communications, we must either sacrifice the maximum number of users or the update rate in order to allow for the communications between the Reference Units and Locators to be suspended and instead to have the Reference Units relay their data to the Base Station. As this is a temporary solution and we do not expect to run tests with the full number of Locators in the near future, we can assume that it is acceptable to cut the maximum number of users in order to free up time within which the second layer of communications could occur. Details of this relaying scheme, if the need for it arises, can be considered future work.

The protocol described in this section would meet all the needs for communication with and control of the Locator devices. As previously mentioned, a proof-of-concept of this protocol was implemented, and some of the details and lessons learned will be described in the following section.

### **3.9. Protocol Implementation**

This section describes the work done in implementing a proof-of-concept version of the Data Channel protocol described in the previous section. The goal of this implementation was to

show that communications are indeed possible using the “time slot” system with the Xemics DP1205 modules on the Data Channel boards and that Locator units can be timed to transmit their ranging signals and communicate with their Data Channel units in 10 ms slots.

The protocol that was implemented is a simplified version of the protocol presented in the previous section. It assumes a single Reference Unit is attached directly to the Base Station, which communicates with multiple Locators. Because the rotary DIP switches on the Data Channel boards have 16 positions, a protocol with 16 slots for 16 possible Locator IDs (numbered 0 through F in hexadecimal) was implemented. The board configured with slot 0 automatically became the Reference Unit, and all other slots were Locators, except for slot F, which was excluded due to implementation issues that will become obvious later.

In this implementation, the MSP430 timer was used to keep track of the 10 ms time slots. These timer “ticks” were adjusted to account for certain transmission and reception start-up times, which will be discussed in much detail later. The code was activated when the timer ticks. The Reference Unit’s timer was not reset to keep its time base constant, while the Locator’s timer was reset upon receiving the synchronization signal.

We will now describe the general operation of the protocol, which is shown in Figure 25, as it was implemented. The Reference Unit stays in receive mode, except in slot 0, in which it switches to Transmit mode and sends a synchronization and data packet, as will be described below. The Locator normally stays in sleep mode, but it wakes up via its timer to receive synchronization and data in slot 0, and it also wakes up in its assigned slot to transmit its data, which for this test consists of temperature and movement data. If the Locator has not seen a synchronization signal for 25 seconds (the time until failure calculated in the previous section), it switches into a constant receive mode in an attempt to regain synchronization. It should be noted that at the time of initial implementation of this protocol, the packet length was set at 17 bytes as opposed to the lengths suggested in the previous section. In addition, forward error correction was not yet implemented, but was implemented and tested separately after this protocol scheme had been confirmed to work.

The Xemics modules have several features that assist in the implementation of the protocol. The modules feature a serial SPI-compatible bus that provides access to a 16-byte transmit buffer, a 16-byte receive buffer, and configuration and command registers. Through these registers, the entire operation of the module can be configured, such as the exact operating



frequency and data rate. The ability to configure the frequency channel is important, because in a final system, the Data Channel boards would need to implement a frequency hopping scheme, as this is required by the FCC for the 900 MHz ISM band.

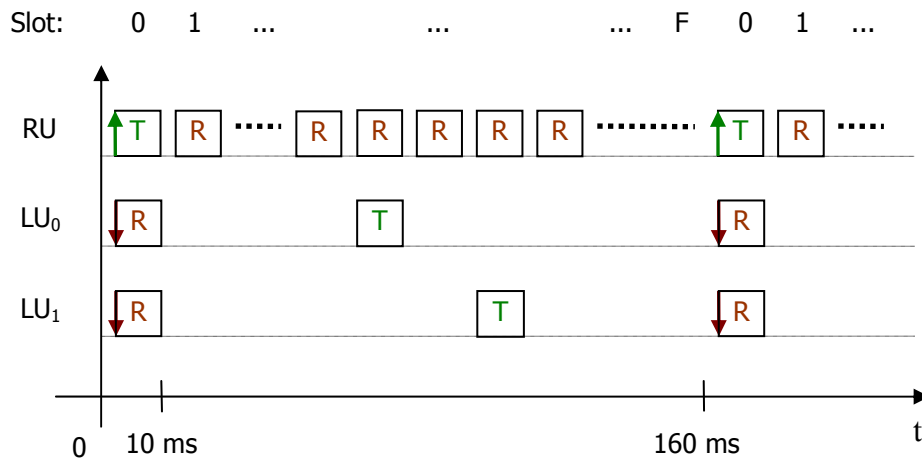


Figure 25: Basic Protocol Overview

The Xemics module has four modes that are selected through configuration lines: transmit, receive, standby and sleep. In transmit mode, the module begins transmitting as soon as a byte is written to the transmit buffer (this behavior is configurable). The receive section features a preamble and unique identifier detection and begins filling the receive buffer as soon as this pattern is detected. The module also features two interrupt lines that can be configured to signal events such as byte received, transmission complete, etc. In standby mode, the module keeps its oscillator running so that it can be powered up faster, but the actual transmit and receive circuitry stays asleep. Finally, in sleep mode, the module is completely off.

The firmware that interfaces the microcontroller code to the Xemics module is a custom written driver that includes all necessary functions to configure and access the Xemics module's functionality. To transmit data, the driver simply writes all payload data (assuming that error correction and checking codes have already been included) plus the preamble and unique identifier bytes to the transmit buffer, including wait states while the buffer is full in the case that the data is longer than 16 bytes, and waiting for the completion of transmission. To receive, the firmware switches the Xemics module to receive mode and configures one of the interrupt lines to signal the "byte received" event, upon which the driver reads the received byte into a buffer on

the microcontroller. This is repeated until the expected number of bytes has been received or a timeout is reached.

A smaller problem that was encountered in the drivers was that the Xemics module's "transmission complete" signal, which is provided on an interrupt line, is actually set before the last bit to be transmitted has actually passed through the RF stages of the module. If the module is placed into standby or sleep mode immediately upon the detection of the transmission complete signal, this last bit is corrupted. This problem has been confirmed by Xemics technical support. So the firmware drivers include a short delay, equivalent to the transmit time of one bit, before placing the module into sleep mode.

### **3.9.1. Synchronization and Timing**

An important interrupt signal provided by the Xemics module is one that is triggered upon detection of the unique identifier; it is used to implement the synchronization feature of the protocol. When the microcontroller firmware detects this interrupt signal, it can reset its internal counter that provides timings for the 10 ms time slot measurement, thus synchronizing to the transmitted signal. Measurements, which are described in the Experimental Results chapter, show that when one transmitter sends a synchronization signal to multiple receivers, the maximum difference of the reception of the synchronization signal between the multiple receivers is 41  $\mu$ s, and typically within about 7.5  $\mu$ s. This is several orders of magnitude below the guard time in the time slots (1 ms), which shows that this synchronization scheme is viable.

However, an issue arises when using this kind of synchronization – one must keep in mind that the unit transmitting the synchronization packet must also stay synchronized with those units receiving the signal. Because there is a fair amount of set-up time involved with sending a synchronization packet (starting up the Xemics module, loading bytes into its transmit buffer, etc.), the transmitting unit must take care that the actual time the synchronization signal is seen at the receiving units matches with its own timer tick. In order to do this, an implementation is sought in which the transmitting unit begins transmitting early, specifically by the amount of time it requires the synchronization signal to reach the receiving units. This method will now be described in detail.

Before we develop the timings necessary for the protocol, we must make note of all timings that affect the operation of the Xemics module and the MSP430 microcontroller. The MSP430 is configured to run at a speed of approximately 4 MHz, giving an instruction cycle time

of 250  $\mu\text{s}$ . The microcontroller takes up to six cycles to execute an instruction, so the maximum instruction execution time is 1.5  $\mu\text{s}$ . The interrupt latency is also 6 cycles or 1.5  $\mu\text{s}$ . As will be shown in the Experimental Results, the 32.768 kHz timer is highly accurate (on the order of ns). This timer frequency gives a period of 30.5  $\mu\text{s}$ , which is the maximum accuracy to which we can time events on the microcontroller.

For the Xemics module, certain timings are required for the module to switch between its modes. These times are shown in Table 10. Additionally, it was measured that on the SPI interface between the Xemics module and the MSP430, writing or reading one byte takes approximately 40.43  $\mu\text{s}$ . The selected data rate of 19200 baud gives about 416.67  $\mu\text{s}$  per byte. This transmission time was also measured, and determined to be as expected, with about 416  $\mu\text{s}$  per byte and an overhead of 153  $\mu\text{s}$ , which includes the time it takes to write one byte to the Xemics transmit buffer. Specifically, it was also measured that transmitting 17 bytes takes 7157  $\mu\text{s}$ . Finally, it was measured that the time it takes for transmitted data to be seen at the receiver (the “over-the-air” delay that includes some delay through the transmit and receive chains) is approximately 136  $\mu\text{s}$ .

To From	Sleep	Standby	Transmit	Receive
Sleep	(0)	2000 $\mu\text{s}$	2350 $\mu\text{s}$	2850 $\mu\text{s}$
Standby	0	(0)	350 $\mu\text{s}$	850 $\mu\text{s}$
Transmit	0	0	(0)	600 $\mu\text{s}$
Receive	0	0	150 $\mu\text{s}$	(0)

Table 10: Xemics Module Mode Switch Times

In general, when a unit is attempting to receive a packet, it attempts to do so over most of the duration of the slot. A receive timeout of 9500  $\mu\text{s}$  was selected, because it leaves 500  $\mu\text{s}$  or time for 330 to 2000 instructions in the slot. Transmitting 17 bytes takes 7175  $\mu\text{s}$ , which leaves 2325  $\mu\text{s}$  guard time in the slot, which is sufficient for our implementation, which specifies at least 2 ms guard time total (1 ms at each end of the slot). An overview of this situation is presented in Figure 26.

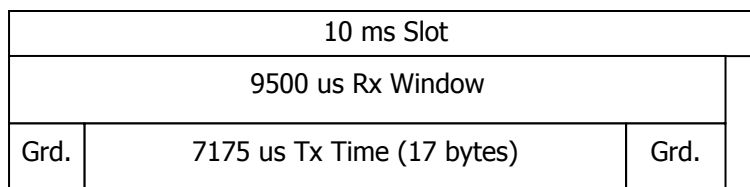


Figure 26: Timeslot Overview

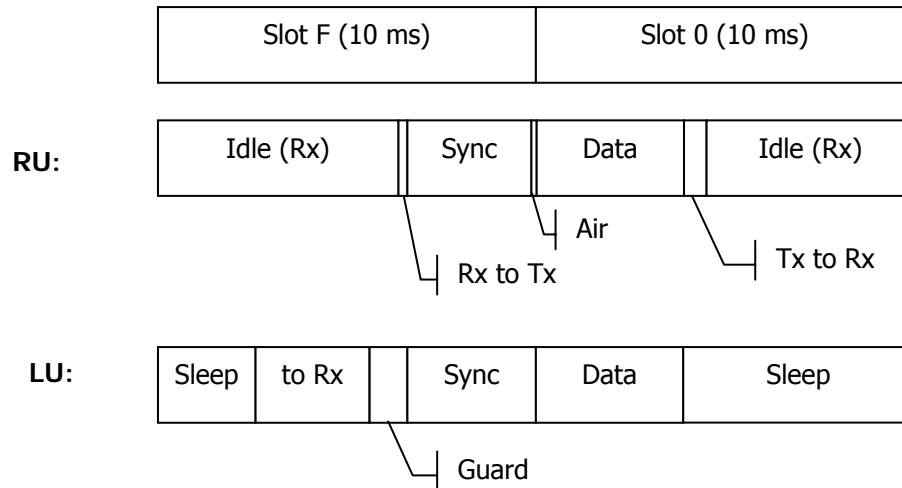
The board that is acting as the Reference Unit remains in receive mode for most of the duration of a “cycle” of 16 times 10 ms, or 160 ms. This also means that for most slots, there is no switching penalty from the Xemics module mode switching because the module can simply stay in receive mode. Reception can be timed to begin exactly at the beginning of the slot, and the transmitting board can implement the 1 ms guard time. Every time a reception is initiated, the Xemics firmware drivers must write to the Xemics module registers, which takes about 160  $\mu$ s, so the timer must be set to tick 160  $\mu$ s early for all slots except slot 0.

In slot 0, the synchronization signal transmitted by the Reference Unit must arrive at the Locators at the exact time of the beginning of slot 0 – this of course means that the actual time that the timer ticks on the Reference Unit must be adjusted so that it begins transmitting early. The timings, which are as follows, are illustrated in Figure 27.

- Xemics mode switch from receive to transmit (labeled “Rx to Tx” in figure) = 150  $\mu$ s (timed exactly by MSP430 timers)
- Time to initialize transmission = 80  $\mu$ s (estimated time to write 2 bytes to Xemics buffer); included in figure together with the switching time above
- Time to transmit pattern and unique identifier bytes (“Sync”) = 3270  $\mu$ s (measured)
- Over-the-air delay (“Air”) = 136  $\mu$ s (measured)

This gives a total time of 3636  $\mu$ s – this is how much earlier the Reference Unit must begin its transmission process compared to the beginning of slot 0. This means that, as previously mentioned, no communication can happen in slot F; however, a workaround to this limitation is described later. After the Reference Unit has transmitted the synchronization signal, the following things will happen in the beginning of slot 0:

- Transmit remaining 10 bytes of packet (“Data”) = 3905  $\mu$ s (measured and calculated)
- Time to switch Xemics module back to receive mode (“Tx to Rx”) = 600  $\mu$ s (timed exactly) – this is so that at the beginning of slot 1, the Reference Unit is already in receive mode and there is no mode switching penalty.
- Total time used in slot 0: 4505  $\mu$ s – this leaves 5495  $\mu$ s in the slot, which could even be used for additional data from the Reference Unit to the Locators.



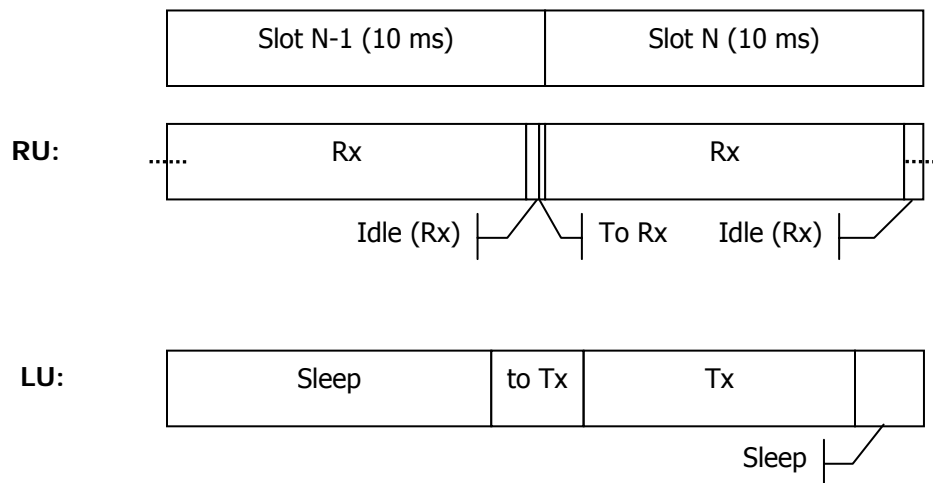
**Figure 27: Synchronization**

Figure 27 also shows the implementation of the Locator Units' timings. One must keep in mind that as opposed to the Reference Unit, the Locator spends most of its time in sleep mode to conserve power, so one must take into account the longer Xemics module mode switching times. In slot 0, the Locator knows that it can expect a synchronization signal at the beginning of the slot. In order to receive this signal, the Locator must wake up early, during what is actually slot F, to prepare to receive the synchronization and data packet. These timings are as follows:

- Wake-up time to receive (labeled "to Rx" in figure) = 2850  $\mu\text{s}$  (timed exactly by MSP430 timers)
- Time to initialize reception = 160  $\mu\text{s}$  (estimated time to write 4 bytes to Xemics buffer); included in figure together with the switching time above
- Guard time in case Reference Unit transmission starts early ("Guard") = 1000  $\mu\text{s}$  (timed)
- Time to receive 7 bytes of pattern plus unique identifier ("Sync") = 3270  $\mu\text{s}$  (measured)
- Over-the-air delay = 136  $\mu\text{s}$  (measured); not shown in figure

This means the Locator needs to wake up a total of 7416  $\mu\text{s}$  before the beginning of slot 0. Logically, this also means that slot 0 is extended by 7416  $\mu\text{s}$ , which the Locator needs to adjust for when resetting its timer. As with the Reference Unit, in slot 0, the time it takes to receive 10 bytes is 3905  $\mu\text{s}$  (measured), leaving 6095  $\mu\text{s}$  in the slot (no mode switch time to sleep). Again, one should note that no communication can take place in slot F, since all boards will be busy mode-switching.

When a Locator unit needs to transmit data in its slot, it should begin transmitting 1 ms into the slot to implement the guard time. However, to wake up from sleep it takes a total of 2430  $\mu\text{s}$ ; therefore, it must actually wake up from sleep and initialize transmission 1430  $\mu\text{s}$  before the beginning of the slot it should transmit in. With a transmit time of 7175  $\mu\text{s}$  for 17 bytes of data, that means the Locator will be done transmitting 8175  $\mu\text{s}$  into the slot – which should give it enough time (1325  $\mu\text{s}$ ) before the Reference Unit times out on the previously described 9500  $\mu\text{s}$  receive timeout. This situation is shown in Figure 28.



**Figure 28: Data Transmission**

As previously mentioned, this protocol implementation is limited in that it does not allow transmissions in the final slot; this is due to the Reference Unit having to switch from receive to transmit mode and then transmitting a synchronization packet, which cuts into the time available in that slot. One can see that with this implementation, this problem would still exist even when expanded to 100 Locators. However, there are several approaches to solving this problem. For example, one might note that, considering the results of the Data Channel boards' timing accuracy, the guard time of 1 ms could be reduced by a slight amount without impacting the performance of the system, and this could be used to allow for enough time for mode switching. Alternatively, one could imagine a system where there are 101 slots for the Data Channel, and only 100 for ranging signal transmissions, meaning that although the Data Channel and ranging signal transmissions would not be aligned for most of the time, the ranging signal transmissions would still allow for updates to be provided once a second. The impact of increasing the Data Channel cycle time to 1.001 s should not be noticeable to the user.

Finally, it should be mentioned that this “time shifting” of the 10 ms time slot timer ticks is not the only method for synchronizing all units. An alternative that was tested and confirmed to work is using yet another Data Channel board as a dedicated “beacon”, the only task of which is to provide regular synchronization packets for all boards in the system. This method works well for experimental setups, but one must consider that in a real-life scenario such a beacon would have to be able to communicate with all Data Channel boards in the system (both on Reference Units and in Locators inside the building), which does not match with assumptions previously made about Locators not always being in range of all units outside the building.

Overall, and as the Experimental Results chapter will confirm, this proof-of-concept implementation of the protocol showed that the time-division multiplexing of Locator’s ranging signal transmissions can be managed by the Data Channel boards.

## **Chapter 4. Digital Waveform Generation**

The waveform used for the ranging signals in the PPL project is one that is not practical to produce using analog methods; therefore, it is clear that a digital approach to generating this waveform must be taken. This approach has the added benefit that new waveforms can be created and generated without any hardware changes, and in theory, this approach could even be used to dynamically modify waveforms on the fly. Figure 29 shows the relationship of the waveform generation subsystem to the rest of the Locator device.

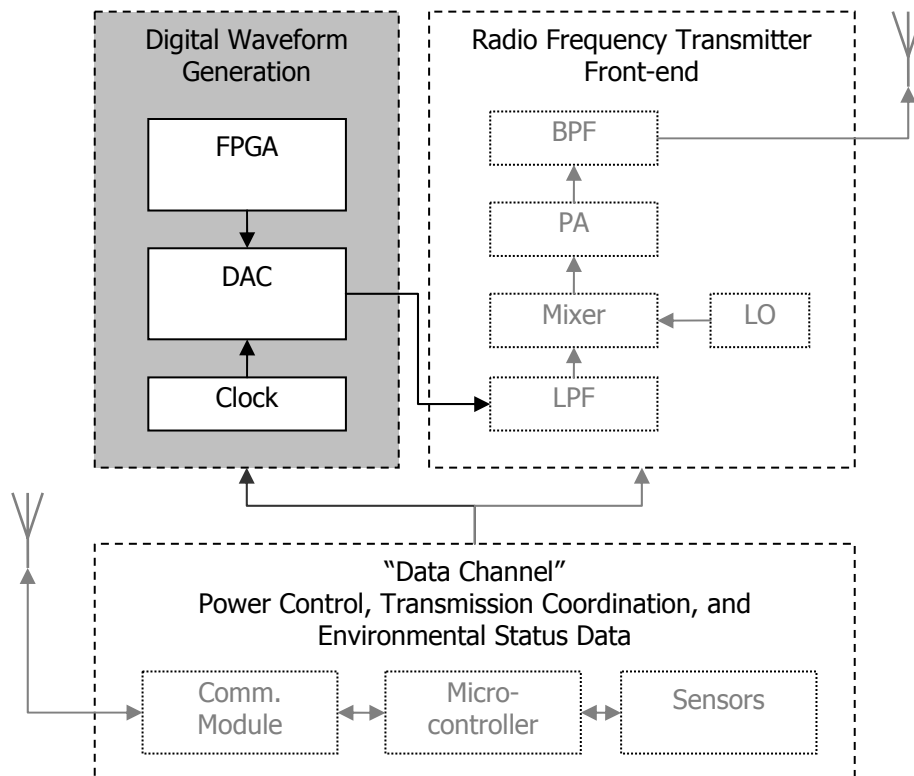


**Figure 29: Digital Waveform Generator as Part of Overall Locator Design**

The previous version of waveform generation hardware (see Section 2.3 for details) used a Xilinx Viretx-2 field programmable gate array (FPGA) and an Analog Devices AD9736 digital to analog converter (DAC), with an FPGA storing the waveform in its block RAM and providing a data clock and the data to the DAC over LVDS lines using DDR clocking. Although this method may be appropriate, the prototype boards that implemented it are relatively large because they feature extra components, take too much power and are in general “overkill” for the current requirements.



To design new waveform generation hardware, several design decisions had to be made. The major ones were that new DAC was selected and a way to provide it with data was devised, and these decisions must be made with size, power control, and other factors such as low turn-on times (for time-division multiplexing) in mind. Figure 30 shows a block diagram of the concept of this hardware.

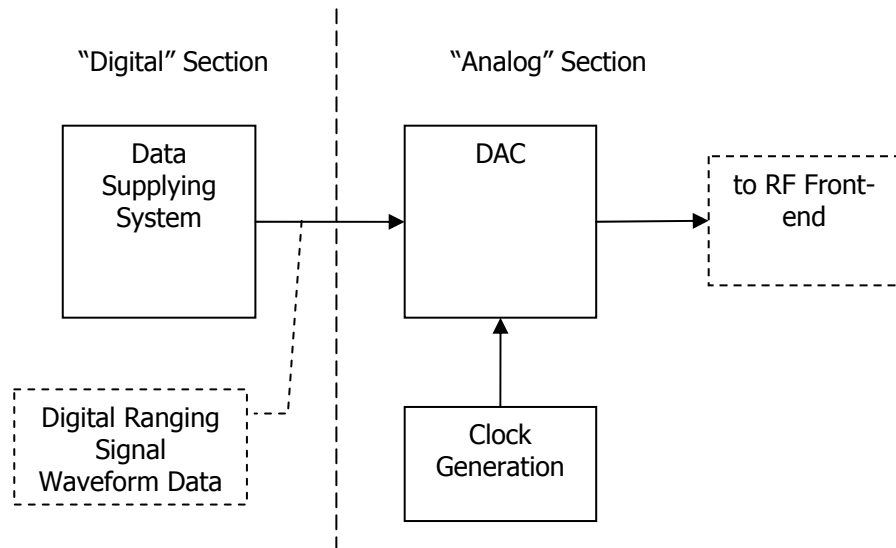


Figure 30: Digital Waveform Generator Concept

This chapter presents the redesign of the Digital Waveform Generator hardware. The following sections will discuss the selection and design of these parts of the system. This is followed by details on the implementation of the new generation of hardware.

#### 4.1. Digital-to-Analog Converter Design

The selection of an appropriate DAC is crucial because it is one of the two major components of the waveform generator system, and must fit the specifications as well as possible. The DAC to be used on the new boards had to be capable of generating signals of a bandwidth of up to 150 MHz, meaning a 300 MSPS sampling rate, at a resolution the same as or, optimally, better than the current DAC, which supports 14 bits. Other criteria were a low noise profile and enough output power to provide at least -40 dBm per subcarrier. In addition, the data interface was an important selection criterion, as it determines the range of different data generation circuits that the DAC can be connected to.

The two major vendors for DACs that were investigated were Maxim and Analog Devices, as they are both known for their large selection of analog parts, and the parts had

previously been used by members of the PPL team. Other vendors (such as Macom or National) were also investigated but no suitable parts were found.

Maxim offers only a handful of DACs within the desired sampling frequency range. The only DACs with sampling rates at 300 MSPS or above were specified as 500 and 600 MSPS, available in both 14 and 16-bit variety, with an LVDS interface. Of these, the DAC that best fits the parameters is the MAX5888, a 16-bit, 500 MSPS DAC with an LVDS data interface, good analog performance characteristics, and a relatively low power consumption of about 44 mA at 100 MSPS sampling rate [2].

Analog Devices offers a larger range of higher-frequency DACs, however again there is only a smaller number of DACs available that match the given parameters. For example, the AD9755 is a 14-bit, 300 MSPS DAC, with the advantage of having two data ports that accept data at half the sampling rate, which allows for much easier interfacing. However, it is recommended to select a DAC that has a somewhat higher sampling frequency than the one needed to produce the bandwidth for the desired signal, as this will avoid any problems with running the part at its nominal top speed, and will avoid spurious components from the clock signal on the output. Another possible part was the AD9726 [1], which is a 400 MSPS, 16-bit DAC with an LVDS data interface, and very similar analog performance characteristics as the MAX5888. We will compare this part to its Maxim counterpart in more detail.

The Maxim part has a relatively simple interface; it has only one clock input and single data rate data inputs, which means they sample their data at each rising edge of the clock signal. The Analog part has a more involved interface, with two clock inputs, one for the overall DAC sampling clock and one for the DAC data, and one clock output, which can be used to feed the device that is providing the data. In addition, it features a serial peripheral interface (SPI) that gives access to some internal configuration registers, such as the DAC calibration. In terms of current consumption, the Maxim part is clearly better with only about 44 mA drawn from a single 3.3 V supply (at 100 MSPS sampling rate), while the Analog part requires a 2.5 V and a 3.3 V rail, and it draws a total of about 209 mA (at 400 MSPS sampling rate). See Table 11 for a summary of the DAC comparison to this point.

<b>Feature</b>	<b>MAX5888</b>	<b>AD9726</b>
Sampling Rate	500 MSPS	400 MSPS
Resolution (bits)	16 bits	16 bits
Interface	LVDS, SDR	LVDS, SDR and DDR
Clocks	single sampling clock	sampling clock in, data clock out, data clock in
Power	44 mA at 100 MSPS 3.3 V rail	209 mA at 400 MSPS 2.5 V and 3.3 V rails
Start-up time	10 ms	5 – 20 ms
Additional Features	-	SPI interface for configuration, clock synchronization

**Table 11: DAC Comparison**

It seems that the Maxim part would be optimal simply due to its lower current consumption; however, the Analog part has two additional features that make it superior. The AD9726 supports double data rate (DDR) data transfer, which has the advantage that the circuitry supplying the data can be optimized in such a fashion that it only needs to run at half the sampling rate (details will be shown in the following section). Most importantly however, the Analog part features an internal clock synchronization system. While the data flowing into the DAC must be aligned to the data clock, the sampling clock can have any phase relation to the data clock, and as long as the two clocks are at the same frequency, the DAC will automatically align the data to the sampling clock correctly. These separate clock inputs provide for much more flexibility, because systems supplying data to the DAC should be able to more easily supply their own, correctly aligned data clock with the data, instead of attempting to align their data to the already existing sample clock. These advantages make it clear that the AD9726 is the better DAC for this design.

#### **4.1.1. Sampling Clock**

Having selected this DAC for our system, we must turn our attention to another important aspect regarding the DAC, which is the generation of the sampling clock. For this purpose, a design was proposed with the assistance of an outside consultant; it is illustrated in Figure 31. This design is based on a circuit currently in use on several PPL RF front-end boards to generate the local oscillator clocks, and on one of two recommended clock configurations from the DAC datasheet. This design is based on a voltage-controlled oscillator (VCO) that is controlled by an Analog Devices ADF4110 integer phase-locked loop (PLL). The output of this circuit is then fed through a 1:4 transformer in order to boost the voltage levels. At the DAC, the differential inputs

are high impedance, so the signal must be biased appropriately (1.25V) and terminated with the appropriate impedance (200  $\Omega$  is used instead of 50  $\Omega$  due to the 1:4 transformer). The DAC requires a minimum differential voltage of 0.5 V, which this circuit was expected to provide.

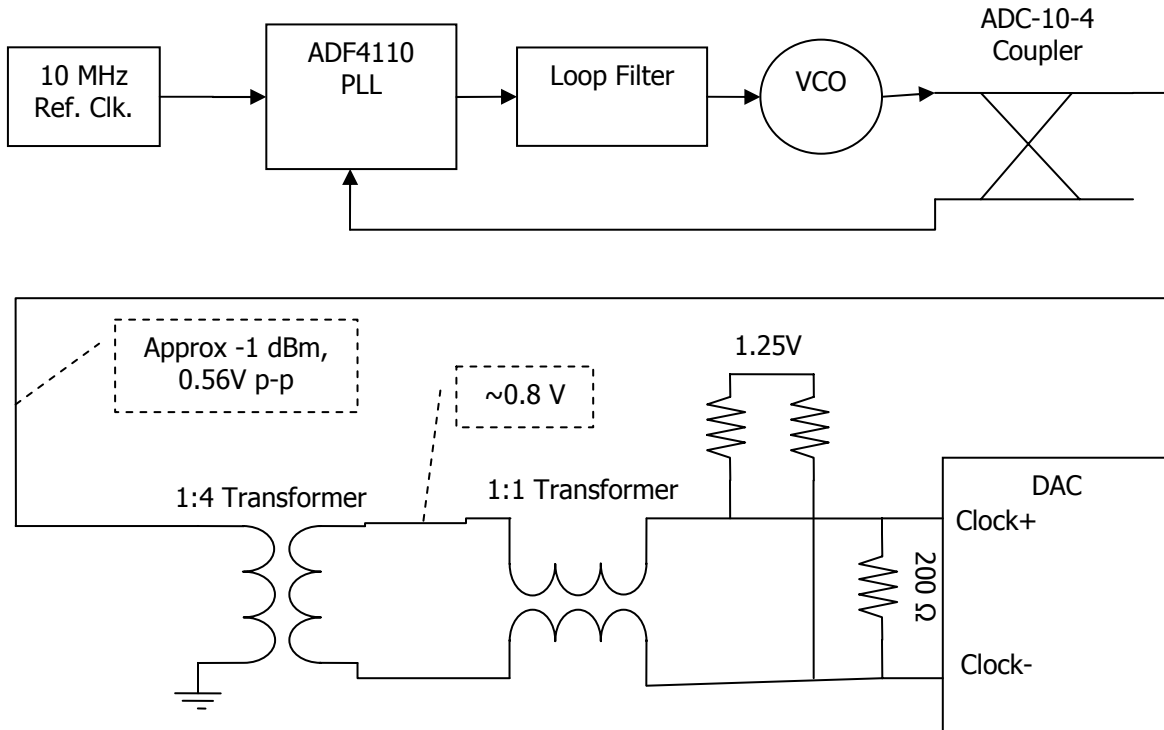


**Figure 31: Proposed DAC Clock Generation Circuit**

An advantage of this design was that it can be adapted for different sampling frequencies. The VCO has a certain range of frequencies it can be tuned to by the PLL IC. In addition, the VCO can be exchanged for other models that provide different frequencies. For this design, the Sirenza VCO191-220U and VCO191-294U were chosen as alternatives, as they provide frequency ranges of 210-230 MHz and 279-308 MHz, respectively. For the implementation, the VCO191-220U and a sampling frequency of 220 MSPS was initially chosen, as a higher sampling frequency was not yet required.

Unfortunately, when the first boards had been populated, it was determined that the circuit did not provide the voltage levels that were expected as they are labeled in the figure above, and the minimum differential voltage of the clock signal required by the DAC inputs was not reached. A solution to this problem was sought, and a modification to the above circuit was developed based on the second of the two clock configurations recommended in the DAC datasheet. This configuration involves the addition of an active LVPECL driver, which outputs

voltage levels appropriate for the DAC. Luckily, this modification could be implemented using a MAX9375 “Anything-to-LVPECL Translator”, which accepts differential or single-ended signals with as little as 100 mV swing and up to 2 GHz frequency. This IC could be mounted on the board in place of the 1:1 transformer, as shown in Figure 32, and with some modifications to the associated passive components, the clock circuit was made fully operational. These modifications can be included in a new revision of the hardware.

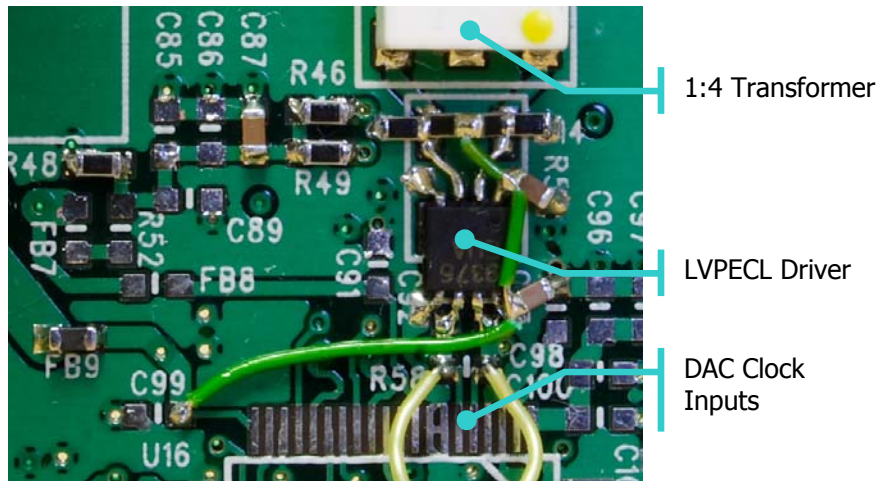


Figure 32: Modifications to Clock Circuit

The DAC and the supporting clock generation circuitry represent the “analog” portion of the Digital Waveform Generator, and we will now turn our attention to the purely digital portion of the system.

## 4.2. Data Supplying System Design

In designing a system to supply data to the digital-to-analog converter, there were several factors that had to be kept in mind. The most important of these was speed and power – the circuitry needed to provide data at up to 300 MSPS while still consuming less power than the current hardware. A factor in conserving power was for the circuit to have low turn-on and turn-off times, as this allows for a lower duty cycle. Two possible designs were considered. The first was to use the existing design idea of an FPGA providing the data. The second alternative was to use a high-speed memory combined by a small amount of logic, for example a CPLD, to control the memory. This section describes the selection process for this part of the design.

FPGAs are generally regarded as problematic in low-power applications because they are perceived to have long turn-on times and high current consumption. Most larger FPGAs are

volatile, meaning they do not store their configuration when powered down, which in turn means that they require external PROM chips that they must load their configuration from whenever they are powered on, which can take a relatively long time (on the order of several hundred milliseconds or more). In addition, FPGAs can draw on the order of several hundred mA or more while running. Therefore, an alternative solution was sought.

#### **4.2.1. High Speed Memory and CPLD**

The major alternative to FPGA-based designs was a system in which data is supplied directly from a non-volatile random-access memory. In such a system, some kind of address counter would be needed to control the address lines of the RAM, and a way to load a waveform into the RAM would be needed as well. This makes it clear that a smaller custom logic device such as a CPLD would be necessary. CPLDs have the additional advantage that they are usually nonvolatile, meaning they stay configured even when power is turned off and they power on very quickly. However, research into existing CPLD devices shows that despite these advantages, suitable devices are not available. A search across manufacturers such as Xilinx, Altera, Atmel, Cypress, Lattice Semi, Actel and Quicklogic showed that CPLDs offered generally have an I/O to speed tradeoff, the limits of which are just under the requirements for this system. This is due in part by the fact that the CPLDs researched do not support DDR, which means they must run at the full system speed of 300 MSPS. In addition, most common standalone memories, such as those available from Cypress or Micron, are not available in a size/speed combination that is appropriate for our applications. For example, the faster synchronous SRAMs offered by Cypress are available only at a minimum size of 9 MB, and a maximum speed of 250 MHz. The amount of data that needs to be supplied is small compared to this: 8192 16-bit samples give a total size of 131072 bits or 16 kilobytes. Finally, most of these SRAMs require on the order of several hundred milliamps while running, very similar to what an FPGA would consume. Therefore, it becomes clear that a “CPLD and RAM” solution may be too impractical and inflexible, and an FPGA solution would be optimal if its shortcomings can be overcome.

#### **4.2.2. Field Programmable Gate Array**

At WPI, the most experience has been gathered with FPGAs from Xilinx, and available support and experience are a large factor in deciding what vendor to choose. However, a search of some of the same manufacturers listed above, such as Altera, Lattice Semi and Quicklogic,

was made in order to determine what alternatives are offered by other manufacturers. In general, it appeared that the two manufacturers with the largest selection of FPGAs, Xilinx and Altera, actually have very similar offerings. For example, the Altera Cyclone series is very similar to the Xilinx Spartan series, and the Altera Stratix is similar to the Xilinx Virtex family in terms of size and speed, and most other features. Because of these similarities, it was appropriate to choose the Xilinx families, as they were already well-supported at WPI. These parts were investigated with respect to size, power, and speed.

As mentioned earlier, the major problem perceived with volatile FPGAs their configuration time when powered up. This is because most FPGAs are configured to use a serial configuration interface, and are commonly not run at their maximum possible configuration rate. However, most Xilinx FPGAs support an 8-bit parallel configuration interface called “SelectMAP” which can operate at speeds of up to 50 MHz. If we select a relatively small FPGA so that the configuration bitstream is kept small, such as from the Spartan-3 family, we can reduce the configuration times to acceptable rates. Figure 33 shows a table of configuration times for different Xilinx parts. Referring to the Spartan-3 datasheet [24], we see that the smallest FPGA that supports enough Block RAM for our purposes is the part XC3S200, with 216 Kbits. This FPGA can be configured in as little as 2.62 ms, which suits our purposes very well. Some work was done to confirm these configuration rates by measuring configuration times on a Spartan-3 demo board, which showed that at a 5 MHz configuration clock, serial configuration took 209 ms, which matches well with the times given in the table, which show configuration times at 50 MHz clock speed.

Table 7: Spartan-3 Configuration Data Frames and Programming Times

Device	# of Frames	Frame Length in Bits	Configuration Bits	Total # of Bits (Including header)	Approx. SelectMap Download Time (50 MHz) in ms	Approx. Serial Download Time (50 MHz) in ms	Approx. JTAG Download Time (33 MHz) in ms
XC3S50	368	1,184	435,712	439,264	1.10	8.79	13.31
XC3S200	615	1,696	1,043,040	1,047,616	2.62	20.95	31.75
XC3S400	767	2,208	1,693,536	1,699,136	4.25	33.98	51.49
XC3S1000	995	3,232	3,215,840	3,223,488	8.06	64.67	97.68
XC3S1500	1223	4,384	5,205,088	5,214,784	13.04	104.30	158.02
XC3S2000	1451	5,280	7,661,280	7,673,024	19.18	153.46	232.52
XC3S4000	1793	6,304	11,303,072	11,316,864	28.29	226.34	342.94
XC3S5000	1945	6,816	13,257,120	13,271,936	33.18	265.44	402.18

Figure 33: Xilinx Spartan-3 Configuration Times (Source: Xilinx XAPP452)

Next, it was investigated whether the XC3S200 is capable of operating at speeds fast enough to support our 300 MSPS operation. A test design for logic to supply waveform data was implemented in the Xilinx design environment based on the final design that is described in Section 4.3.3. This design operates using double data rate transmission, requiring the maximum clock speed in the design to be only half the sampling rate. Using the Spartan-3 datasheet and the Xilinx design tools, it was determined that the maximum speed that the design could run at was 212 MHz. This shows that the Spartan-3 is indeed capable of operating fast enough, if we assume DDR operation. In fact, we see that theoretically, operation of up to 400 MSPS (the limit of the DAC), or 200 MHz DDR clock rate, would be supported by this design, which is much more than the required 300 MSPS. As the Experimental Results chapter will show, this was indeed possible.

Finally, the expected current draw by this design was considered. Using a combination of the datasheets and the Xilinx XPower tool, we the design used for testing above was analyzed. For this design, the XC3S200 was estimated to draw about 329 mA. While this value seems high, one must consider that due to the short configuration times of the FPGA, a low duty cycle can be achieved. If we assume that we will be using the “10 ms time slot” system developed in Chapter 3, and we estimate a start-up time of the digital section of about 5 ms (which includes the FPGA configuration time of 2.62 ms), we see that the duty cycle of the FPGA circuitry can be reduced to as little as 1.5%. This will be discussed in detail in Section 5.2.2.

One should note that Xilinx offers a “low-power” version of their Spartan-3 FPGAs, known as Spartan-3L, which generally are very similar to the Spartan-3 series except that they draw somewhat lower currents, and have a special “hibernate” mode. However, if one reads the datasheets in detail, the advertised “hibernate” mode is nothing more than actually powering off the FPGA. The smallest device in this series is the XC3S1000L, which has five times the logic resources of the XC3S200, resulting in a longer configuration time, and some of the current-saving advantages are lost. In addition, these devices are only available as ball grid array packages, which we would like to avoid, as we will see below. Therefore, it seems that the XC3S200 was indeed the optimal choice.

### **4.2.3. FPGA Configuration**

In order to support the SelectMAP parallel configuration, the Xilinx XCF-P series PROMs must be used. The smallest of these is the XCF08P, which can hold up to 8 Mbits of configuration information. Although this is relatively large compared to the required bitstream



size of about 1 Mbit, it is the smallest available PROM that supports SelectMAP configuration and therefore the advantage of faster configuration is greater than that of some wasted resources. New designs can be programmed into this PROM using the provided JTAG programming interface, which is also supported by the FPGA and the Xilinx tools. Although the PROM features the ability to generate a configuration clock, in order to achieve the highest possible configuration rate of 50 MHz, an external oscillator must be used to drive the PROM (which in turn provides the configuration clock to the FPGA). Adding a 50 MHz oscillator also has the advantage of being able to route this clock signal to the FPGA for use as a system clock in cases where the DAC's clock is not functional.

#### **4.2.4. Package Selection**

The XC3S200 is available in four different package options, ranging from a 100-pin quad flat pack to a 256-pin ball grid array package. While the larger packages generally support a higher package density and a higher user I/O count, they have the disadvantage that one cannot mount them by hand, or debug or modify them without difficulties. Therefore, it was decided that the smallest possible package should be used. Two limiting factors in this case are the number of available I/O pins, and the support for simultaneously switching outputs (SSO). SSO guidelines state that in order to prevent large ground bounce, the number of simultaneously switching pins per pair of  $V_{CC0}$ -GND connections on the package must be limited. For the smallest available package, known as VQ100, and the LVDS standard, this limit is seven switching pin pairs per I/O bank. As the banks of the VQ100 package only support three or four pairs of LVDS pins, this limitation should not affect this package. However, one must take care when judging the total number of I/O pins available. The VQ100 package has many pins with dual functions, such as some pins for “digitally controlled impedance” (DCI), or for reference voltages for specific I/O standards, or for configuration. Although our design uses no DCI or I/O standards that require reference voltages, we must keep in mind that by using the parallel SelectMAP configuration, we are occupying more pins than a serial configuration would. Subtracting the pins needed for configuration and the power supply and ground pins, there are 51 user I/O pins remaining. In our design, we require at least 18 differential pairs to connect to the DAC (16 data and two clock lines), and we see that this requirement is satisfied. Finally, it is important to note that because the design will be operating close to the speed limitations of the FPGA, one should select the latest revision of the FPGA (Rev. E) and the highest available speed grade (-5) for best

performance in terms of items such as slew rate, DCM performance, and LVDS I/O standard performance.

Having selected the major components of the system, the FPGA and the DAC, details of the design of the Digital Waveform Generator hardware will now be presented.

### **4.3. Hardware Implementation**

In this section, some of the details of the hardware design of the Digital Waveform Generator boards will be presented, including issues such as power control, interfaces, PCB layout, and FPGA design.

Figure 34 shows an overview of the components in the Digital Waveform Generator. The most important of these, i.e. the FPGA, configuration PROM, DAC, and DAC clock generation, have already been discussed in previous sections. As is apparent from this diagram, the power distribution for this board is somewhat complex, as there are several different supply voltages required by the DAC and FPGA. In addition, it was decided to separate the power supplies of the analog and digital portions of the board in order to avoid noise passing between these parts of the board; these will be referred to as the “analog” and “digital” portions of the system, as shown in the figure. The power system will be discussed in more detail below.

An element of this diagram that has not previously been mentioned is the level shifter. It was decided to include a MAX3001E bi-directional level shifter because the FPGA’s I/O banks are operating on 2.5 V, and it will most likely be necessary to interface to hardware that operates on higher voltage levels, such as the Data Channel hardware or the digital interfaces of the DAC and PLL, which all operate on 3.3 V. The level shifter is connected to a total of eight free pins on the FPGA. A 3.3 V supply line can even be passed from the analog power supply to the level shifter. This has the advantage that the FPGA can program registers as necessary on the DAC and the PLL without the need for an external board, such as the Data Channel, performing this task.

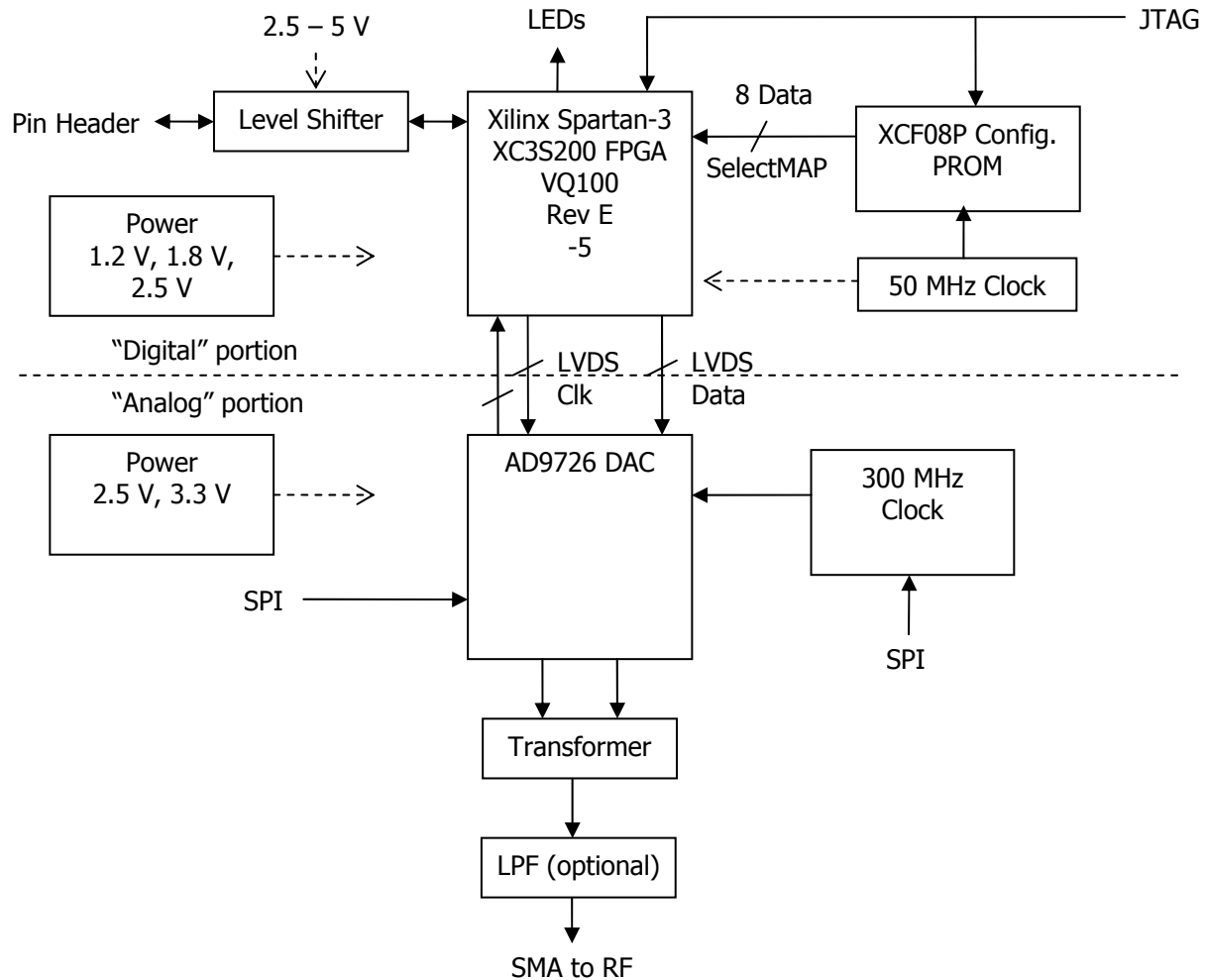


Figure 34: Digital Waveform Generator Block Diagram

#### 4.3.1. Power Supply Design

An important feature of the waveform generation hardware is to save power by shutting down when it is not needed. Therefore, special attention must be paid to the power distribution system of the board. There are several voltages required by the different components of the board: the FPGA requires 1.2 V and 2.5 V, the PROM requires 1.8 V and 2.5 V, and the DAC and various other components require 2.5 V and 3.3 V. We would like to be able to power down the PROM separately from the FPGA when it is not needed. In addition, the 50 MHz oscillator that supplies the configuration clock to the PROM should optionally stay enabled when the PROM is powered down, in case it is being used as a system clock for the FPGA as well. Figure 35 shows a distribution system for the digital components of the system that accommodates these requirements. For the analog components in the system, shown in Figure 36, no special

separation of the power supplies is needed, because all components of the analog system will be enabled together during normal operation.

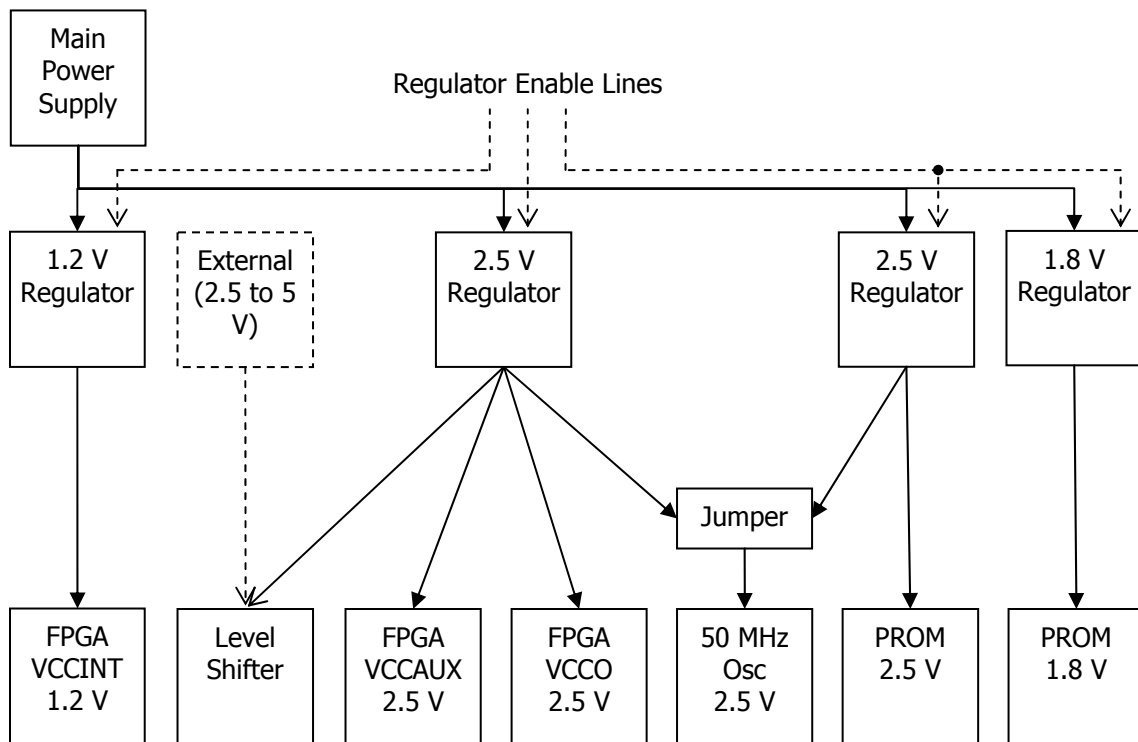


Figure 35: Digital Side Power Distribution

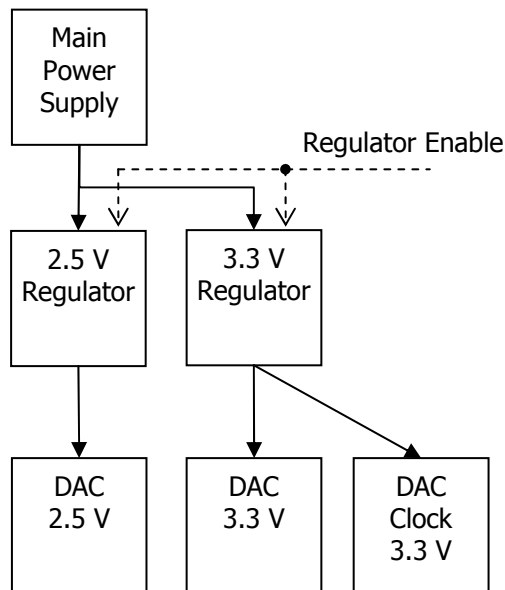


Figure 36: Analog Side Power Distribution

We see from this design that a total of four regulators are required for the digital portion and two regulators are required for the analog portion. Table 12 shows estimates of current

consumption values that we can use to judge what current flow these regulators must support. Note that some elements of the system were not included, such as debug LEDs, or the level shifter (which consumes only about 1 mA). In addition, some of the estimates in this table are based on tools such as the Xilinx XPower analysis tool, and may change as the design is changed. Therefore, we must design with a safety margin in mind in case a component draws more current than expected.

Device	Voltage	Typ. (mA)	Max. (mA)
FPGA	1.2 V	57	80
FPGA	2.5 V	272	
50 MHz Osc.	2.5 V		30
PROM	1.8 V	10	
PROM	2.5 V	40	
DAC Clock	3.3 V	15	18
DAC	2.5 V	141	158
DAC	3.3 V	68	78

**Table 12: Current Consumption Estimates**

Table 13 shows the regulators that were chosen based on these requirements. Each of these regulators features an individual enable line. It was decided to tie together the enable lines for the analog section, as all components will be powered on together, as previously mentioned. In addition, the enable lines for the PROM were tied together. The FPGA enable lines were left separate because one of the regulators has an active high enable line, while the other has an active low enable line. In addition, it is recommended to enable the FPGA's 2.5 V supply before enabling the 1.2 V supply to prevent current surges [24]. The four resulting enable lines are brought out on a pin header to allow the required power sequencing to be generated by an external source, such as the Data Channel board.

Power Supply	Regulator	Max. Current
FPGA 1.2 V	TI TPS76912	100 mA
FPGA 2.5 V	TI TPS79525	500 mA
PROM 1.8 V	TI TPS76918	100 mA
PROM 2.5 V	TI TPS76925	100 mA
Analog 2.5 V	TI TPS71202	250 mA
Analog 3.3 V	(dual-channel)	(each channel)

**Table 13: Regulator Selection**

### **4.3.2. PCB Design**

As previously mentioned, it was decided to separate the analog and digital portions of the waveform generation hardware in order to prevent electrical noise leaking between the two portions, especially to prevent digital switching noise from leaking to the analog components. To this end, it was decided to also physically separate the two sections of the design onto two sides of the PCB being designed. This has the advantage that with a multi-layer PCB, ground planes can be used to protect the two sides from noise. It was decided to implement a six-layer PCB for optimal separation and to route the many signal and control lines. The layers were defined as follows:

- Layer 1 (Top): Digital components and routing
- Layer 2: Digital power and some routing
- Layer 3: Ground plane
- Layer 4: Analog power and some routing
- Layer 5: Ground plane
- Layer 6 (Bottom): Analog components and routing, also flooded with ground copper

This separation of the layers gives another advantage. Both the DAC and the FPGA packages are of the quad flat pack style, with 80 and 100 pins, respectively. The only connections passing between the analog and digital side, other than the main power supply and the previously mentioned connection to optionally supply 3.3 V to the level shifter from the analog side (which is heavily decoupled), are the LVDS connections to and from the DAC – sixteen data pairs and two clock pairs. Investigating the pin layout of the packages, which are shown in Figure 37, it is clear that the possibility exists to mount the two devices directly “back-to-back” on the top and bottom layer of the PCB in order to minimize the length of the traces.

This approach was taken, and it was possible to route all LVDS lines in this fashion. Figure 38 shows a part of the finished layout, in which several trace pairs (circled in dashed lines) routed in close quarters between the FPGA and the DAC can be seen. It is important to keep the lengths of all LVDS lines very similar, in order to minimize skew across the data and between the individual pairs themselves. The trace length across all LVDS lines was measured to be approximately  $275 \pm 69$  mils, which is small enough to prevent any skew problems.



to the pins as possible, but with this design that is clearly not possible. However, care was taken to place the decoupling capacitors as close to their power and ground pins as possible.

Figure 39 shows the top “digital” side of a completed Digital Waveform Generator PCB. One can see the FPGA in the bottom right and the PROM in the bottom left portion of the board. The three SMA connectors are connections for supplying an external 10 MHz reference for the PLL, supplying an alternative input for the DAC clock (such as via a signal generator), and the DAC output. The pin headers on the board interface to such things as the PLL and DAC’s SPI ports, the board’s JTAG chain, and the level shifter, which is connected to the FPGA. Connections from the FPGA to the SPI interfaces of the PLL and DAC can be established simply by placing a jumper cap on the respective pins of the two ten-pin headers that can be seen at the left of the board.

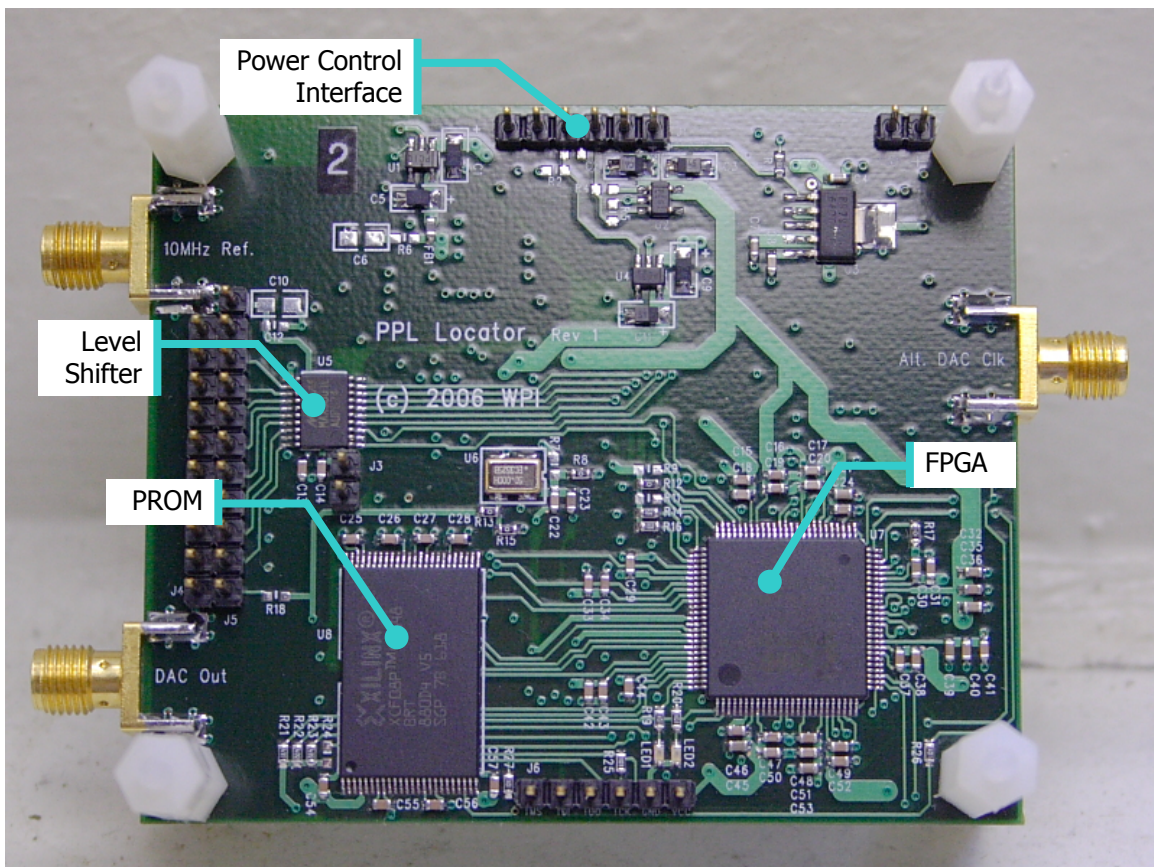


Figure 39: Completed Digital Waveform Generator Board, Top (Digital) Side

Figure 40 shows the bottom “analog” side of a completed Digital Waveform Generator PCB. One can see the DAC is on the lower left, with the clock generation circuitry occupying the upper half of the board.



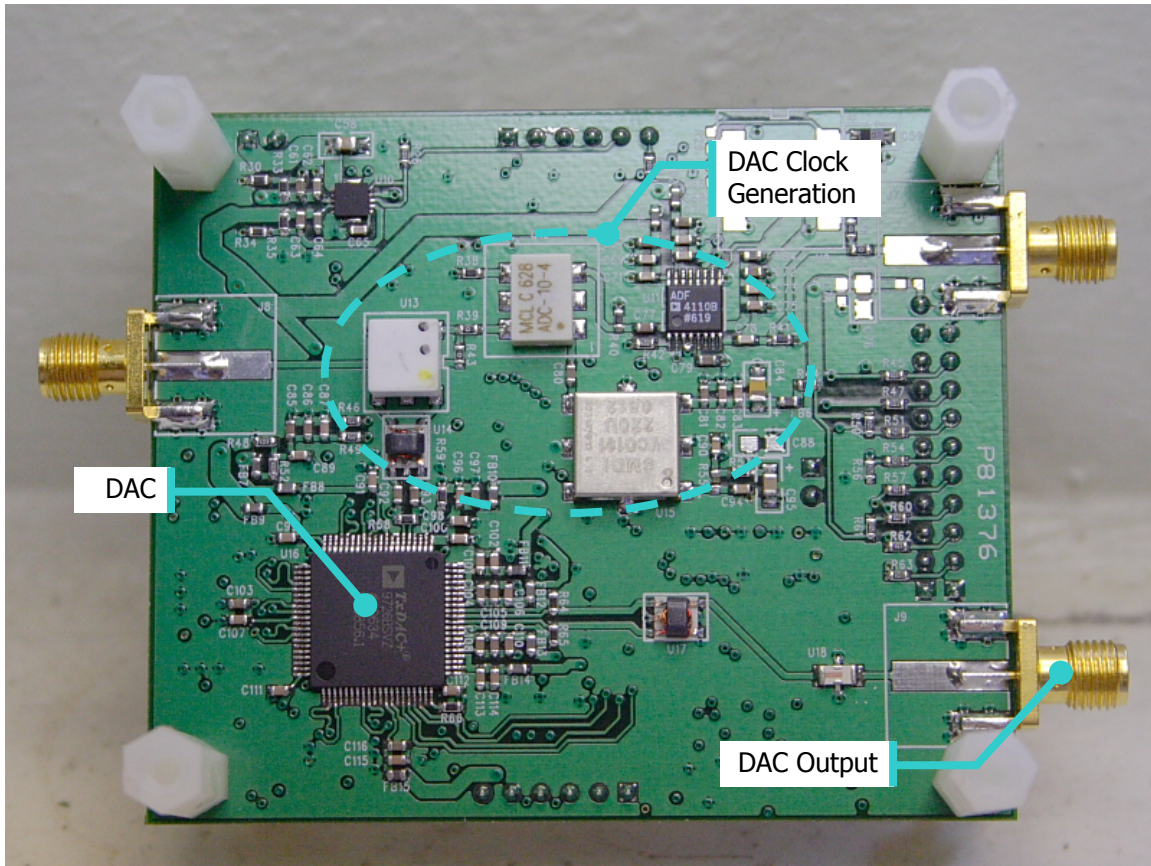


Figure 40: Completed Digital Waveform Generator Board, Bottom (Analog) Side

#### 4.3.3. FPGA Digital Design

Finally, we will describe the design of the hardware that is instantiated inside the FPGA that generates the waveform data for the DAC. The basic principle of the hardware is that the waveform data is loaded from a block memory, which is controlled by an address counter that is simply an up counter. However, we must support speeds of up to 300 MSPS, and this requires DDR operation in the FPGA. In this type of data transfer, data is provided on both the rising and the falling edge of the clock signal, which therefore has half the frequency of the sampling rate. This is illustrated in Figure 41.

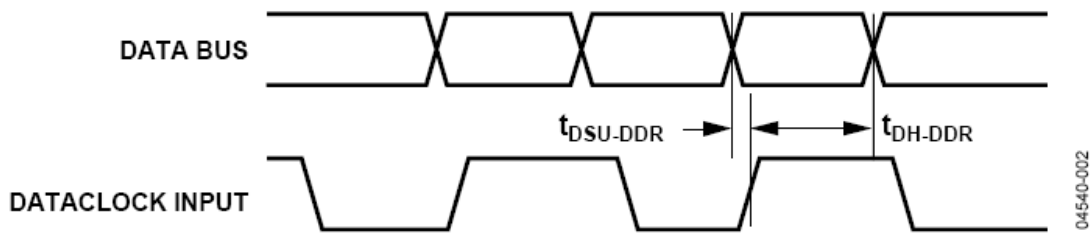
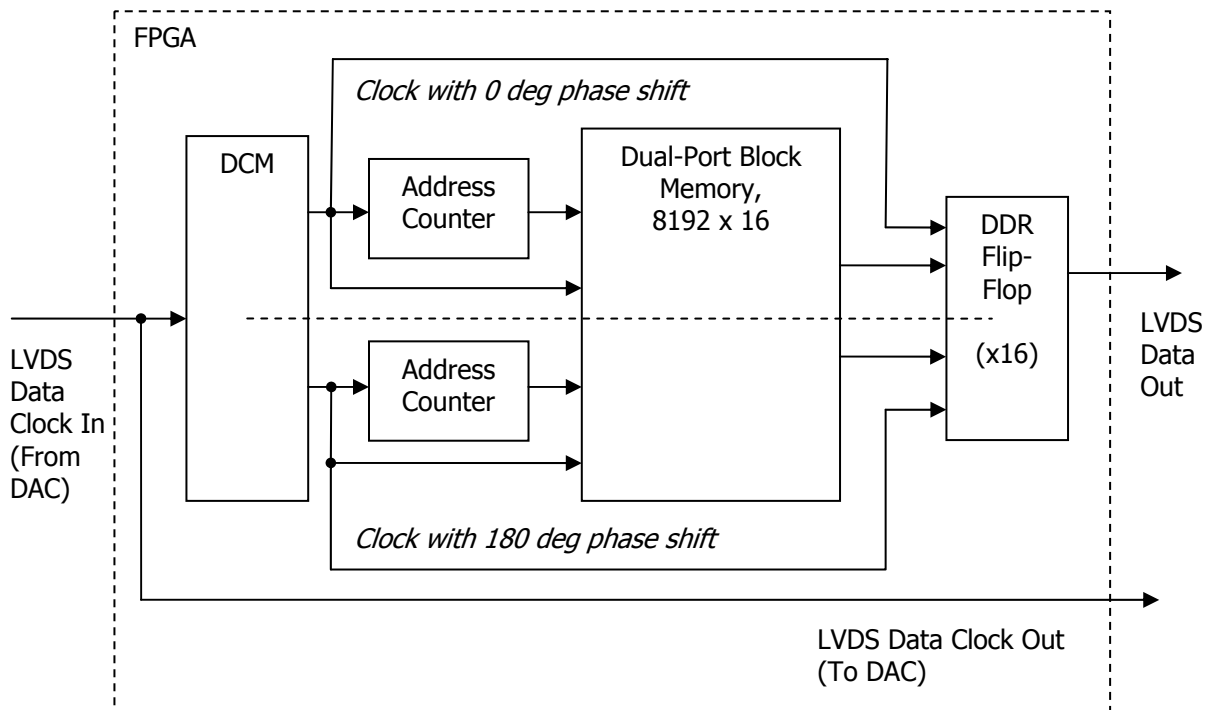


Figure 41: DDR Timing Diagram (Source: AD9726 Data Sheet)

DDR can be implemented with a special type of flip-flop that is supported in hardware by the Spartan-3 series, which accepts two data and clock signals that are 180 degrees out of phase, and outputs a data stream consisting of the two “merged” data signals by sampling each data input at the rising edge of its respective clock input. Therefore, we see that the logic that provides data to this flip-flop can simply be rising-edge clocked at half the frequency of the output data, and this logic can be replicated to form the two inputs to the DDR flip-flop.

In the design for the Digital Waveform Generator, which is shown in Figure 42, a Spartan-3 Digital Clock Manager is used to create the two clock signals, which are 180 degrees out-of-phase, and then these two signals are used to drive an address counter each, which in turn accesses a dual port block memory that contains the waveform data. The data is then loaded from the dual-port memory into the DDR flip-flop, where it is combined into one data stream.



**Figure 42: FPGA Internal Hardware Design**

One issue that had to be kept in mind is that at the output of the FPGA, the data bus must be aligned to the data clock. To verify the alignment, a second Spartan-3 Digital Clock Manager was instantiated in the FPGA and configured to add a variable phase shift to the data clock leaving the FPGA. By phase shifting the data clock, one could observe the behavior of the DAC output, as noise on the DAC output indicates a misalignment of the data bus and data clock. Using this method to determine the characteristics of DAC output when the data clock and data

bus are aligned showed that in the above design the signals were indeed well aligned, as there was no additional noise on the DAC output.

As will be shown in the Experimental Results chapter, this design works successfully, both in terms of power consumption and waveform generation, at speeds of up to 400 MSPS, thereby exceeding the required sampling rate and allowing for generation of signals of up to 200 MHz bandwidth.

## **Chapter 5. Experimental Results**

This chapter presents the results of tests that were performed to confirm the functionality and characterize the performance of both the Data Channel and Digital Waveform Generator printed circuit boards. The Data Channel boards were designed to provide wireless, bi-directional communications in order to implement a time-division multiplexing protocol that allows for multiple Locators to be used in the PPL system at once and that communicates commands and status information. The Digital Waveform Generator boards were designed to generate the custom ranging signal waveform with 150 MHz bandwidth while consuming as little power as possible. The tests described in this chapter verify that the design of this hardware, as described in the previous chapters, was successful.

### **5.1. Data Channel**

Tests were performed on the Data Channel boards to verify that they are functioning correctly, to characterize their performance with respect to factors such as baud rate and antenna configuration, and to verify that they can indeed be used to implement the TDM system for supporting multiple Locators. First, the characterization of the hardware performance will be described. Then, extensive tests that measure both the performance of the RF communications and the accuracy of the microcontroller's timers are presented, followed by the results of the proof-of-concept implementation of the Data Channel TDM protocol.

#### **5.1.1. Hardware Performance**

During February and March 2006, a total of ten Data Channel boards were populated and tested, and all were shown to function within expected parameters. The boards were numbered #1 through #10, and each board was characterized with respect to current consumption and RF characteristics. The following characteristics were measured, averaged across all boards, and verified against expected values from part datasheets. Note that all current measurements were performed at the main power supply input, so some approximations regarding the contributions of different modules had to be made.

- Basic Current: 3 mA (only MSP430 running at 4 MHz)
  - Analog Circuitry (accelerometer and conditioning circuit): 0.6 mA
  - Each LED: 4.1 mA

- Xemics module in Transmit mode (15 dBm): 62 mA
- Xemics module in Receive mode: 15 mA
- Transceiver Module (tested at a nominal center frequency of 915.05 MHz and 4800 baud)
  - TX Power: 14.3 dBm
  - RX Sensitivity: -111.2 dBm
- Other Specifications
  - Voltage References confirmed at nominal voltages of 3.3 and 3 V
  - Estimated Lifetime of three Energizer EN91 batteries: 600 hrs at 10mA, 150 hrs at 30 mA, 60 hrs at 70 mA
  - Weight: 4.6 oz including batteries and antenna

In addition, the functioning of the accelerometer was tested both by measuring different test points on the board, as well as by using code on the MSP430 to read the output of the movement detection circuit and display it on a PC via the RS232 interface. A similar test involving the serial interface was performed with the temperature sensor and the battery voltage reading.

In terms of battery life, one should note that when the entire board is in “sleep mode”, i.e. all hardware except for the 32.768 kHz crystal is powered down, it should consume only on the order of a few  $\mu\text{A}$ . The crystal must stay enabled in order to keep the timers on the MSP430 running, because only the timers can trigger an automatic wake-up of the microcontroller and therefore the rest of the board. Using the battery life values given above, one can see that even if the board were to be operated at full transmit power constantly ( $\sim 65\text{mA}$ ), it can run for several days, and if the radio communications are reduced and power-saving modes are used, the boards can even run for months on one set of batteries.

### **5.1.2. Outdoor / Indoor Range Tests**

The goal of this test was to compare Packet Error Rates (PERs) at different data rates and antenna configurations when communicating from outside a building to the inside. This test was also used to confirm coverage of a building in the indoors-only environment.

The firmware for this test operates the boards in one of two modes, “master” or “slave”. The master board transmits a configurable number of packets each time the distress button is pressed (for this test 128), and waits for a response from the slave for each packet sent. Each

packet has a known format: it begins with a single ID byte that is used to keep track of which packets were transmitted during each run (in this test, a different ID was used for each location tested), and then contains a configurable number of bytes with the same pattern (for this test, 9 bytes of 0xAA were used). The slave board continuously attempts to receive packets (for 0.1 s at a time, with a very brief delay on the order of microseconds in between each receive attempt). For each received packet, it analyzes the packet for correctness, and if the packet is correct, it sends an identical packet as a response.

Board #3 was used as the master, and board #4 was used as the slave. The slave board was placed inside a cardboard box in the back window of a car. The car was parked in various locations around the Atwater-Kent building (see Figure 43), once on Salisbury Street (the “Street” location), and once behind the building (the “Back” location). For the indoors-only variation of this test, the slave was left on a desk in AK301a (the “Lab” location). The master was carried throughout the building. In the measurements for this test, “Front” indicates the hallway in AK that is parallel to and closest to Salisbury St., and “Back” indicates the corresponding hallway in the back of AK. All tests were done with the board in motion (normal to fast walking speeds), and the board was walked almost the entire length of each hallway with measurements being taken almost continually.



**Figure 43: Slave “Street” (left) and “Back” (right) Location**

The antenna configuration for this test was varied among half-wave (HW) and quarter-wave (QW) antennas, as was the data rate (4800, 9600, 19200, 38400, and 76800 baud). No attenuators were used for the antennas to achieve maximum range. A total of ten runs were performed, with the configurations shown in Table 14.

Run #	Baud Rate	Slave Location	Slave Antenna	Master Antenna
1	4800	Street	QW	QW
2	9600	Street	QW	QW
3	19200	Street	QW	QW
4	38400	Street	QW	QW
5	76800	Street	QW	QW
6	4800	Street	HW	QW
7	19200	Street	HW	QW
8	9600	Street	HW	HW
9	19200	Back	QW	QW
10	19200	Lab	QW	QW

**Table 14: Outdoor / Indoor Test Runs**

Raw test results are presented in Table 20 in Appendix A. Some other things to note are that the outside temperature during the tests was approximately 3°C and the battery voltage of the boards was regularly checked and confirmed to be in the range 4.4 to 4.9 V.

From runs 1-5, we can draw performance comparisons concerning the baud rate, as shown in Figure 44. During these tests, a clear increase of performance was noted in runs 1-5 in the “Back” locations when the master was near one of the corridors that connect the back hallway to the front hallway of AK on the second and third floors.

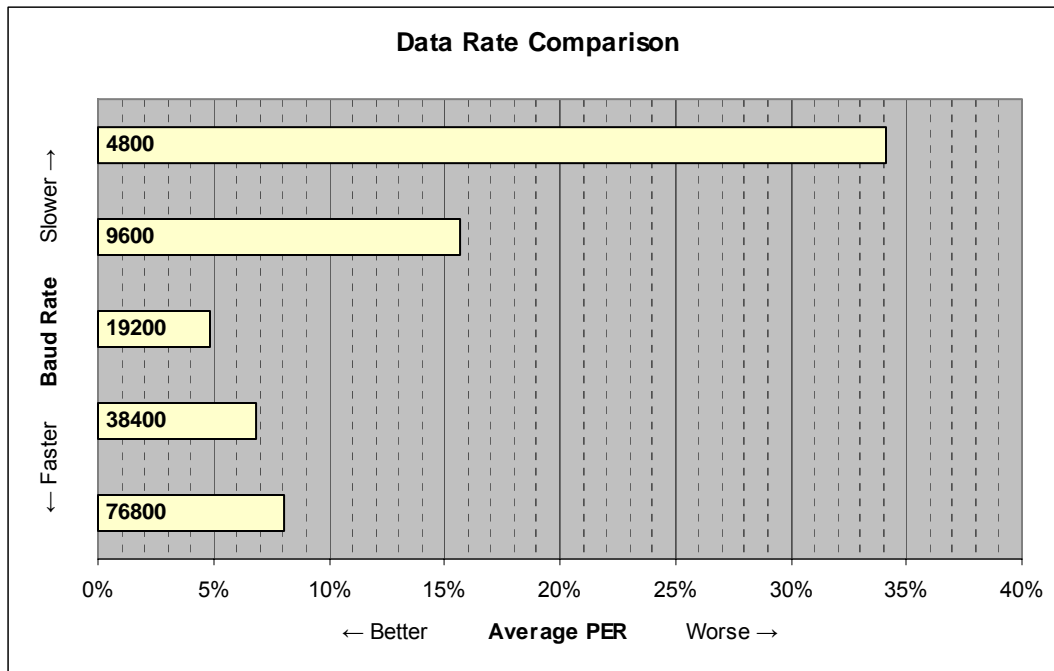


**Figure 44: Range Test Data Rate Results**

The relatively poor performance at 4800 and 9600 baud is surprising (compare to Section 5.1.4). However, one should keep in mind these tests measured packet error rate, as compared to bit error rate, meaning that a single bit error in a packet would cause the entire packet to be recorded as invalid. Therefore, it is possible that at lower data rates, because time to transmit one packet is longer, the chance for interference simply is higher. At the higher data rates, the behavior is as expected, with the performance decreasing slightly for the higher data rates. The optimal data rate is clearly 19200 baud.

Because runs 3-5 exhibited the expected data rate vs. PER relationship, we will use those runs to compare PER vs. distance, as shown in Figure 45. One should note that although this was not recorded in detail, communication was confirmed to be possible to the back entrance of AK during all test runs; this was especially confirmed during run 8 (HW/HW) from the “Street” to the “Back” location – therefore verifying that two units, both outside the building, would be able to communicate with each other.

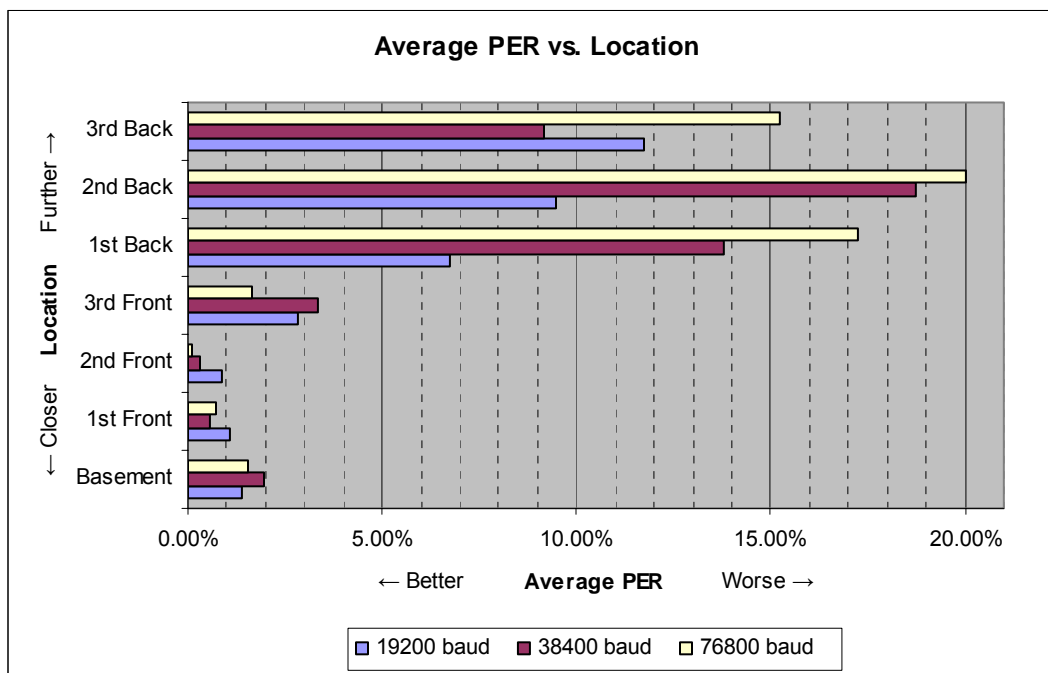


Figure 45: Range Test Distance Results

The performance decrease versus increasing distance is as would be expected, although the weaker performance on the second floor back hallway at higher data rates is somewhat surprising; it is possible that it may be due to the configuration of the building.



During runs 6-8, the antenna configuration was varied, and the results of this comparison are shown in Figure 46. Note that the graph bars are labeled in the order “Master / Slave”, and that this plot is intended to show a comparison of three pairs of antenna configurations. The QW/QW vs. QW/HW comparisons were performed for the worst and best-case data rates. The QW/QW vs. HW/HW comparison was performed at data rate of 9600 baud; this was selected because it is neither very good (because it may be difficult to see an increase in performance) or the worst (to avoid the possibility of the worst-case actually being due to some kind of system problem). In addition to these tests, a subjective but clear increase in performance was noted in a quick check of the HW/HW configuration at 19200 baud from the street to the third floor back hallway. A full HW/HW test at 19200 baud was not run because this antenna configuration is unlikely.

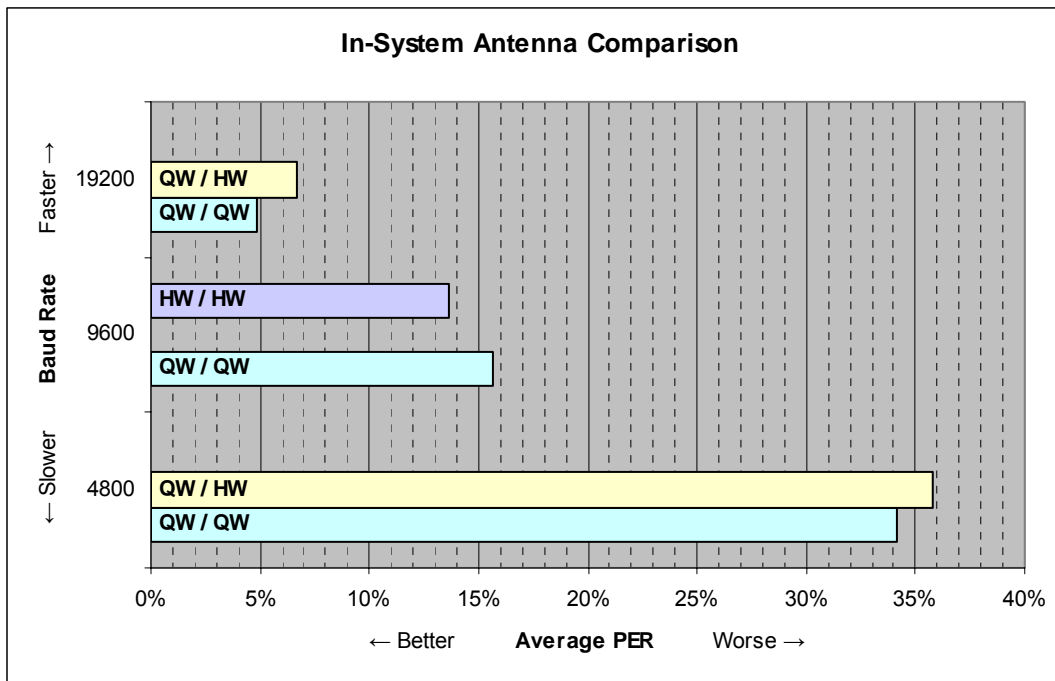
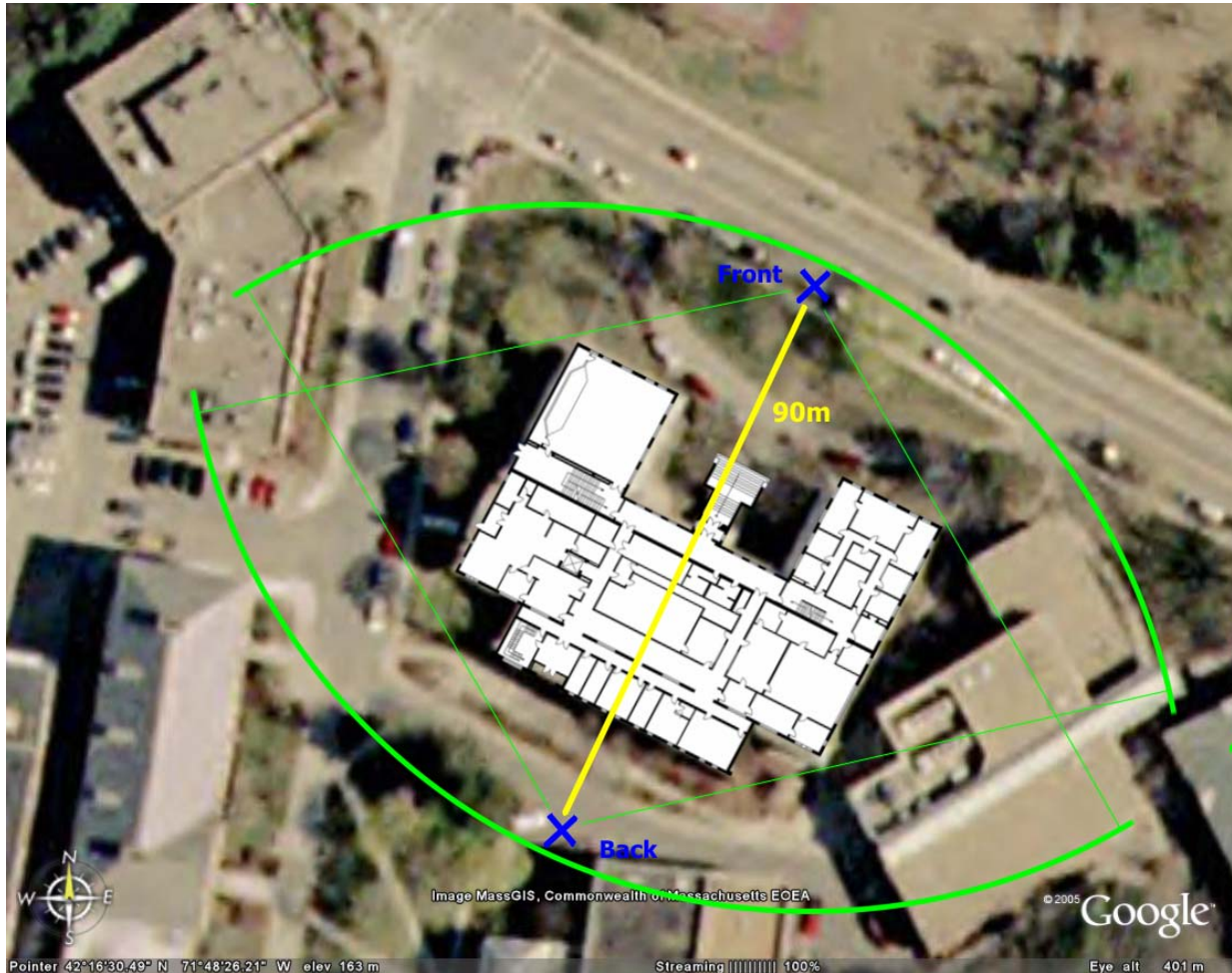


Figure 46: Range Test Antenna Results

In terms of antenna configuration, the results – although the decreased performance of HW/QW vs. QW/QW is surprising – match well with those of the Antenna Configuration Test (see Section 5.1.5).

Runs 9 and 10 were intended to show coverage of the Atwater-Kent building at the optimal data rate and antenna configuration of 19200 baud and QW/QW antennas. Figure 47 shows an overview map of the building and surrounding area, with the “Front” and “Back”

locations plotted. The arches in the plot indicate the coverage of the entire building. Note that although this test only confirms a total distance of 90 m, several separate tests were performed to confirm a coverage range of up to 100 m.



**Figure 47: Range Test Results Overview Map**

This test shows that the entire Atwater-Kent building can be covered at 19200 baud (and most likely at higher rates) with the QW antennas from Salisbury Street, the Salisbury Labs building, and from inside the building (AK301a).

In general, this series of tests confirms expected behavior of the boards, except in a few cases as noted. One should note that these tests consisted of measurements of the packet error rate, meaning that absolutely no bit errors were allowed in each packet, and each packet had to make a full round-trip. Therefore, the addition of forward error correction to the protocol should result in a better test result with more robust communications, which is an item that should be performed as future work.

### 5.1.3. Outdoor Range Test

This test intended to confirm that the boards could communicate over a minimum of about 800 m ( $\frac{1}{2}$  mile) outdoors, with the units being within line-of-sight of each other.

The set-up for this test was very similar to the Outdoor / Indoor Range Tests (Section 5.1.2). The same firmware and boards were used, with the slave placed in the same way in the back window of a car and the master carried in the same manner. The car with the slave board was parked in a parking lot on a hill on Highland St. between Lancaster and Tuckerman (aka. Harvard) St., this gives a more or less straight-line view down Highland St. to the west for over 1 km, as shown in Figure 48. The distances were measured using Google Earth [11] from the parking lot to the far sidewalk corner of each street, where the master was located during each measurement. This test used different quarter-wave antennas, which were shipped with the ChipCon evaluation boards. The same half-wave antennas were used as in the previous range test, and again no attenuators were used. The data rate was fixed at 19200 baud.



**Figure 48: Outdoor Range Test Locations**

Raw results are shown in Table 21 in Appendix A; these results are plotted in Figure 49 below. One should note that because the QW/QW configuration was showing a continuously dropping performance, the test was aborted before reaching the full test range. During all tests, the parking lot was in line-of-sight of the board, however, there may have been parked cars, lampposts and traffic lights in the path. There was intermittent traffic on Highland St. during the test, although, subjectively, it did not seem that passing traffic affected communications.

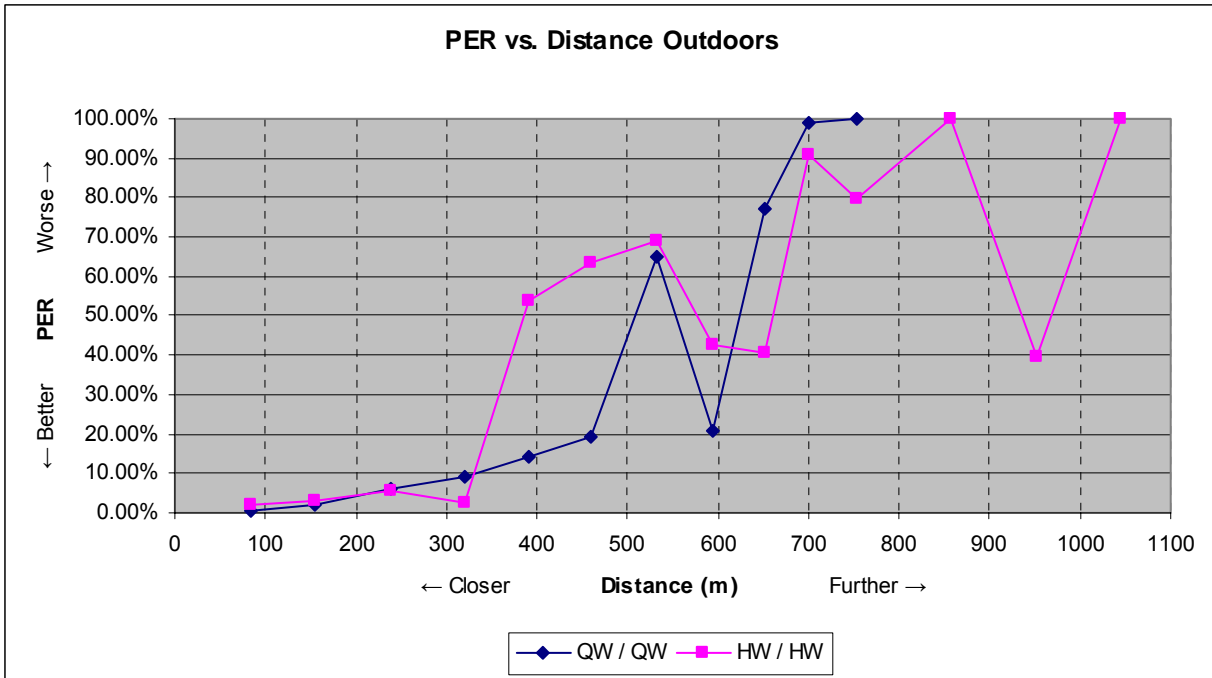


**Figure 49: Outdoor Range Test Results**

The results of this test show that with the QW/QW configuration, the boards can communicate over about 600 m, and in the HW/HW configuration apparently for almost a full km. In the latter configuration, the drop in performance between about 400 and 550 m may be explained by more parked cars and larger buildings around West Street, and the reason for sudden increase in performance at about 950 m (or, conversely, the drop in performance before this location) is not quite clear. Overall, these results show that the boards are able to communicate outdoors over a range of at least 600 m. As in the previous section, one should keep in mind that these tests were performed without any kind of error correction, so the addition of this feature will most likely cause a decrease in the packet error rates that were measured in this experiment.

#### **5.1.4. Data Rate vs. Receiver Sensitivity Test**

This test intended to measure receiver sensitivity at different baud rates as a follow-up test to compare to the results of the Range Tests. This test is similar to that performed to measure the receiver sensitivity of the boards after they were populated, except that the data rates were varied.

A signal generator was set to a center frequency of 915 MHz with FM modulation and a modulation rate of half the baud rate, except at 38400 and 76800 baud, where a modulation rate

of 9600 was used because the signal generator has a limitation of 10 kHz on the modulation rate. The frequency deviation was set to 100 kHz. An oscilloscope was used to observe the raw clock and data output of the Xemics module on board #3. The signal generator amplitude was increased from -120 dBm until no more errors were observed (by visual inspection) on the output data.

See Figure 50 for a plot of the results. These measurements are compensated for a loss through the cable measured to be about 1dBm.

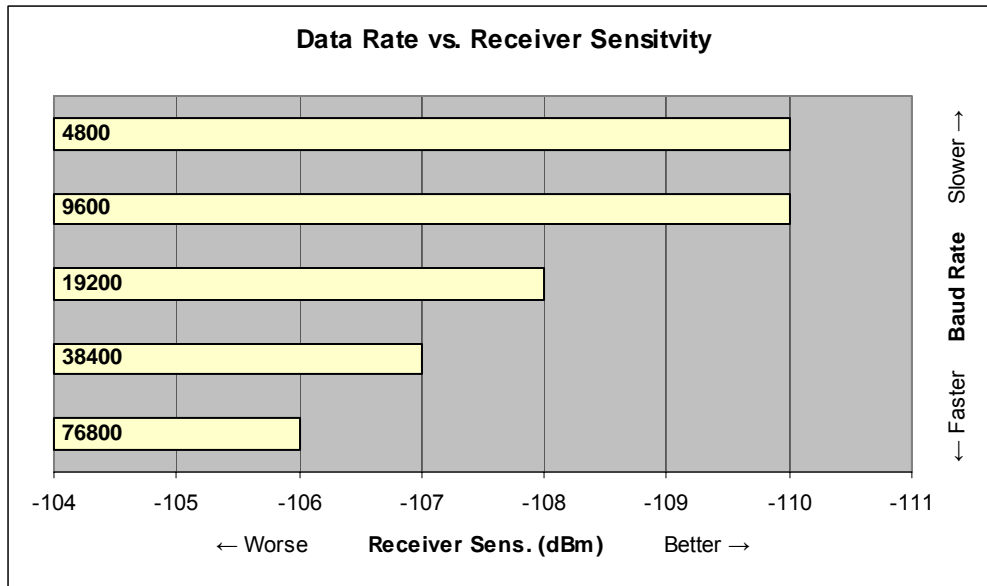


Figure 50: Data Rate vs. Receiver Sens. Results

This test confirms the generally expected relationship of decreased receiver sensitivity for an increased data rate; however, this decrease is only fairly small. Because these results do not explain the decreased performance at 4800 and 9600 baud in the Range Tests in Section 5.1.2, we can assume that the longer transmit time of the packets at those baud rates simply gave a bigger chance for interference during those tests, resulting in the higher packet error rate.

### 5.1.5. Antenna Configuration Test

This test intended to compare the performance of different antenna combinations on transmitter and receiver. This is a follow-up test to compare to the results of the Range Tests in Section 5.1.2.

Antennas were attached to each a signal generator (thus acting as a transmitter) and a spectrum analyzer (acting as the receiver), similar to what is shown in Figure 51. The signal

generator was set to transmit a 915 MHz signal at 15 dBm, and the average amplitude of the received signal was measured at the spectrum analyzer.

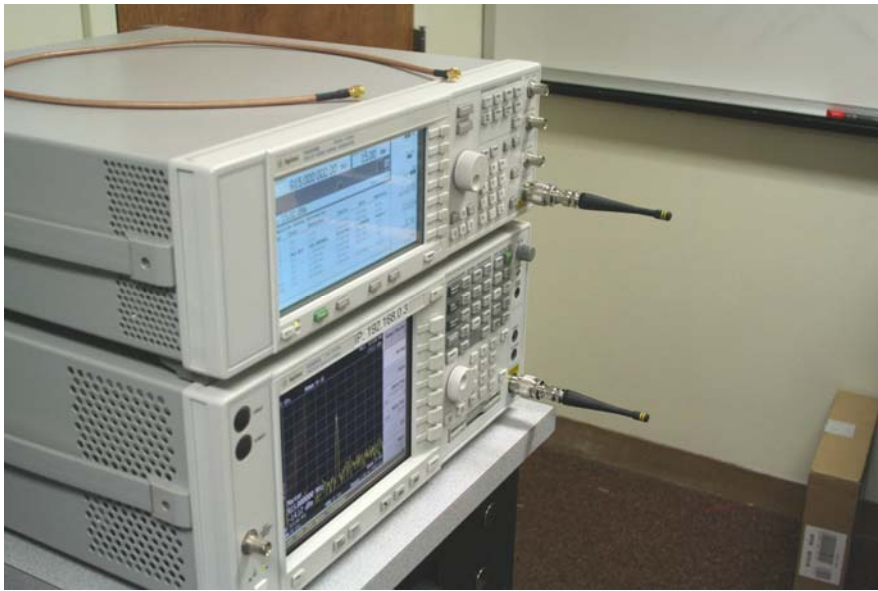


**Figure 51: Antenna Configuration Test Set-Up**

See Figure 52 for a plot of the results. The antennas labeled as “QW2” are the antennas that were shipped with the ChipCon evaluation boards, and the “RH” antenna is the reduced-height antenna (part nr. ANT-916-CW-RH from Linx Technologies). The other antennas are those ordered from “Antenna Factor”: The “HW” half-wave is part nr. ANT-916-CW-HW and the “QW” quarter-wave is part nr. ANT-916-CW-QW.

Although the expected result that the HW/HW configuration is better than the QW/QW configuration was confirmed, and these results match well with the results of the Range Tests, there are several surprising results. The difference in the QW / HW configuration, which was not shown in an earlier test, was confirmed in two separate reruns of that test. Apparently, mismatches in the antenna size cause a decrease in performance. The reduced-height antenna performs relatively well. The improved performance of the “QW2” antennas that were shipped with the ChipCon kits led to the investigation of obtaining more of these antennas to replace the existing antennas. Since it is unlikely that the half-wave antennas will be used on the Locator devices due to their size, it seems that using only quarter-wave antennas throughout the system would be optimal.

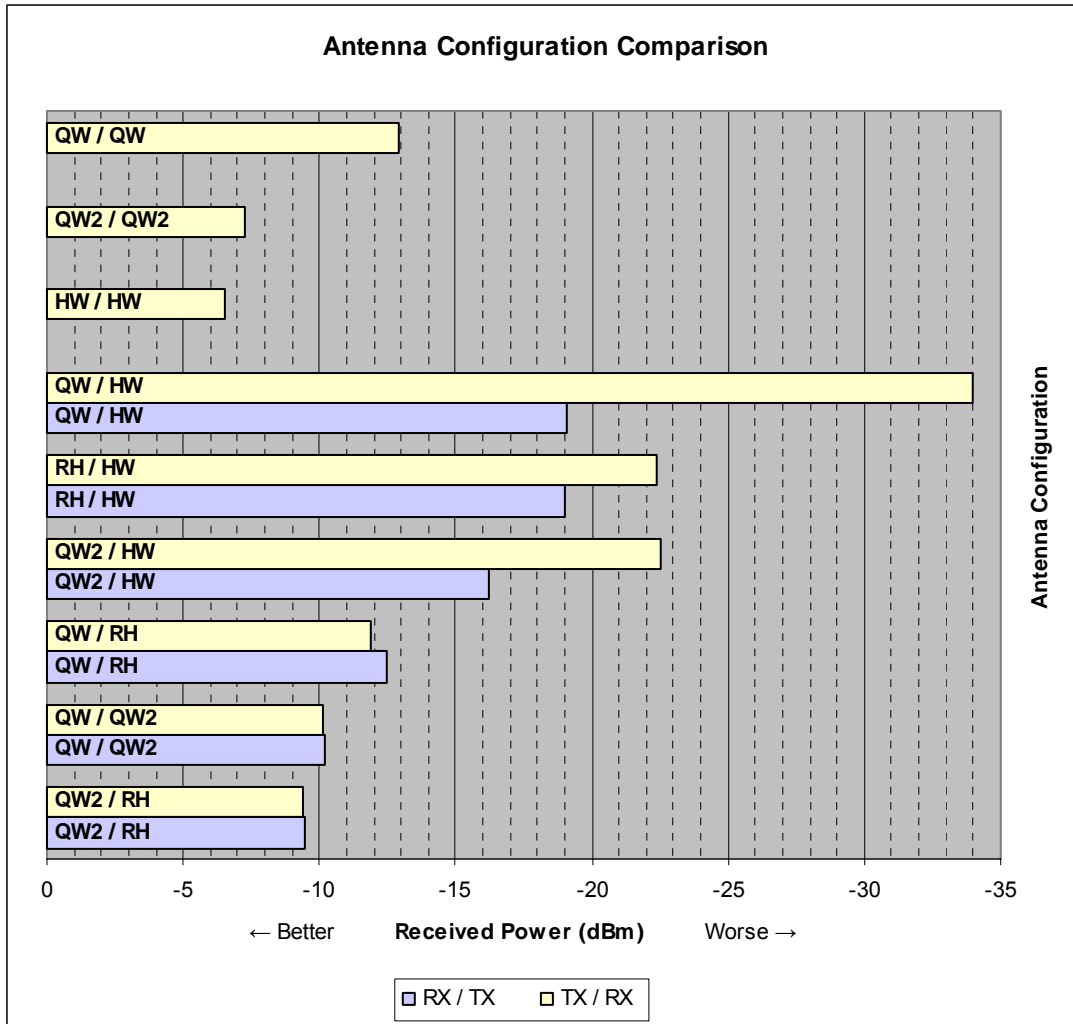


Figure 52: Antenna Configuration Test Results

### 5.1.6. Timer Accuracy Test

The goal of this test was to evaluate the accuracy of the MSP430 microcontroller timers by measuring a 10 ms period generated by the timers, as it would be in the implementation of the Locator TDM system.

Custom test firmware was used that toggles a pin on the board (in this test, board #3) every time the timer, which is run off a 32.768 kHz crystal, reaches its 10 ms tick time; the width of a positive pulse of this signal was measured using an oscilloscope. Due to not being able to set the timer ticks to an exact 10ms, 327 ticks of the 32.768 kHz crystal were used, giving an expected period of about 9.97924805 ms.

The worst-case period fluctuation  $\Delta T$  over multiple clock cycles is  $\Delta T = \frac{n}{f \cdot (1 - ppm)} - \frac{n}{f \cdot (1 + ppm)} = \frac{-2 \cdot ppm \cdot n}{f \cdot (p - 1) \cdot (p + 1)}$  where  $n$  is the number of clock cycles at  $f$  Hz over the period and  $ppm$  is the rating of the crystal. At 20 ppm (actual value of crystals on board) and 32.768 kHz over 327 cycles, the maximum fluctuation should be 399.2 ns.

It is important to note that under normal operating circumstances, other interrupts may block execution of the Timer interrupt, delaying the interrupt for up to around ten clock cycles (6 cycles latency plus execution of any other code before interrupts are re-enabled), or longer in case interrupt nesting is not enabled (as is the case in a few of the shorter interrupt handlers). However, in practice this should not have a large impact because the instruction cycle time is only 250 ns. In the code used in this test, the only other interrupts are for the distress button, the Xemics module, and the RS232 UART, and none of these peripherals were used, so there should be no such disturbances of this kind.

Almost 24,000 measurements were taken over a time of about 30 minutes. In short, the results show a mean period of 9.97899347 ms with a deviation range of 166.7 ns. With this fluctuation, one can calculate the accuracy to be 8.35 ppm. This shows that the accuracy of the system is within the expected oscillator accuracy.

### 5.1.7. Timer Drift Test

The goal of this test was to evaluate the accuracy of the MSP430 timers by measuring how fast two boards' clocks drift apart. This test is very similar to the Timer Accuracy Test in Section 5.1.6, but two boards' 10 ms signals were compared, and the time it takes for those signals to drift about 1 ms apart from their original offset was measured. The boards (#3 and #7) were placed directly next to one another so it is safe to assume they were both at room temperature. This test was run three times. Note that the drift time was measured manually using a stopwatch so this might introduce a slight error, but care was taken to reduce this to as little as possible. See Table 15 for a summary of results.

Run	Time Taken	Actual Drift	Calc. Accuracy
One	493.63 s	1.000328 ms	1.0132 ppm
Two	455.81 s	1.000448 ms	1.0974 ppm
Three	443.59 s	1.000690 ms	1.1279 ppm
<b>Average</b>	464.34 s	1.000489 ms	<b>1.0795 ppm</b>

Table 15: Timer Drift Test Results



Using the Equation 1 from Section 3.3 for worst-case time until failure  $\Delta t$  with  $ppm = 20$  ppm, which was the actual value of crystals on board, and  $\Delta t = 1$  ms, we can see that the worst-case time until failure  $t_f$  is 25 s. The results of this test show that the accuracy of the system is well within the expected oscillator accuracy. However, because these tests only compared two boards at room temperature, one should always use the calculated worst-case time until failure values for protocol implementations.

#### **5.1.8. Synchronization Accuracy Test**

The goal of this test was to determine how accurately two boards can be synchronized by sending a synchronization signal from a third board. This is important because it determines, among other things, what the minimum guard time in the TDM protocol must be, and how well two boards can be synchronized for other purposes, such as synchronizing Reference Units to sample the received ranging signal at the same time. Although this latter function is not specified as part of the Data Channel's tasks, it was at one point during developments considered as a possibility, which is part of the reason why these extensive tests were performed.

The firmware for this test used a version of the Xemics drivers that utilized the Xemics modules' "pattern match" interrupt that triggers at the very beginning of a packet, when the preamble and pattern bytes are recognized (3 and 4 bytes, respectively). When this interrupt is seen, the board pulses one of its pins. The code has some similarities to the Range Test code (Section 5.1.2), as the boards can be placed into a master and slave mode, and the master transmits the same 10-byte packet. However, since the synchronization interrupt is triggered before the entire packet is received; the received packet is not verified for correctness at the slave and not echoed back. In this version of the code, the slave stays in continuous receive (with very brief interruptions) and the master transmits a fixed number of sync packets (2048) at 19200 baud, with a brief delay between each packet, giving approx. 3 minutes for one run.

For this test, one board is configured as the master, and two slave boards are placed into receive mode and their pins measured with the automatic measurement capabilities of a two-channel oscilloscope to determine the average and maximum time offsets between when the boards receive the synchronization signal. The slave boards were each about two feet away from the master. This test was run on all possible permutations of two slave boards, plus some additional tests, giving a total of over 46 runs.

See Table 22 in Appendix A for raw data. The first 45 runs cover all permutations of master/slave board combinations. From these runs, the average across all maximum offsets was 29.7  $\mu\text{s}$  and the average of the standard deviation of all offsets was 1.24  $\mu\text{s}$ .

Because no large variances were noticed across the boards, the board combination for the final run (46) was selected from run 13 because it exhibited the worst-case accuracy, but the other parameters were within normal range. For this test, the master board's transmissions were initiated ten times, giving 20480 packets sent. The results for this test are within the expected ranges, and they give a worst-case offset of about 41  $\mu\text{s}$ .

A test for spurious interrupts was also performed. One board (#7) was put into receive mode with no other board transmitting for about 10 minutes on two separate occasions, to verify that the pattern match could not be easily triggered by noise or other transmissions. No false-positive interrupts were triggered during this time. In addition, no spurious interrupts were observed during the entire test.

A final test was run at a later time in the same configuration as Run 13, except that 4096 packets were sent. In this test, the temperature of slave 1 (board #2) was increased to approximately 42°C using a heat gun, as compared to a normal board temperature of about 27°C. The results of this test are very similar to all other tests.

In summary, we can see that typically (meaning three times the standard deviation, averaged across all tests or, assuming a normal distribution, over 99% of the time), one can expect two boards to be synchronized to within 7.5 $\mu\text{s}$ , with a worst-case (from over 100,000 measurements) of 41 $\mu\text{s}$ . This performance does not seem to depend on the board combination used or on temperature. As this is much lower than the previously selected guard time of 1 ms, we see that this synchronization method is clearly suited for our purposes.

This test series was followed up with a test that used the synchronization interrupt to reset the boards' 10 ms timers. The results of this test showed that this method of synchronizing the boards' timers is indeed successful, and is as accurate as predicted by the results above. This test showed that the stage is set for implementing the Data Channel communications protocol.

### **5.1.9. Time Division Multiplexing Protocol**

This section shows the results of the implementation of the proof-of-concept Data Channel protocol described in Section 3.9. Please refer to that section on details of the implementation. This protocol was tested to be functional by using three Data Channel boards,

with one acting as the Reference Unit and two other boards acting as Locator units  $LU_0$  and  $LU_1$ , configured to IDs 4 and 8, respectively. The results shown here are three sets of digital traces showing debug codes generated on the pins of the Data Channel Boards. The various codes are explained in the figures and in this text.

Figure 53 shows an overview of one 160 ms communications cycle with all 16 slots (compare to Figure 25 in Section 3.9). For this trace, one can see that in slot 0, the Reference Unit transmits a synchronization signal, which is received by both Locator units. One can see that each Locator unit wakes up at the correct time with respect to the slot it has been configured for, and transmits its data to the Reference Unit, which successfully receives it.

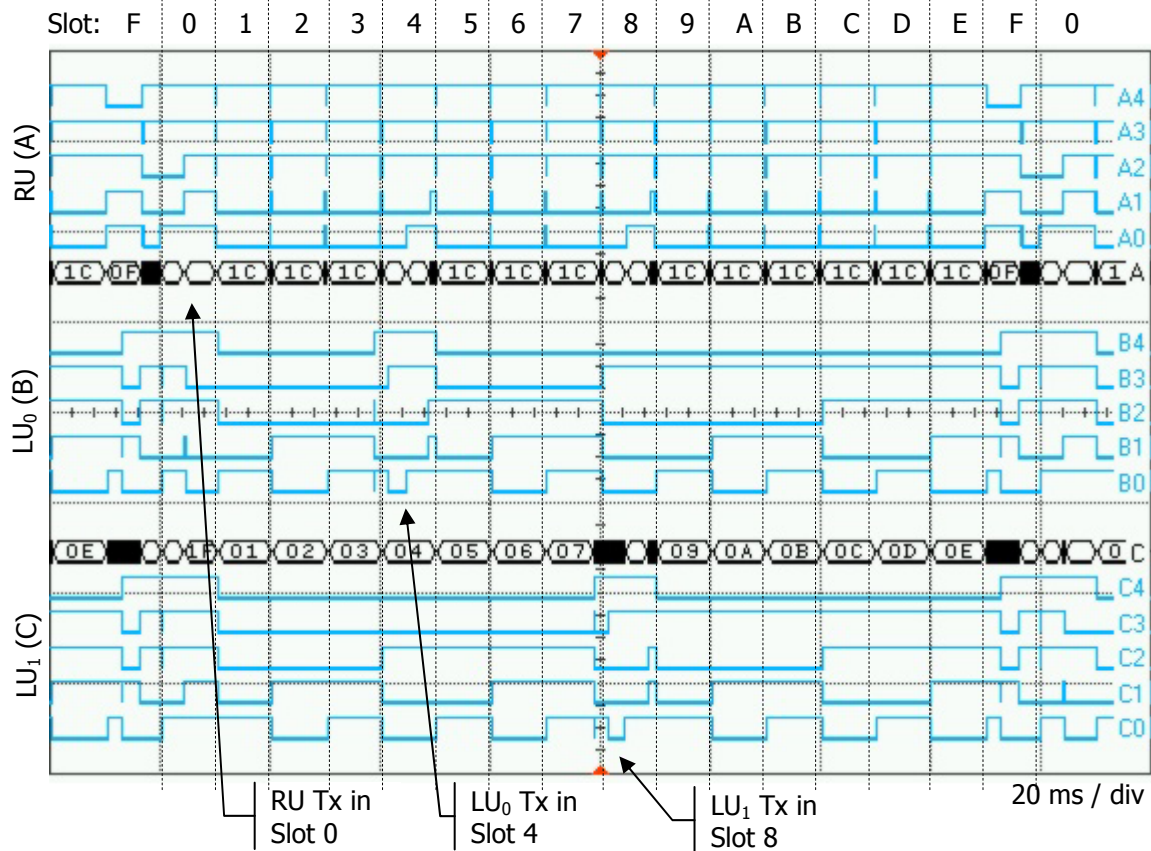
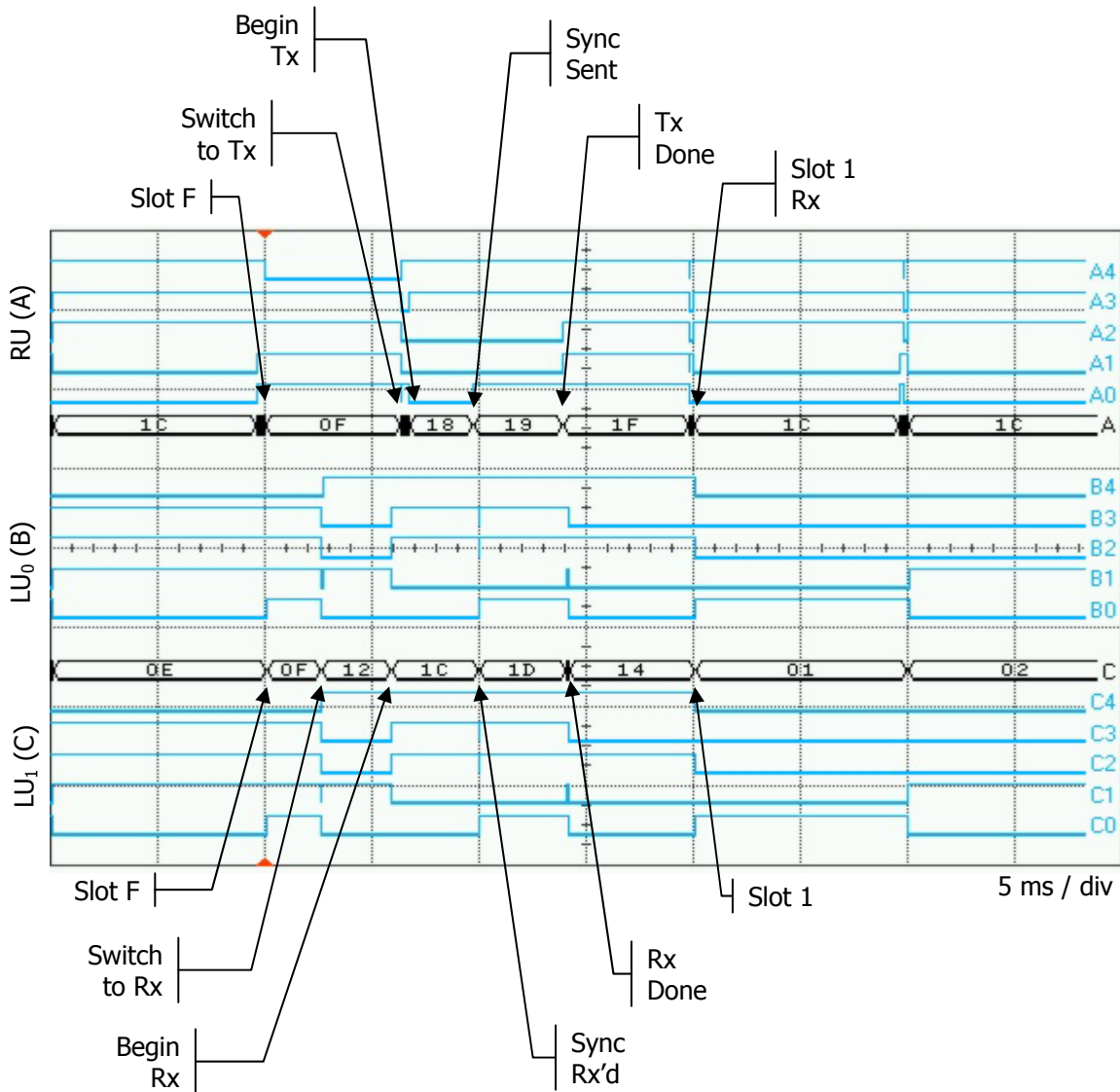


Figure 53: Actual Protocol Overview

Figure 54 shows the details of a synchronization procedure (compare to Figure 27 in Section 3.9.1). One can clearly see both the Reference Unit and Locator units wake up early, during slot F, to transmit resp. receive the synchronization signal.



**Figure 54: Actual Synchronization**

Figure 55 shows how LU<sub>1</sub>, which is configured to slot 8, wakes up early in slot 7 to begin transmitting data and how this transmission is received by the Reference Unit (compare to Figure 28 in Section 3.9.1).

The version of the protocol used in these tests was fairly simple, for example with no support for forward error correction. However, as these tests were intended to show that the “10 ms time slot” system works in general, these tests were successful. In addition, it is important to note that the protocol shown in this section was used as the basis for a general-purpose communications system between one “master” Data Channel board and several “slave” boards, and this system was used in supporting PPL experiments for over half a year.

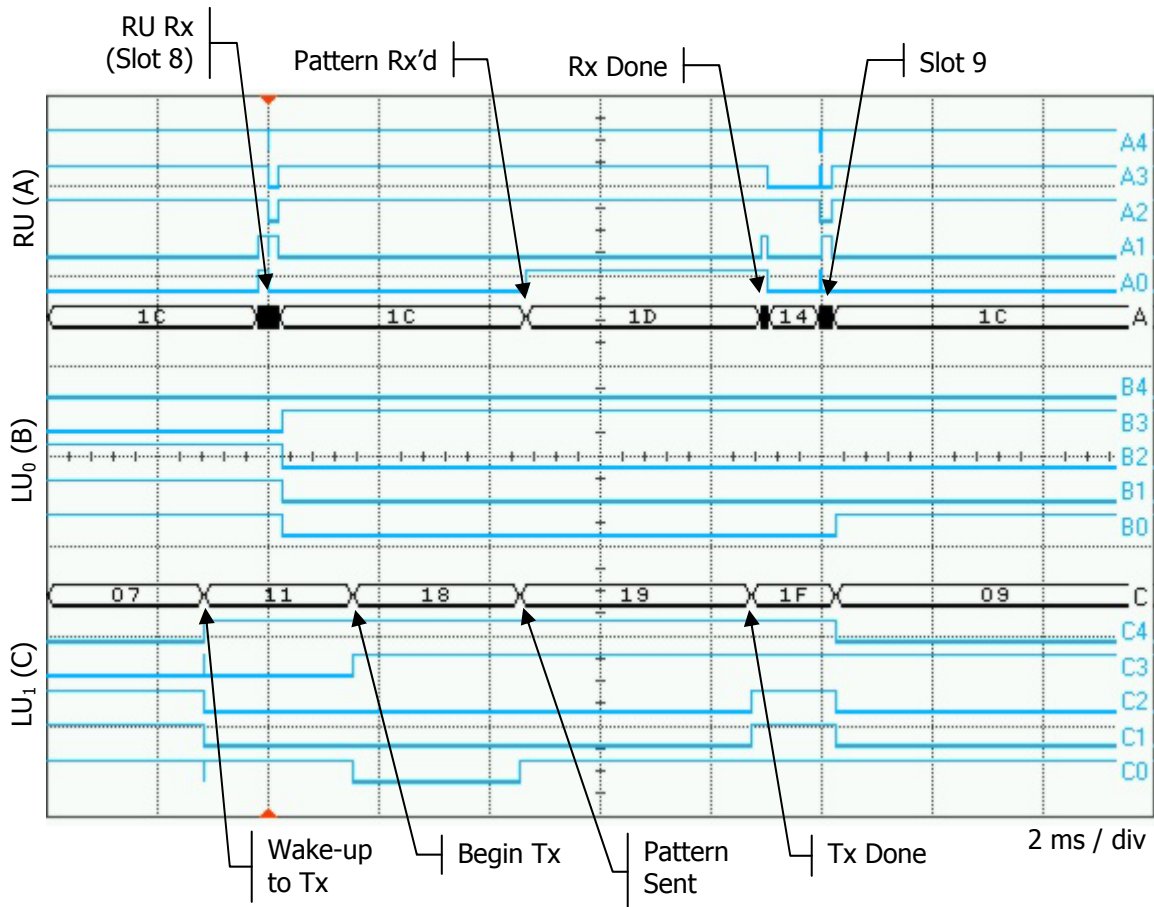


Figure 55: Actual Data Transmission

## 5.2. Digital Waveform Generator

This section describes tests that were performed to show the correct functioning of the new Digital Waveform Generation hardware. At the time of writing, a total of three boards were completed to final specifications, which included the update to the clock generation circuit. An additional completed board without this modification was used for applying an externally generated sampling clock to test a larger range of sampling frequencies. After the boards were verified to be functional, a series of tests to characterize the performance of the boards was performed; these will be described here. In addition, an analysis of the power consumption of this board is presented.

### 5.2.1. RF Characterization

This series of tests was intended to compare the previous generation of hardware to the new design, to compare performance at different sampling frequencies. Throughout these tests,

the new Digital Waveform Generation hardware is referred to as the “new” and the previous generation is referred to as the “old” hardware. One should note that because power levels per subcarrier required for the new Locator RF front-end hardware currently under development is -40 to -50 dBm, the full-scale range output of the DAC on the new boards was reduced to accommodate for these levels.

Two waveforms were used for these tests: a single tone 10 MHz waveform and a multi-carrier waveform consisting of 50 carriers spread equally across the bandwidth, beginning at about 10% of the bandwidth and spanning to about 90% of the bandwidth. This waveform is shown in Figure 56 in the frequency domain for the case of 200 MSPS; the first carrier is at 10.01 MHz and the last carrier is at 88.97 MHz.

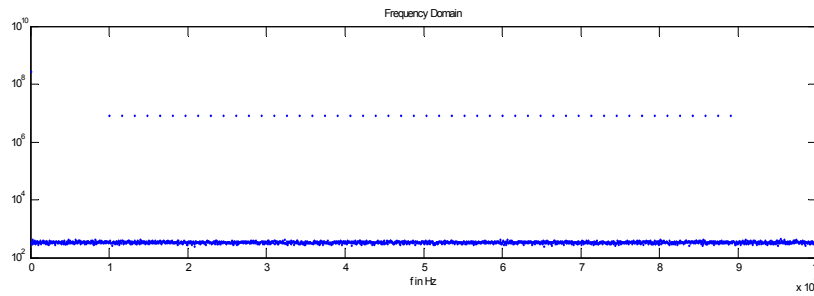


**Figure 56: Multi-Carrier Test Waveform**

The first test performed compared the per-carrier signal-to-noise ratio (SNR) of the old vs. the new hardware. This test involved measuring the noise floor of the signal and comparing it to the average power per subcarrier of the multi-carrier waveform. This test was performed before the full-scale range output power of the new boards was reduced from its maximum level, and the old board was left at its default output level. Table 16 shows the results of this test.

Board	Noise Floor	Average Power per Subcarrier	SNR
Old	-123 dBm	-33.8 dBm	89.2 dB
New	-119 dBm	-27.8 dBm	91.2 dB

**Table 16: SNR Comparison Results**

While this test shows that the new hardware has a higher output level in this configuration, the output power needed to be reduced so that the performance of the boards could be characterized at the output levels that they will be operating at in the final system.

The first measurements presented show a comparison of the harmonic distortion for the different board and clock combinations. This test was performed by loading a waveform onto the

boards that consisted of a single 10 MHz carrier, and then using the automatic measurement capabilities of a spectrum analyzer to measure the power level of the harmonics. The carrier and first two harmonics are presented in Table 17.

Board	Sampling Clock	Clock Source	10 MHz Carrier Power (dBm)	First Harmonic (dBc)	Second Harmonic (dBc)
Old	200 MSPS	Sig. Gen.	-8.23	-71.11	-88.84
New	200 MSPS	Sig. Gen.	-16.42	-78.20	-92.75
New	220 MSPS	Sig. Gen.	-16.42	-78.12	-92.51
New	300 MSPS	Sig. Gen.	-16.41	-78.20	-92.79
New	400 MSPS	Sig. Gen.	-16.41	-79.69	-90.54
New	220 MSPS	Onboard	-16.41	-75.84	-83.51

Table 17: Harmonic Distortion Test

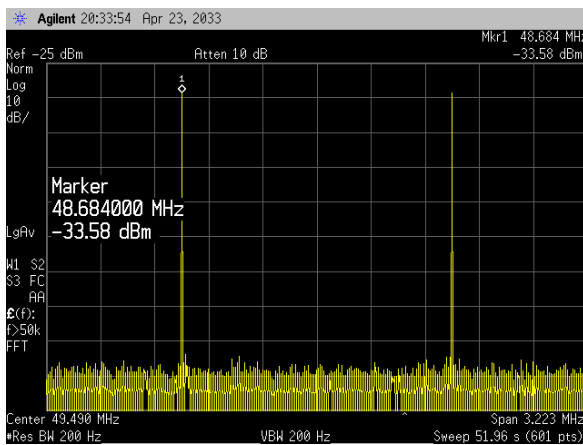
Taking into consideration the fact that the carrier power of the old board was slightly higher than that of the new boards, this test shows that the new boards perform as well or better than the old boards in terms of harmonic distortion, even when operating with the on-board clock.

The next test performed consisted of a visual inspection of several regions of the multi-carrier waveform. These regions included the first and last 10% of the bandwidth of the signal (where there are no carriers), and the space in between three pairs of carriers at the beginning, middle and end of the signal. In addition, the overall output levels of all carriers was inspected for flatness. During these tests, statistics on the average carrier power and the difference between the first and last carrier power (to illustrate flatness) were gathered and are shown in Table 18.

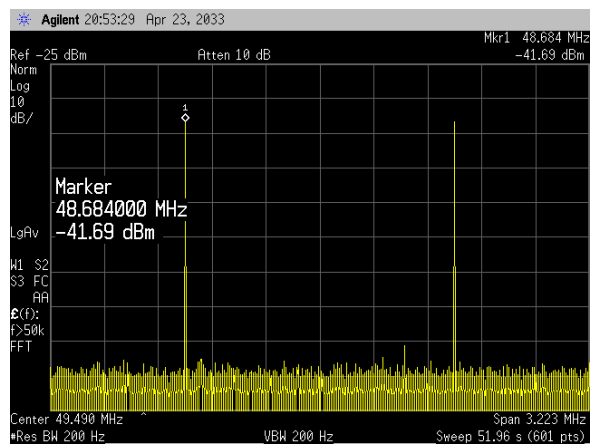
Board	Sampling Clock	Clock Source	Average Power per Carrier (dBm)	Diff. First to Last Carrier (dB)
Old	200 MSPS	Sig. Gen.	33.963	3.13
New	200 MSPS	Sig. Gen.	42.093	3.00
New	220 MSPS	Sig. Gen.	42.087	3.01
New	300 MSPS	Sig. Gen.	42.070	2.92
New	400 MSPS	Sig. Gen.	42.050	2.89
New	220 MSPS	Onboard	42.093	3.06

Table 18: Signal Power Levels

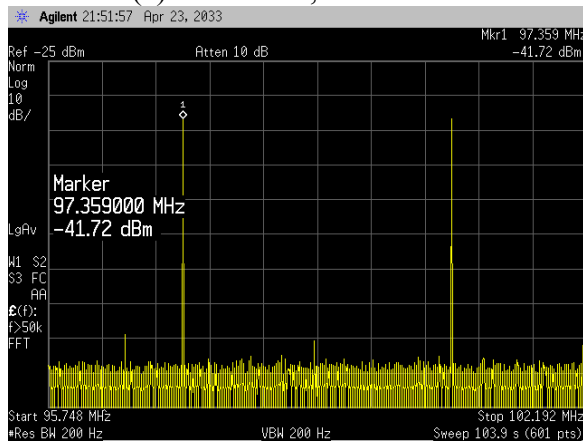
As before, these results show that the new boards operate within their required specifications, and their flatness is slightly better than that of the old boards. Several screen captures will now be presented to compare the noise levels in different waveforms. Figure 57 shows a comparison of four different signals, captured at the center of the multi-carrier waveform (the 25<sup>th</sup> and 26<sup>th</sup> carrier are shown). One can see that, except at a sampling frequency of 400 MSPS, the new boards perform as well as the old boards, with almost no spurious carriers visible above the noise floor.



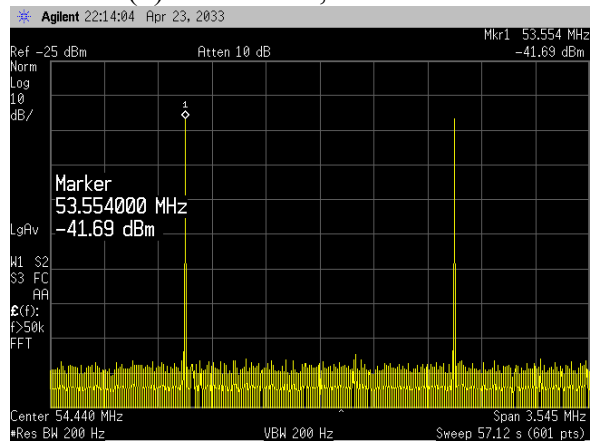
(a) Old Board, 200 MSPS



(b) New Board, 200 MSPS



(c) New Board, 400 MSPS

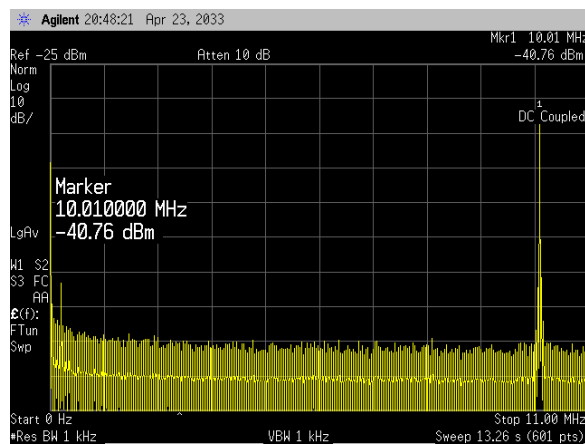


(d) New Board, 220 MSPS onboard

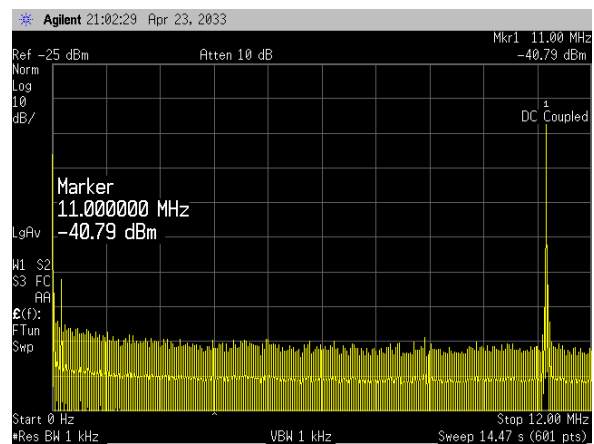
Figure 57: Spurious Signal Comparison



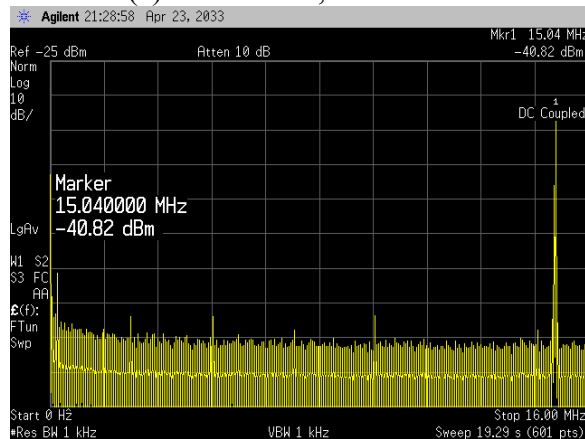
Figure 58 shows a comparison of different sampling rates on the new boards using the lower 10% of the bandwidth of the signal as examples. As in the previous results, we see that these images show the effect of increasing sampling frequency on the spurious levels. However, one should note that the original specifications only called for a maximum sampling frequency of 300 MSPS, and at this sampling frequency, relatively few artifacts were observed within the limits of signal itself.



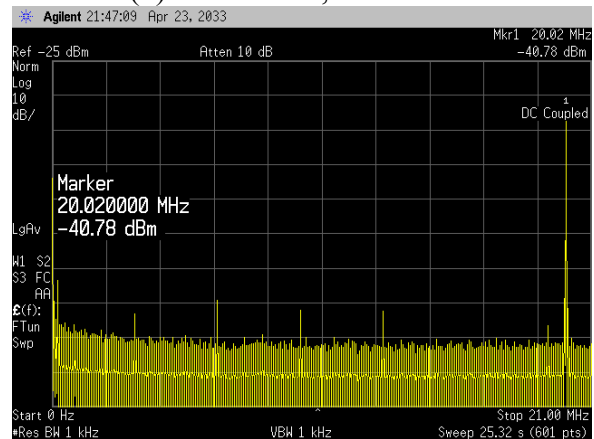
(a) New Board, 200 MSPS



(b) New Board, 220 MSPS



(c) New Board, 300 MSPS



(d) New Board, 400 MSPS

**Figure 58: Sampling Clock vs. Spurious Levels**

Finally, Figure 59 and Figure 60 show the full spectrum of the Digital Waveform Generator board operating at 220 MSPS with the onboard clock and 400 MSPS, respectively. As has been shown in the previous discussion, the new boards can be evaluated as being fully operational and a replacement for the previous generation of waveform generation hardware.

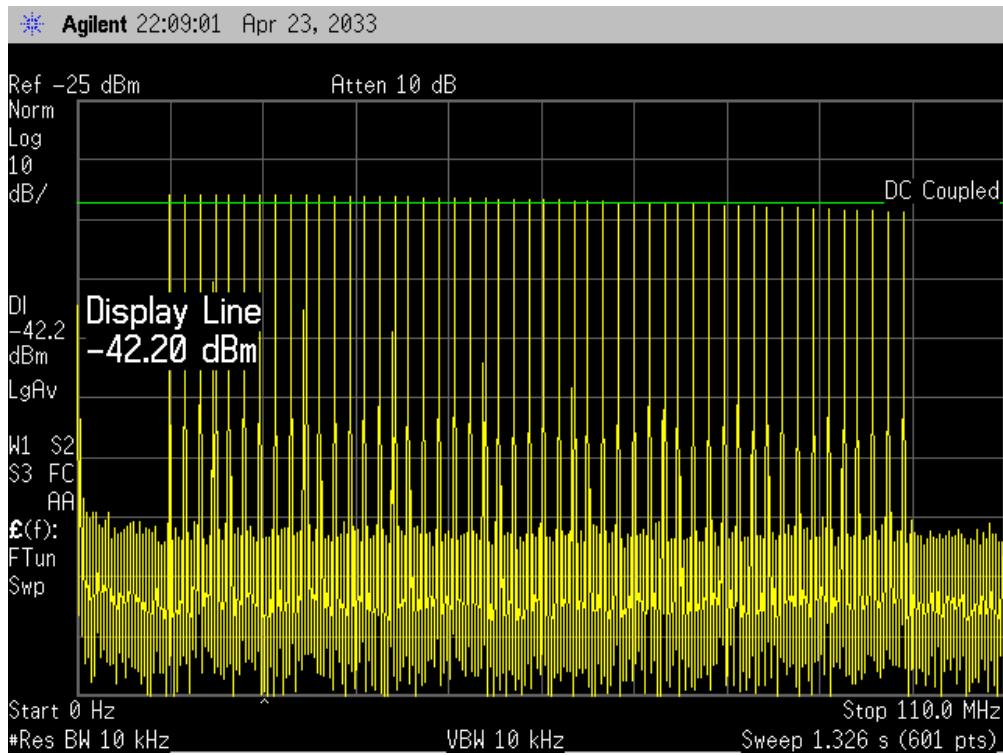


Figure 59: Output Spectrum at 220 MSPS with On-board clock

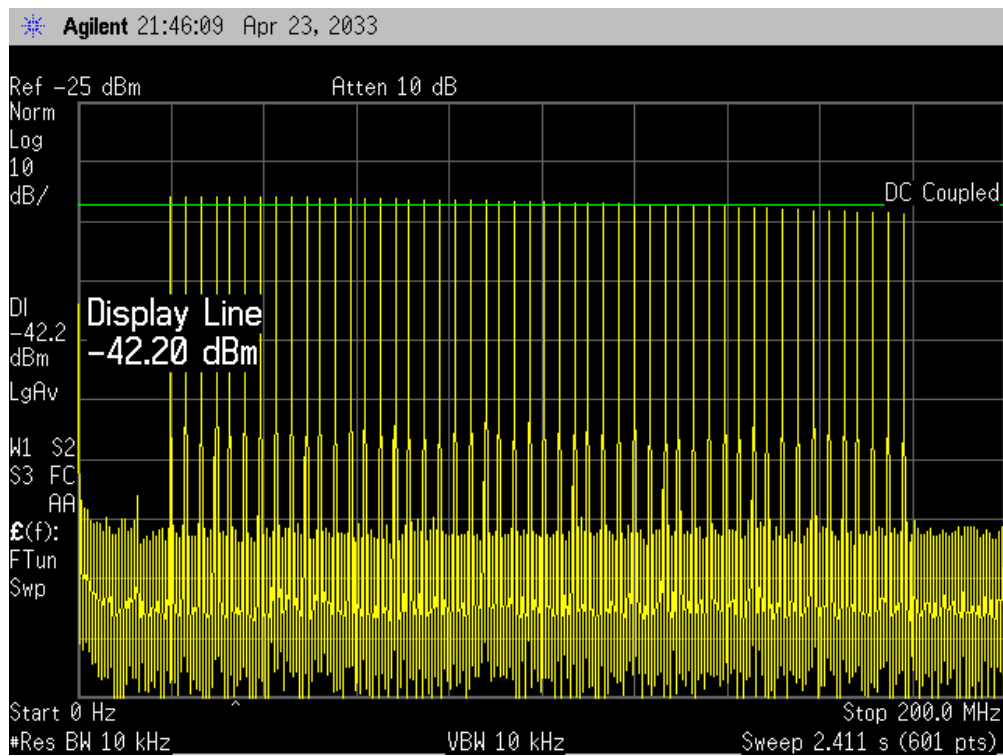


Figure 60: Output Spectrum at 400 MSPS

### **5.2.2. Power Analysis**

The previous section showed that the new generation of Digital Waveform Generation hardware provides twice the sampling rate of the previous generation of hardware, with approximately the same or slightly better RF characteristics. Next to the size reduction accomplished by this new version of the hardware, another major achievement was the reduction in power consumption. In this section, we will compare the old and new waveform generation hardware in terms of their power consumption, and will estimate the battery life of the new Locator hardware.

Measurements performed on the previous generation hardware show that the boards take approximately 1.28 seconds from the application of power to the main supply until the output of the DAC is seen. While running, the hardware takes about 509 mA. It can be assumed that most of the start-up time is dedicated to FPGA configuration, which is done in a serial fashion, and therefore the hardware is limited to a high start-up time. With this high start-up time, it is clear that with respect to the previously described “10 ms time slot” protocol, no kind of duty cycle reduction can be accomplished. Even if it were possible to rapidly enable and disable the RF front-end in order to implement such a protocol, the waveform generation hardware would still consume a constant 509 mA, and this kind of a current draw is completely impractical in a small, battery-powered system. From this we see that the ability of the new Digital Waveform Generator to be able to turn on and off different sections of the circuitry and to be able to power up rapidly were important aspects of the design.

The new waveform generation hardware was also measured in terms of current consumption. These measurements were performed by using a Data Channel board to control the enable lines of the regulators on the Digital Waveform Generation boards, as they would be in a final system. The results are as follows:

- All disabled: 0 mA
- PROM Enabled: 1.4 mA
- FPGA
  - Unconfigured (i.e. static current consumption): 65.3 mA
  - With simple counter (50 MHz clock): 144 mA
  - With full waveform generation implementation (220 MSPS): 343 mA
- DAC and Clock Generation enabled (220 MSPS): 67.5 mA

We see from these results that at a speed of 220 MSPS (the frequency of the on-board clock), the system draws approximately 411 mA total. At higher sampling rates up to 400 MSPS, the current consumption has only been observed to be marginally higher, by approximately 50 mA. One should note that the current consumption of the PROM while active cannot be measured directly because the FPGA needs to be active as well, but the datasheet specifies a maximum of 50 mA. We must also take note of how long each of these parts of the board stays active. As expected, the FPGA's configuration time was measured to be slightly less than 3 ms. The DAC has a start-up time of about 20 ms. The reference oscillator for the DAC clock takes approximately 10 ms to stabilize, and the settling time of the PLL IC is specified to be within several hundred  $\mu$ s, so we can assume that the DAC clock will have stabilized by the time the DAC is active. At the time of writing, the new RF transmitter front-end is still under development, so only estimates of its start-up time and current consumption exist. We will assume the RF Front-end consumes about 368 mA and is capable of starting up within 20 ms. The sequencing for all these timings is represented in Figure 61. Finally, another point to make is that research into different battery vendors shows that cell phone sized batteries, which are realistic for a Locator type device, usually have capacities of up to 1400 mAh.

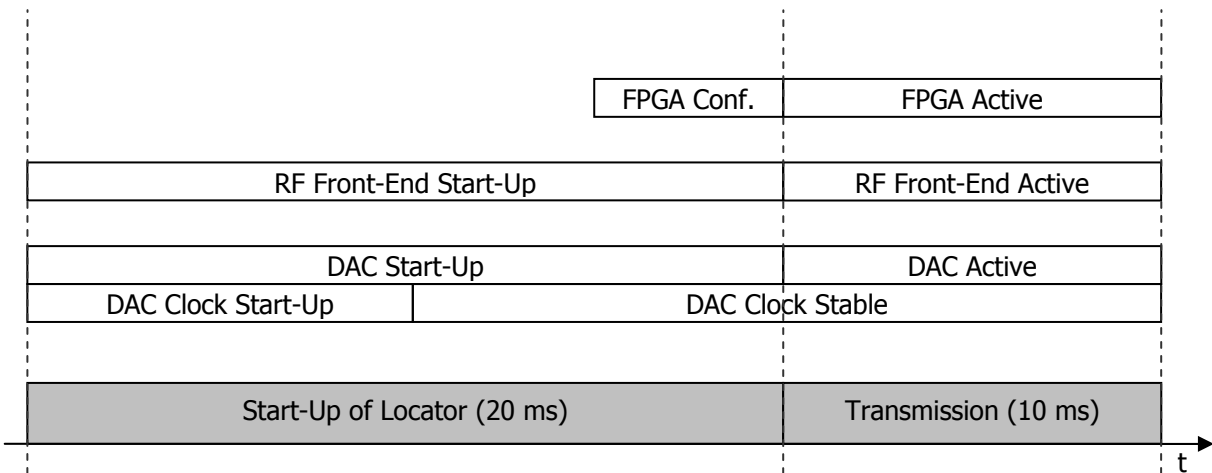


**Figure 61: Locator Power-Up Sequencing**

Using these numbers, we can now estimate what the average power consumption of the Locator device would be. For this calculation, we will assume that the hardware is active for a 10 ms time slot out of one second, and that the DAC, clock generation hardware, and RF front-end hardware are enabled 20 ms prior to this, while the FPGA is enabled 5 ms prior to the slot. In addition, we assume the Data Channel is active in transmit mode for 10 ms and in receive mode

for 10 ms out of one second. Figure 62 shows a graphical representation of the power consumption with these timings. Using this information, we can now estimate the possible battery life of the entire Locator device. The calculations are shown in Table 19, from which we can see that we can project the battery life to be at least 72 hours.

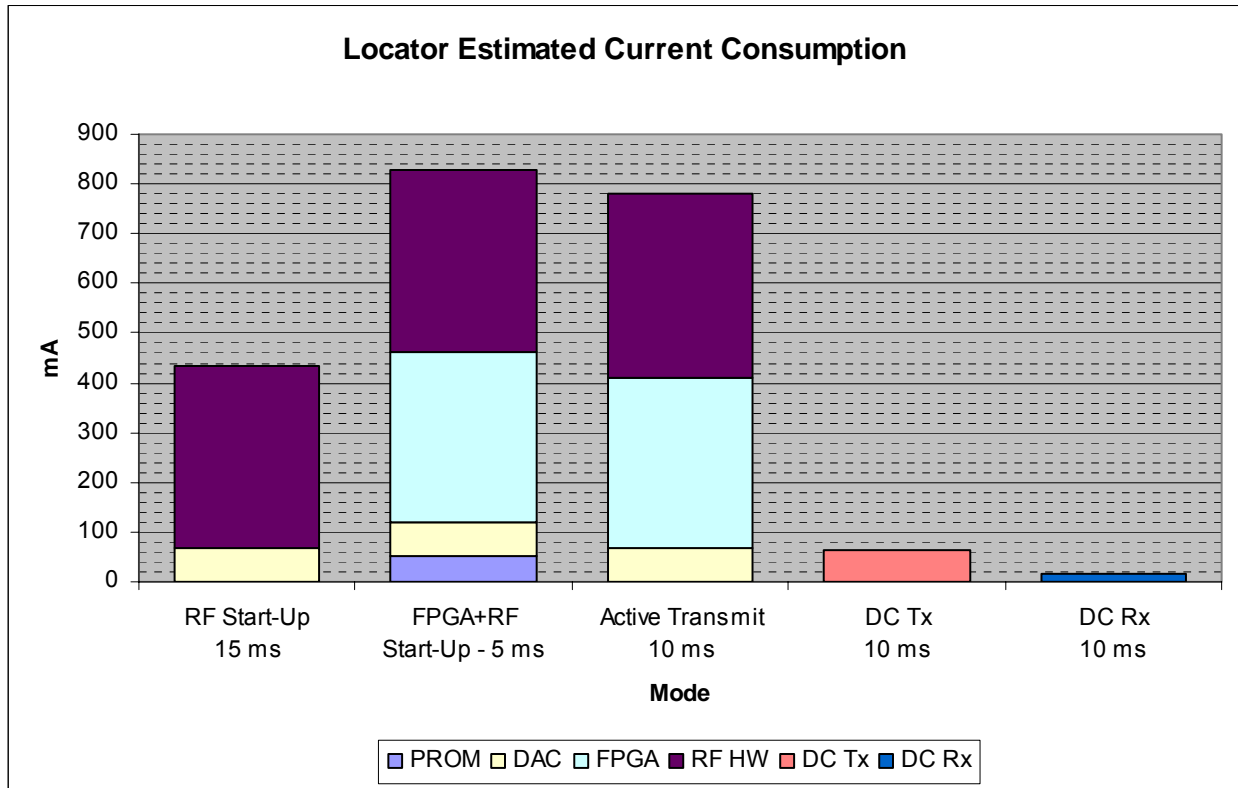


Figure 62: Power Consumption and Timing

Mode	Current	Time	Duty Cycle	Equivalent Current
RF Start-Up	436 mA	15 ms	1.5%	6.54 mA
FPGA+RF Start-Up	829 mA	5 ms	0.5%	4.145 mA
Active Transmit	779 mA	10 ms	1%	7.79 mA
DC Tx	65 mA	10 ms	1%	0.65 mA
DC Rx	17 mA	10 ms	1%	0.17 mA
<b>Total:</b>				19.295 mA
<b>Battery Life with 1400 mAh Battery:</b>				<b>72.56 hrs</b>

Table 19: Battery Life Calculation

These battery life estimates are calculated for a system that is fully active, i.e. providing location updates once a second. If a longer battery life is desired, one could sacrifice the update frequency to even further reduce the duty cycle. In addition, as has been described, the Data Channel gives the Locator the ability to power down completely into a “sleep mode”, so that only

a very small amount of current is consumed. The Locator devices should be able to remain in this sleep mode for very long periods of time, on the order of weeks, or even months. In such a sleep mode, the Data Channel could regularly wake up for short periods of time in order to listen for a command to power back on, as could be issued when the Locator device arrives at the scene of an incident.

One can clearly see from these results that the new generation of Digital Waveform Generator hardware is superior to the previous generation. Although testing of the boards in a “real-life” experimental situation has not occurred yet, given the results of this testing, one can be confident that they will perform well as replacements for their predecessors.

## **Chapter 6. Conclusion and Future Work**

The research described in this thesis involved the design, implementation and testing of the *Data Channel* and the *Digital Waveform Generation* subsystems of the Locator units of Precision Personnel Locator project. The first chapters of this thesis presented a brief history of the PPL project and the design requirements for these subsystems, which were derived from the overall project requirements. This was followed by a description of the design of each subsystem, including some background theory, discussions of the design alternatives and the rationale for the design decisions made. Then, the details of the implementation of the subsystems were explained, followed by the results of performance testing and characterization.

The Data Channel hardware was successfully implemented as a small printed circuit board and tested to be able to serve its purpose of being a low-power communications platform capable of accurately controlling the transmissions and power usage of the Locator devices, in addition to collecting and communicating environmental status data. The rationale behind the decision to implement a bi-directional communications channel separate from the existing ranging signal transmissions was presented.

Another goal that prompted the development of the Data Channel hardware was requirement to support multiple Locator devices. An investigation into various methods for implementing this functionality was carried out, including a brief comparison of Frequency Domain Multiplexing and Time Division Multiplexing. Alternative designs were also considered, such as a scheme in which Locators transmit in a completely random fashion.

To achieve these goals, the Data Channel subsystem was designed to include a low-power microcontroller, a bi-directional wireless communications module capable of operating in the 900 MHz ISM band, and sensors to measure ambient temperature and detect non-movement of the device. A distress button was also added that can be pressed by the user to trigger a distress signal to be sent to the outside of the building. The Data Channel hardware is capable of interfacing to various other hardware, such as the Digital Waveform Generator.

A proof-of-concept version of a specialized communications protocol that allows up to 100 Locators to provide location updates once a second via time-division multiplexing was implemented in firmware on the Data Channel boards. This protocol functions by synchronizing the boards to a common time base, thereby giving them the ability to direct each Locator device to transmit its ranging signal waveform for 10 ms out of every second. In addition, this protocol

provides for the communication of commands and the reporting of status information, such as temperature and movement data, back to the Base Station.

Lastly, the Data Channel hardware was extensively tested with respect to many different parameters, such as communication range, timing accuracy, and the ability to synchronize to a common time base in order to implement the communications protocol.

Because the Data Channel printed circuit boards are also useful as a general-purpose microcontroller and wireless communications platform, they are actively being used for several tasks outside of their original specifications. These additions include interfacing to a variable-gain amplifier on the receiver units, to a phase-locked loop IC used for the local oscillator of the current transmitter and receiver, to an analog switch allowing for multiple antennas to be multiplexed to on receiver, and lastly, controlling all these functions wirelessly through the communication protocol that was developed. The Data Channel boards have proven to be a useful addition to the PPL project.

The second of the two subsystems, the Digital Waveform Generator, was also implemented as a small printed circuit board and tested in its function of generating the ranging signal waveforms while consuming a relatively low amount of power. These boards replace and offer more features than an earlier version of waveform generation hardware, which was only specified for bandwidths of up to 100 MHz and which had no power reduction capability. The specifications for the new hardware included the ability to generate waveforms of up to 150 MHz bandwidth, to consume less power, and to be smaller in size than the previous hardware, thereby making them more suited for implementation in an actual, hand-held, battery-powered Locator device.

The design process of the Digital Waveform Generator hardware began with a discussion on the selection of a digital-to-analog converter and how its clock signal can be generated. An Analog Devices DAC was selected, and a phase-locked-loop based circuit capable of generating a clock signal for the DAC was designed. Alternative means to supplying the DAC with ranging waveform data were reviewed, which led to the selection of the Xilinx Spartan-3 FPGA for this purpose. It was shown that this design is suited for a low-power application because of the ability to rapidly configure the FPGA through a parallel interface at a high clock frequency. Careful attention was paid to details of the printed circuit board layout including the power distribution



system, the physical separation of the analog and digital components, and routing of high-speed differential signals.

Testing of the new Digital Waveform Generator hardware design showed that it meets and even exceeds the original specifications. The boards were shown to be able to generate a waveform of up to 200 MHz bandwidth with good RF characteristics. This higher bandwidth is important in producing waveforms that span the frequency bands that were recently granted to the PPL project by the FCC for experiments. In addition, the ability to selectively power down parts of the boards and quickly power them back on was essential, as it gives ability to reduce their duty cycle and consume less power overall. The resulting in a battery life estimate for the complete Locator device while deployed and active at an incident site was shown to be over 72 hours. Achieving this excellent battery life was an important goal of the design of the Locator hardware.

The Digital Waveform Generator boards will be used during experiments of the overall PPL system after the completion of this thesis. This will show how well the boards perform in a “real-life” environment as compared to bench testing.

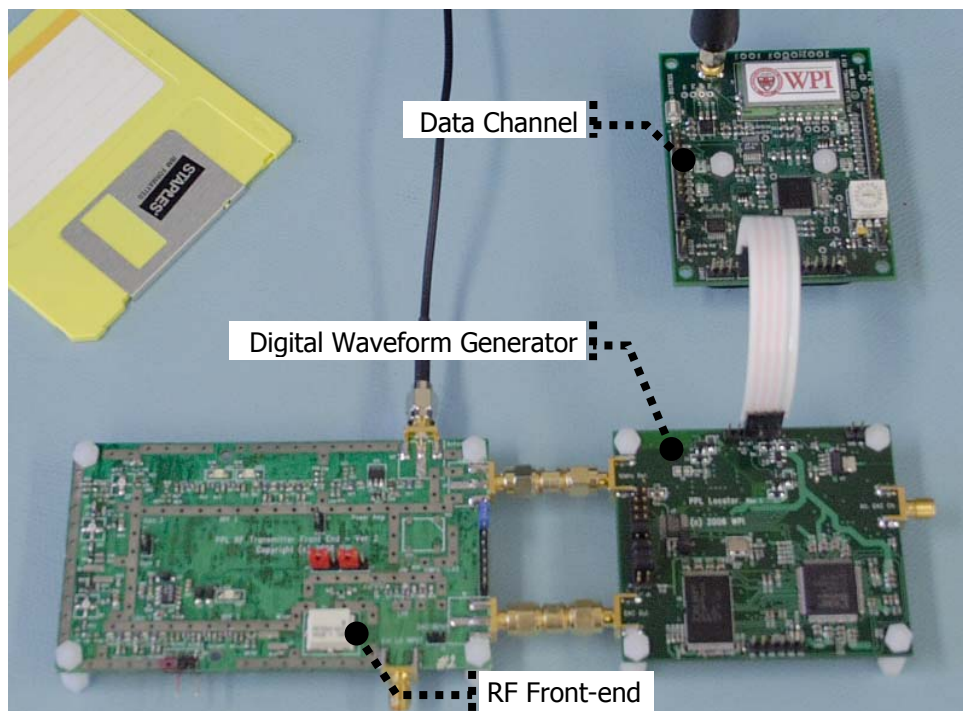


**Figure 63: Newly Developed Locator Hardware**

Figure 63 shows the new generation of Locator hardware. The Data Channel and Digital Waveform Generator PCBs are shown in the top right and bottom right of the image,

respectively. The waveform generator hardware is shown linked directly to a new RF Front-end transmitter, which is currently under development by other members of the PPL team. One should note that these boards are shown in their evaluation configuration; the boards are designed to be stacked together to be able to fit in a smaller package.

## **6.1. Future Work**

As the PPL project continues to evolve, additional hardware will be developed and improvements to the existing systems will be made. It is likely that another generation of prototype Locator hardware will eventually be developed, and the work presented in this thesis can serve as a basis for that design. In addition, there are several areas where more developments can be made.

Although the Data Channel boards have proven to be a reliable communications platform, so far only a proof-of-concept version of the full protocol described in this thesis has been implemented. This is due in part to the fact that it had not yet been necessary to support multiple transmitters. In addition, there had been no need for a support of multiple Reference Units, because all boards have generally been within communication range of one another.

As the PPL system is further improved, one can also expect to see larger-scale experiments, in which it may become necessary to begin supporting multiple Reference Units. Other improvements to the Data Channel protocol include the support for frequency hopping, or the ability to dynamically configure Locators into specific slots, which would be useful in a situation with a large number of users. Lastly, extensive tests, such as the range tests described in this thesis, need to be repeated with improvements such as the addition of forward error correction.

The Digital Waveform Generator boards have so far only been tested on the laboratory bench using spectrum analyzers and oscilloscopes. A next step for these boards is to be combined with the new RF Front-end hardware, so that these boards can be used in a “real-life” experiment that compares them to the existing transmitter hardware they will be replacing. The accuracy of the location estimates produced by the PPL algorithms when applied to the data from the old and new hardware would serve as the best indicator of their performance. Lastly, once the full set of new Locator hardware is completed, the support of multiple Locator devices using time-division multiplexing can be tested.

The Precision Personnel Locator project will continue to strive for the goal of precise indoor location tracking, and the work presented in this thesis represents a step towards this goal.

## **Chapter 7. References**

- [1] 16-Bit, 400 MSPS D/A Converter. Analog Devices, 2005. Dec. 2006  
<[http://www.analog.com/UploadedFiles/Data\\_Sheets/AD9726.pdf](http://www.analog.com/UploadedFiles/Data_Sheets/AD9726.pdf)>.
- [2] 3.3V, 16-Bit, 500MSPS High Dynamic Performance DAC with Differential LVDS Inputs. Maxim, Dec. 2003. Dec. 2005 <<http://datasheets.maxim-ic.com/en/ds/MAX5888.pdf>>.
- [3] Anderson, John R. United States Fire Administration. Department of Homeland Security. Abandoned Cold Storage Warehouse Multi-Firefighter Fatality Fire, Worcester, Massachusetts. USFA-TR-134, Dec. 1999. Nov. 2006  
<<http://www.usfa.dhs.gov/downloads/pdf/publications/tr-134-508.pdf>>.
- [4] Bicket, John, Daniel Aguayo, Sanjit Biswas, and Robert Morris. Architecture and Evaluation of an Unplanned 802.11b Mesh Network. Proc. MobilCom '05, Cologne, Germany, Aug. 28 –Sept. 2, 2005. Nov. 2006  
<<http://pdos.csail.mit.edu/papers/roofnet:mobicom05/roofnet-mobicom05.pdf>>
- [5] "Bluetooth." The Official Bluetooth® Wireless Info Site. Dec. 2006  
<<http://www.bluetooth.com/bluetooth/>>.
- [6] Cyganski, David, John Orr, and William R. Michalson. A Multi-Carrier Technique for Precision Geolocation for Indoor/Multipath Environments. Proc. ION GPS/GNNS, Sept. 9-12, 2003.
- [7] Cyganski, David, John Orr, Ryan Angilly, and Benjamin Woodacre. Performance Limitations of a Precision Indoor Positioning System Using a Multi-Carrier Approach. ION NTM 2005, Jan 24-26, 2005.
- [8] Duckworth, James, Hemish K. Parikh, and William R. Michalson. Radio Design and Performance Analysis of Multi Carrier-Ultrawideband (MC-UWB) Positioning System. ION NTM 2005, Jan. 24-26, 2005.
- [9] Elert, Glenn, ed. "Speed of a Skydiver (Terminal Velocity)." The Physics Factbook. Nov. 2006 <<http://hypertextbook.com/facts/JianHuang.shtml>>.
- [10] Elert, Glenn, ed. "Speed of the Fastest Human, Running." The Physics Factbook. Nov. 2006 <<http://hypertextbook.com/facts/2000/KatarzynaJanuszkiewicz.shtml>>.
- [11] Google Earth. <<http://earth.google.com/>>.
- [12] IEEE 802.11 Working Group. Dec. 2006 <<http://www.ieee802.org/11/>>.
- [13] Kazemi, Frederick D. Platform for Precision Personnel Location System. Worcester Polytechnic Institute. 2004.

- [14] Kremoski, Haris, Ivan Seskar, and Predrag Spasojevic. An ORBIT Testbed Study of 802.11b DCF: Throughput, Latency, and the Capture Effect. Proc. IEEE Tridentcom 2006, Barcelona, Spain, Mar. 1-3, 2006. Nov. 2006 <[http://www.orbit-lab.org/attachment/wiki/Orbit/Documentation/Publications/trident06\\_camera.pdf](http://www.orbit-lab.org/attachment/wiki/Orbit/Documentation/Publications/trident06_camera.pdf)>.
- [15] Manual on Uniform Traffic Control Devices, 2003 ed. U.S. Department of Transportation, Federal Highway Administration, 2004. Nov. 2006 <<http://mutcd.fhwa.dot.gov/>>.
- [16] Mixed Signal Microcontroller. Texas Instruments, Aug. 2006. Dec. 2006 <<http://focus.ti.com/lit/ds/symlink/msp430f1611.pdf>>.
- [17] Orr, John A. Development of a System for Tracking and Location of Firefighters and Other Emergency Personnel Inside Buildings. Worcester Polytechnic Institute. 23 December 1999.
- [18] Orr, John A. Firefighter and other Emergency Personnel Tracking and Location Technology for Incident Response. Worcester Polytechnic Institute. 11 July 2001.
- [19] Papoulis, A. and S. U. Pillai. Probability, Random Variables and Stochastic Processes, 4th ed. New York, NY: McGraw-Hill Companies, Inc., 2002.
- [20] Parikh, Hemish K., William R. Michalson, and R. James Duckworth. Performance Evaluation of the RF Receiver for Precision Positioning System. ION GNSS 2004, Sept. 21-24, 2004.
- [21] Precision Indoor Personnel Location and Tracking for Emergency Responders. 22 Sept. 2006. Worcester Polytechnic Institute. Nov. 2006 <<http://www.ece.wpi.edu/Research/PPL/News/Workshop2006/>>.
- [22] Precision Personnel Locator Project: System Requirements Workshop. 22 Sept. 2006. Worcester Polytechnic Institute. Dec. 2006 <<http://www.ece.wpi.edu/Research/PPL/News/Workshop2004/>>.
- [23] Small, Low Power, 3-Axis  $\pm 3$  g iMEMS® Accelerometer. Analog Devices, 2006. Dec. 2006 <[http://www.analog.com/UploadedFiles/Data\\_Sheets/ADXL330.pdf](http://www.analog.com/UploadedFiles/Data_Sheets/ADXL330.pdf)>
- [24] Spartan-3 FPGA Family: Complete Data Sheet. Xilinx, Apr. 26, 2006. Dec. 2006 <<http://direct.xilinx.com/bvdocs/publications/ds099.pdf>>.
- [25] Tannenbaum, Andrew S. Computer Networks. 4th ed. Prentice Hall PTR, 2002.
- [26] The Worcester Fire Fighters Memorial. <<http://www.fallen-heroes.org/>>.
- [27] "Warehouse Tragedy." Worcester Telegram & Gazette. <<http://www.telegram.com/static/fire/>>.

- [28] Wireless Personnel Locator Requirements Assessment. Worcester Polytechnic Institute. Center for Technology Commercialization, Inc., 2004.
- [29] Worcester Fire Department. Group interview. 25 Oct. 2005.
- [30] Worcester Fire Department. Worcester Cold Storage and Warehouse Fire Board of Inquiry Report. Dec. 1999. Nov. 2006  
<<http://www.ci.worcester.ma.us/reports/boardofinquiryreportjan01.pdf>>.
- [31] Workshop on Precision Indoor Tracking and Positioning. Worcester Polytechnic Institute. 2006. Nov. 2006  
<<http://www.ece.wpi.edu/Research/PPL/News/Workshop2006/PDF/WorkingGroups.pdf>>.
- [32] XE1205 Low-Power, Integrated UHF Transceiver. Xemtech, Jul. 6, 2006. Dec 2006  
<<http://www.semtech.com/pc/downloadDocument.do?navId=H0,C193,C196,P2615&id=769>>.
- [33] ZigBee Alliance. Dec. 2006 <<http://www.zigbee.org/en/index.asp>>.

## **Appendix A. Detailed Data Channel Experimental Results**

Table 20 is referenced in Section 5.1.2. The “Received” column is the number of valid responses from the slave that the master received for each of its “Sent” packets. Packet error rate is calculated as the number of packets lost over packets sent.

<b>Run</b>	<b>Baud</b>	<b>Slave</b>	<b>Master</b>	<b>Sent</b>	<b>Recev.</b>	<b>PER</b>
1	4800	Street (QW)	Basement (QW)	256	171	33.203%
1	4800	Street (QW)	1st Front (QW)	256	160	37.500%
1	4800	Street (QW)	1st Back (QW)	256	165	35.547%
1	4800	Street (QW)	2nd Front (QW)	256	159	37.891%
1	4800	Street (QW)	2nd Back (QW)	256	174	32.031%
1	4800	Street (QW)	3rd Front (QW)	256	180	29.688%
1	4800	Street (QW)	3rd Back (QW)	256	171	33.203%
2	9600	Street (QW)	Basement (QW)	384	338	11.979%
2	9600	Street (QW)	1st Front (QW)	384	282	26.563%
2	9600	Street (QW)	1st Back (QW)	512	428	16.406%
2	9600	Street (QW)	2nd Front (QW)	512	449	12.305%
2	9600	Street (QW)	2nd Back (QW)	512	422	17.578%
2	9600	Street (QW)	3rd Front (QW)	512	466	8.984%
2	9600	Street (QW)	3rd Back (QW)	512	432	15.625%
3	19200	Street (QW)	Basement (QW)	1024	1010	1.367%
3	19200	Street (QW)	1st Front (QW)	1024	1013	1.074%
3	19200	Street (QW)	1st Back (QW)	1024	955	6.738%
3	19200	Street (QW)	2nd Front (QW)	1024	1015	0.879%
3	19200	Street (QW)	2nd Back (QW)	1024	927	9.473%
3	19200	Street (QW)	3rd Front (QW)	1024	995	2.832%
3	19200	Street (QW)	3rd Back (QW)	1024	904	11.719%
4	38400	Street (QW)	Basement (QW)	1024	1004	1.953%
4	38400	Street (QW)	1st Front (QW)	1024	1018	0.586%
4	38400	Street (QW)	1st Back (QW)	1024	883	13.770%
4	38400	Street (QW)	2nd Front (QW)	1024	1021	0.293%
4	38400	Street (QW)	2nd Back (QW)	1024	832	18.750%
4	38400	Street (QW)	3rd Front (QW)	1024	990	3.320%
4	38400	Street (QW)	3rd Back (QW)	1024	930	9.180%
5	76800	Street (QW)	Basement (QW)	1280	1260	1.563%
5	76800	Street (QW)	1st Front (QW)	1280	1271	0.703%
5	76800	Street (QW)	1st Back (QW)	1280	1059	17.266%
5	76800	Street (QW)	2nd Front (QW)	1280	1279	0.078%
5	76800	Street (QW)	2nd Back (QW)	1280	1024	20.000%
5	76800	Street (QW)	3rd Front (QW)	1280	1259	1.641%
5	76800	Street (QW)	3rd Back (QW)	1280	1085	15.234%
6	4800	Street (HW)	Basement (QW)	256	188	26.563%
6	4800	Street (HW)	1st Front (QW)	256	174	32.031%
6	4800	Street (HW)	1st Back (QW)	256	171	33.203%
6	4800	Street (HW)	2nd Front (QW)	256	127	50.391%
6	4800	Street (HW)	2nd Back (QW)	256	162	36.719%
6	4800	Street (HW)	3rd Front (QW)	256	181	29.297%
6	4800	Street (HW)	3rd Back (QW)	256	148	42.188%

Run	Baud	Slave	Master	Sent	Recev.	PER
7	19200	Street (HW)	Basement (QW)	1024	1011	1.270%
7	19200	Street (HW)	1st Front (QW)	1024	1009	1.465%
7	19200	Street (HW)	1st Back (QW)	1024	884	13.672%
7	19200	Street (HW)	2nd Front (QW)	1024	1019	0.488%
7	19200	Street (HW)	2nd Back (QW)	1024	891	12.988%
7	19200	Street (HW)	3rd Front (QW)	1024	992	3.125%
7	19200	Street (HW)	3rd Back (QW)	1024	882	13.867%
8	9600	Street (HW)	Basement (HW)	384	346	9.896%
8	9600	Street (HW)	1st Front (HW)	384	336	12.500%
8	9600	Street (HW)	1st Back (HW)	384	323	15.885%
8	9600	Street (HW)	2nd Front (HW)	384	358	6.771%
8	9600	Street (HW)	2nd Back (HW)	384	306	20.313%
8	9600	Street (HW)	3rd Front (HW)	384	350	8.854%
8	9600	Street (HW)	3rd Back (HW)	384	303	21.094%
9	19200	Back (QW)	Basement (QW)	512	227	55.664%
9	19200	Back (QW)	1st Front (QW)	512	416	18.750%
9	19200	Back (QW)	1st Back (QW)	512	512	0.000%
9	19200	Back (QW)	2nd Front (QW)	512	464	9.375%
9	19200	Back (QW)	2nd Back (QW)	512	511	0.195%
9	19200	Back (QW)	3rd Front (QW)	512	487	4.883%
9	19200	Back (QW)	3rd Back (QW)	512	512	0.000%
10	19200	Lab (QW)	Basement (QW)	512	345	32.617%
10	19200	Lab (QW)	1st Front (QW)	512	431	15.820%
10	19200	Lab (QW)	1st Back (QW)	512	508	0.781%
10	19200	Lab (QW)	2nd Front (QW)	512	445	13.086%
10	19200	Lab (QW)	2nd Back (QW)	512	511	0.195%
10	19200	Lab (QW)	3rd Front (QW)	512	508	0.781%
10	19200	Lab (QW)	3rd Back (QW)	512	512	0.000%

**Table 20: Outdoor / Indoor Range Test Raw Results**

Table 21 is referenced in Section 5.1.3; the columns are similar to those in the above table.

Run	Location	Dist (m)	Antennas	Sent	Recev.	PER
1	Lancaster	84	QW / QW	256	255	0.39%
1	Wachusett	154	QW / QW	256	251	1.95%
1	Goulding	239	QW / QW	256	240	6.25%
1	Denny	320	QW / QW	256	232	9.38%
1	N Ashland	390	QW / QW	256	219	14.45%
1	Ormond	460	QW / QW	256	206	19.53%
1	West	533	QW / QW	256	90	64.84%
1	Berkshire	594	QW / QW	256	203	20.70%
1	Fruit	652	QW / QW	256	59	76.95%
1	Howe	700	QW / QW	256	3	98.83%
1	Sever	754	QW / QW	256	0	100.00%
1	Roxbury	856	QW / QW	0	0	
1	Somerset	952	QW / QW	0	0	
1	Russell	1045	QW / QW	0	0	

Run	Location	Dist (m)	Antennas	Sent	Recev.	PER
2	Lancaster	84	HW / HW	256	251	1.95%
2	Wachusett	154	HW / HW	256	248	3.13%
2	Goulding	239	HW / HW	256	242	5.47%
2	Denny	320	HW / HW	256	249	2.73%
2	N Ashland	390	HW / HW	256	118	53.91%
2	Ormond	460	HW / HW	256	93	63.67%
2	West	533	HW / HW	256	79	69.14%
2	Berkshire	594	HW / HW	256	147	42.58%
2	Fruit	652	HW / HW	256	152	40.63%
2	Howe	700	HW / HW	256	23	91.02%
2	Sever	754	HW / HW	256	52	79.69%
2	Roxbury	856	HW / HW	256	0	100.00%
2	Somerset	952	HW / HW	256	155	39.45%
2	Russell	1045	HW / HW	256	0	100.00%

**Table 21: Outdoor Range Test Raw Results**

In Table 22 below (referenced in Section 5.1.8), “MA”, “SL1” and “SL2” refer to the master, slave 1 and slave 2 board numbers, respectively. The “Range” is the maximum synchronization offset obtained across the measurements for those boards, and the Mean and Std. Dev. are also given for those measurements. The statistics shown below those columns were only calculated for runs 1-45.



Run	MA	SL1	SL2	Range (s)	Meas.	Mean (s)	Std. Dev. (s)	
1	3	1	2	3.018E-05	2048	3.034E-07	1.058E-06	
2	4	1	3	3.190E-05	2048	-2.355E-07	1.316E-06	
3	5	1	4	3.002E-05	2048	1.020E-08	1.108E-06	
4	6	1	5	2.686E-05	2048	-1.292E-07	1.050E-06	
5	7	1	6	3.695E-05	2048	-2.598E-07	1.366E-06	
6	8	1	7	2.090E-05	2048	-1.044E-07	9.710E-07	
7	9	1	8	2.264E-05	2048	-2.519E-07	1.106E-06	
8	10	1	9	2.817E-05	2048	-7.714E-07	1.025E-06	
9	2	1	10	2.669E-05	2046	-2.820E-08	1.083E-06	
10	5	2	3	3.325E-05	2048	-6.282E-07	1.185E-06	
11	6	2	4	1.324E-05	2048	-3.966E-07	9.387E-07	
12	7	2	5	3.254E-05	2048	-4.278E-07	1.164E-06	
13	8	2	6	3.756E-05	2048	-5.834E-07	1.131E-06	
14	9	2	7	2.685E-05	2048	-1.034E-06	1.842E-06	
15	10	2	8	3.613E-05	2048	-5.265E-07	1.226E-06	
16	1	2	9	2.667E-05	2047	-5.671E-07	1.106E-06	
17	3	2	10	3.745E-05	2047	-3.840E-07	1.225E-06	
18	7	3	4	3.697E-05	2048	1.216E-07	1.096E-06	
19	8	3	5	3.076E-05	2048	-1.247E-07	1.217E-06	
20	9	3	6	2.447E-05	2048	-9.144E-08	1.088E-06	
21	10	3	7	1.975E-05	2046	-1.500E-07	1.168E-06	
22	1	3	8	2.855E-05	2048	-2.109E-08	1.024E-06	
23	2	3	9	3.190E-05	2048	-9.300E-08	1.138E-06	
24	4	3	10	2.745E-05	2048	1.566E-07	1.139E-06	
25	9	4	5	3.432E-05	2048	-3.195E-07	1.326E-06	
26	10	4	6	3.744E-05	2045	-4.075E-07	1.149E-06	
27	1	4	7	3.221E-05	2048	-8.115E-07	1.528E-06	
28	2	4	8	3.217E-05	2048	-4.233E-07	1.206E-06	
29	3	4	9	2.384E-05	2039	-1.018E-06	1.629E-06	
30	5	4	10	3.139E-05	2046	-1.060E-06	2.086E-06	
31	1	5	6	3.149E-05	2048	-3.082E-07	1.137E-06	
32	2	5	7	2.569E-05	2046	-9.838E-08	1.028E-06	
33	3	5	8	3.506E-05	2048	-1.763E-07	1.291E-06	
34	4	5	9	1.530E-05	2048	-1.080E-07	9.202E-07	
35	6	5	10	3.413E-05	2048	-2.345E-07	1.622E-06	
36	3	6	7	3.734E-05	2048	-1.761E-07	1.299E-06	
37	4	6	8	3.227E-05	2048	-1.476E-07	1.205E-06	
38	5	6	9	2.911E-05	2048	-1.966E-06	1.841E-06	
39	7	6	10	2.733E-05	2047	-8.510E-07	1.765E-06	
40	5	7	8	2.540E-05	2048	-1.643E-07	1.118E-06	
41	6	7	9	3.386E-05	2048	-1.285E-07	1.228E-06	
42	8	7	10	2.863E-05	2048	-2.107E-08	1.156E-06	
43	7	8	9	3.284E-05	2048	-1.315E-08	1.157E-06	
44	9	8	10	3.071E-05	2048	-6.509E-09	1.039E-06	
45	1	9	10	2.686E-05	2048	-3.618E-08	1.118E-06	
46	8	2	6	4.057E-05	20470	-3.172E-07	1.166E-06	
				<b>Avg.</b>	2.967E-05	2047.4889	-3.265E-07	1.236E-06
				<b>Std Dev</b>	5.579E-06	1.4700298	4.013E-07	2.528E-07
				<b>Max</b>	3.756E-05	2048	3.034E-07	2.086E-06
				<b>Min</b>	1.324E-05	2039	-1.966E-06	9.202E-07
				<b>Range</b>	2.432E-05	9	2.270E-06	1.166E-06

Table 22: Synchronization Accuracy Test Results